METABOLIC REGULATION OF HISTONE METHYLATION

A Dissertation

Presented to the Faculty of the Graduate School

of Cornell University

in Partial Fulfillment of the Requirements for the Degree of

Doctor of Philosophy

by

Samantha Jo Mentch

January 2017

METABOLIC REGULATION OF HISTONE METHYLATION

Samantha Jo Mentch, Ph.D.

Cornell University 2017

The one carbon cycle encompasses the folate and methionine cycles to produce one carbon units for a variety of cellular processes. The methionine cycle, in particular, generates S-adenosylmethionine (SAM) from methionine, an essential amino acid. SAM is utilized by histone methyltransferases (HMTs) to methylate histone proteins. Histone methylation plays diverse roles in the establishment of chromatin states and the regulation of gene expression. Histones are methylated by histone methyltransferases (HMTs) and demethylated by histone demethylases (HDMs) the activities of which rely on molecules generated via cell metabolism, such as S-adenosylmethionine (SAM). It has been shown in vitro, physiological concentrations of SAM are close to reported K_M values for histone methyltransferase enzymes. Therefore, histone methyltransferase activity is sensitive to small changes in intracellular concentrations of SAM that could arise from differences in nutrient availability.

Histone methylation has only recently been appreciated as a dynamic epigenetic mark. Of the numerous histone methylation modifications that occur, the importance of H3 lysine 4 trimethylation (H3K4me3), H3K9me3, and H3K27me3 in establishing and maintaining chromatin states and their influence on gene expression are well documented. To better define the relationship between SAM availability, histone methylation and downstream consequences on gene expression, I characterized the metabolic response to methionine restriction using metabolomic, transcriptomic, and epigenomic approaches. Together,

we found a specific response to methionine deprivation lead to decreases in SAM and H3K4me3 providing a link between cell metabolism and epigenetics. We took this one step further, and analyzed the transcriptional response to methionine restriction to determine the effect of metabolic alterations in H3K4me3 on gene expression.

This work provides evidence for a link between metabolic status and histone methylation in cells that could give rise to changes in gene expression–whether transient or permanent–providing a molecular basis for how environmental factors, such as diet, can influence gene expression via cell metabolism.

BIOGRAPHICAL SKETCH

Samantha Mentch is the daughter of Amy and Bob Berkheimer and the oldest of four children–Kim, Bobby, and Iris-Ann. She grew up in a small town in Central Pennsylvania, where she was encouraged to run around barefoot and explore and play outside. A bit of an overachiever, she took every science, math and programming class available and graduated from West Perry High School in 2008. The next fall she was the first in her family to attend college at Susquehanna University in pursuit of her degree in Biology. In one of her first college lectures she was shown the video, "The Inner Life of a Cell" by XVIVO made for Harvard University and was captivated by the coordinated intricacies of a single cell. It was from that moment she decided to pursue research to understand, at the smallest scale, how cells work.

She began research her sophomore year in a physical chemistry lab developing methods to detect DNA quadruplex structures in solutions. Quickly realizing her passion was in cell and molecular biology, she pursued research studying egg maturation in Drosophila, where she carried out her honors thesis research in Dr. David Richards' Lab. In addition, she also pursued research at other universities. She was fortunate to participate in research at The University of Pennsylvania and Harvard Medical School through the Leadership Alliance. While at UPenn, she studied the role of wnt signaling in cancer during the summer of 2010 and worked with the first multicellular organism *in vivo* system to test the histone code hypothesis at Harvard in the summer of 2011. After her summer at Harvard, she knew she wanted to study epigenetics and go to graduate school to pursue a Ph.D. Samantha graduated Suma Cum Laude with a Bachelor of Science in Biology with Honors, a Bachelor of Arts in Chemistry, and a minor in Mathematics from Susquehanna University in 2012.

She began graduate school at Cornell University the following fall and, despite telling everyone she would never join a cancer lab, landed in the lab of Dr. Jason Locasale. There she has studied the interplay of cell metabolism and epigenetics in the context of normal and disease states, including cancer.

Since being at Cornell, she married another Cornell graduate, statistician, high school sweetheart, and her best friend Lucas Mentch. Together they moved to North Carolina so Samantha could finish her research in her thesis lab, which moved to Duke University in the fall of 2015.

Dedicated to my family and my best friend and husband Lucas

ACKNOWLEDGEMENTS

There are many people to thank who have helped me during my Ph.D. journey that culminates in this thesis. First, I would like to thank my husband, Lucas, for always pushing me to be better than I thought I could be. I could not have done this without your constant support and encouragement through the ups and downs. I would also like to thank my family for their understanding and ability to bring me back down to earth when I needed it most.

I am grateful for the friends I made that were essential in keeping me focused and sane. I would like to thank my lab mates especially in this regard. Maria, Bella, Xiaojing, Mahya, and Ahmad were a constant support system that made lab life bearable at some of the most unbearable moments. They've taught me so much in such a short time. I wish them, and the rest of the Locasale Lab continued success.

Much of this work could not have been done without the gracious help of collaborators who supplied valuable materials and support that led to some of the most exciting parts of this thesis. To this end, I extend sincere thanks to Dr. Sailendra (Nath) Nichenametla of the Orentreich Foundation, Dr. Oliver McDonald at Vanderbilt, Dr. Anna Thalacker-Mercer and members of her Lab (Diwakar Gupta and Heather Roman) and Drs. Erin Jones and Mintie Pu of the Lee Lab, both at Cornell University.

Finally, I am incredibly grateful for all the mentors and support I've had along the way that have allowed me to reach the end of this journey. I could not have done it without the experience and advice from those at all the institutions I've had the privilege of being part of. I am especially grateful for my committee members, Drs. Sylvia Lee, Chris Fromme, and Jason Locsale, Dr. Bill Brown, Dr. Marcus Smolka and the BMCB GFAs of Cornell University, Drs. David Richard

and Swarna Basu of Susquehanna University, Drs. Mitzi Kuroda and Sheila Thomas of Harvard University School of Medicine, and Drs. Arnaldo Diaz and Susan Ross of the University of Pennsylvania. You've all given me invaluable opportunities to conduct the highest caliber of research.

TABLE OF CONTENTS

LIST OF TABLES

LIST OF FIGURES

LIST OF ABBREVIATIONS

5-mTF: 5-methyltetrahydrafolate

ATP: Adenosine triphosphate

BHMT: Betaine-homocysteine methyltransferase

BRCA1: Breast cancer 1

CEBP: CCAAT/Enhancer Binding Protein

COMPASS: Complex of proteins associated with SET1

CBS: Cystathionine β-synthase

CHD1: Chromodomain helices DNA-bnding protein 1

ChIP: Chromatin immunoprecipitation

CTD: C-terminal domain

DMG: Dimethylglycine

DNA: Deoxyribonucleic acid

DNMT: DNA methyltransferase

DOT1L: Disruptor of telomeric silencing-like 1

EZH1/2: Enhancer of zeste homologue 1/2

H2AK119ub1: Histone 2A lysine 119 mono-ubiquitination

H3K4me(1,2,3): Histone 3 lysine 4 (mono-, di-, trimethyl)

H3K9me(1,2,3): Histone 3 lysine 9 (mono-, di-, trimethyl)

H3K27me(1,2,3): Histone 3 lysine 27 (mono-, di-, trimethyl)

H3K79me(1,2,3): Histone 3 lysine 79 (mono-, di-, trimethyl

hCys: Homocysteine

HOX: Homeobox protein family

HP1: Heterochromatin protein 1

HMT: Histone methyltransferase

KMT: Lysine methyltransferase

MAT: Methionine adenosyltransferase

MLL: Mixed Lineage Leukemia

mESC: Mouse embryonic stem cell

MS: 5-methyltetrahydrafolate-homocysteine methyltransferase

MYC: V-myc myelocytomatosis viral oncogene homolog

NNMT: Nicotinamide N-methyltransferase

P53BP1: p53-binding protein 1

Pc: Polycomb

PPARγ: Peroxisome Proliferator Activated Receptor Gamma

PRC: Polycomb repressive complex

PRMT: Arginine methyltransferase

RNA: Ribonucleic acid

RNAP II: RNA polymerase II

SAM: S-adenosylmethionine

SAH: S-adenosylhomocysteine

SET: Su(var), Enhancer of Zeste and Trithorax

SUV39H1: Su-var 3-9 Homologue 1

TAF3: TBP Associated Factor, 140kD

TBP: TATA box binding protein

TFIID: Transcription factor II D

THF: Tetrahydrafolate

trx: trithorax

LIST OF SYMBOLS

°C: degrees Celcius

K_m: Michaelis-Menten constant

hr: hour

M: molar

min: minute

mg: milligrams

mL: milliliters

mM: millimolar

U: units

μg: micrograms

μL: microliters

μM: micromolar

$\times$ g: times acceleration due to gravity

CHAPTER 1

INTRODUCTION

1.1 Methionine Metabolism

Methionine, an essential amino acid, is transported into the cell via the amino acid transport system where it is then available for protein synthesis and metabolic conversion via the methionine cycle (Townsend et al., 2004). The methionine cycle is part of one carbon metabolism and utilizes methionine to generate S-adenosylmethionine (SAM). The methyl group in SAM is available for transfer by methyltransferases like histone methyltransferases (HMTs), producing S-adenosylhomocysteine (SAH) in the process. SAH is then converted to homocysteine which can either enter the transsulfuration pathway or be remethylated using 5-methyltetrahydrafolate (5-mTHF) or betaine completing the cycle to regenerate methionine. The methionine cycle itself is a series of complex biochemical reactions whose enzymes are inhibited and activated by the metabolites produced in the process (Hoffman et al., 1980; Finkelstein and Martin, 1984; Finkelstein, 1990). In addition, the methionine cycle provides substrates for polyamine synthesis and the generation of cysteine and glutathione from the transsulfuration pathway (Finkelstein, 1990). It also provides a link between folate metabolism and downstream synthesis of purines and pyrimidines (Figure 1.1). More details on the methionine cycle can be found in Chapter 2.

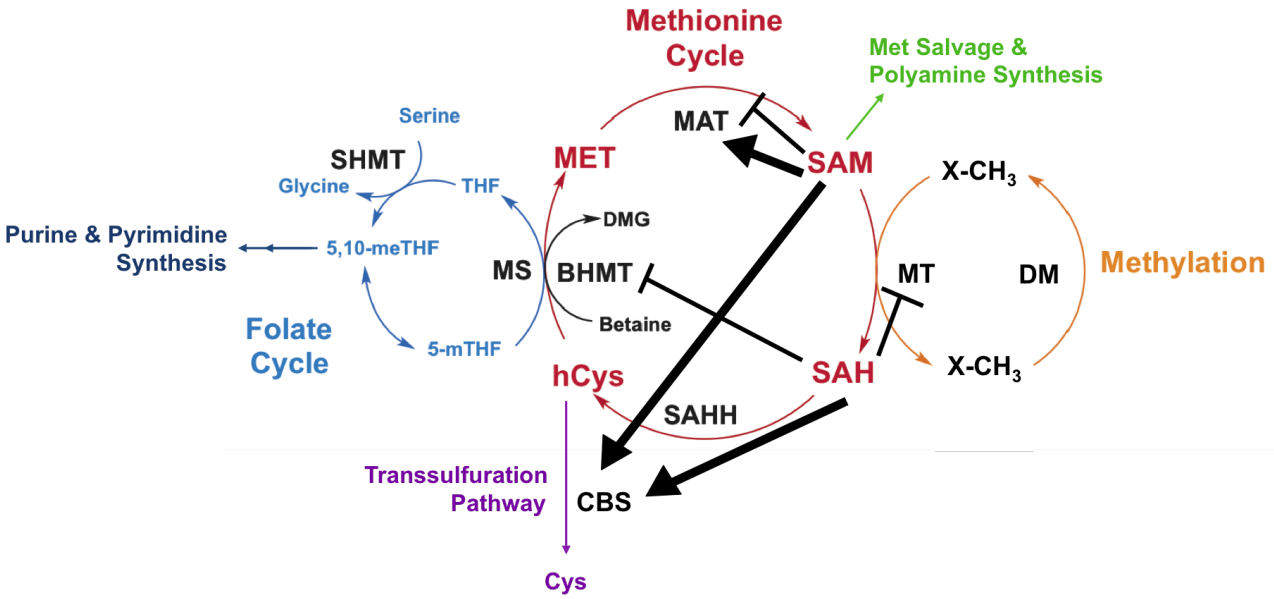

Figure 1.1: One Carbon Metabolism

One carbon metabolism is composed of the folate cycle and the methionine cycle, are connected through remethylation of homocysteine (hCys) by methionine synthase (MS) utilizing 5-methyltetrahydrofolate (5-mTHF) as a methyl donor to regenerate methionine. One-carbon metabolism, and methionine metabolism in particular, is important in the generation of S-adenosylmethionine (SAM) for methylation reactions by methyltransferases (MT). Products of one carbon metabolism are utilized in the methionine salvage pathway, polyamine synthesis, the transsulfuration pathway and purine and pyrimidine synthesis. In addition, products of methionine metabolism, SAM and S-adenosylhomocysteine (SAH), regulate enzyme activity through inhibition (flat top line) or activation (bold arrow). Methionine (MET); Methionine Adenosyltransferase (MAT); Demethylase (DM); S-adeonsylhomocysteine hydrolase (SAHH); betaine-homocysteine S-methyltransferase (BHMT); Cystathionine (Cys); Cystathionine β-synthase (CBS); tetrahydrafolate (THF); 5,10-methylenetetrahydrofolate (5,10-meTHF); Serine hydroxymethyltransferase (SHMT).

Much of the research on methionine metabolism has focused on the methionine cycle in hepatic tissues and cells due to the overwhelming activity observed there and the expression of CBS and liver specific MAT1A and BHMT1 (Figure 1.2) (Finkelstein, 1990). In other cells it is likely the transsulfuration pathway does not play a critical role unless extreme excess of methionine is introduced to the cell.

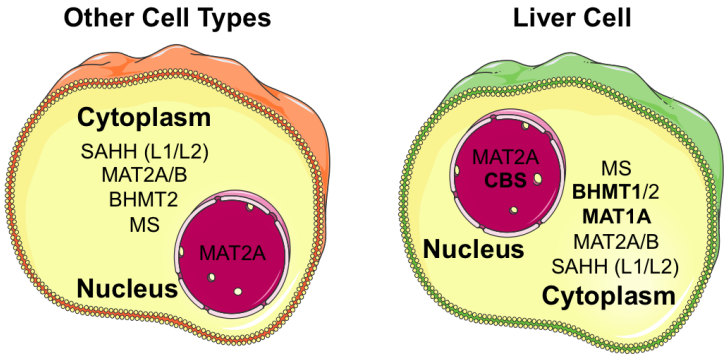

Figure 1.2: Methionine Cycle Enzymes

In most cell types, MAT2B, BHMT2, MS, SAHH are located in the cytoplasm and MAT2A is localized to the cytoplasm and the nucleus. In liver cells, in addition to those enzymes, BHMT1 and MAT1A are transcribed and localized in the cytoplasm and CBS is produced and localized in the nucleus.

Understanding the role of methionine metabolism in diverse cell types will be essential to determine how alterations will effect histone methylation and the role this relationship plays in disease states. Defects in methionine metabolism can give rise to a variety of pathologies including liver disease and cancer (Mato et al., 2008).

1.2 Histones, Nucleosomes, and Chromatin

Nearly all eukaryotic cells use highly conserved histone proteins to organize and package DNA into chromatin. Chromatin is composed of repeating nucleosome arrays, in which 147 bp of DNA wraps around a histone octamer containing two each of the core histones−H3, H4, H2A, and H2B−forming a nucleosome core (Wood et al., 2005) (Figure 1.3), with linker histones H1 and linker DNA in between (Kornberg, 1977). The organization of nucleosomes into higher ordered structures directly impacts the accessibility of the underlying DNA sequences and therefore, gene expression.

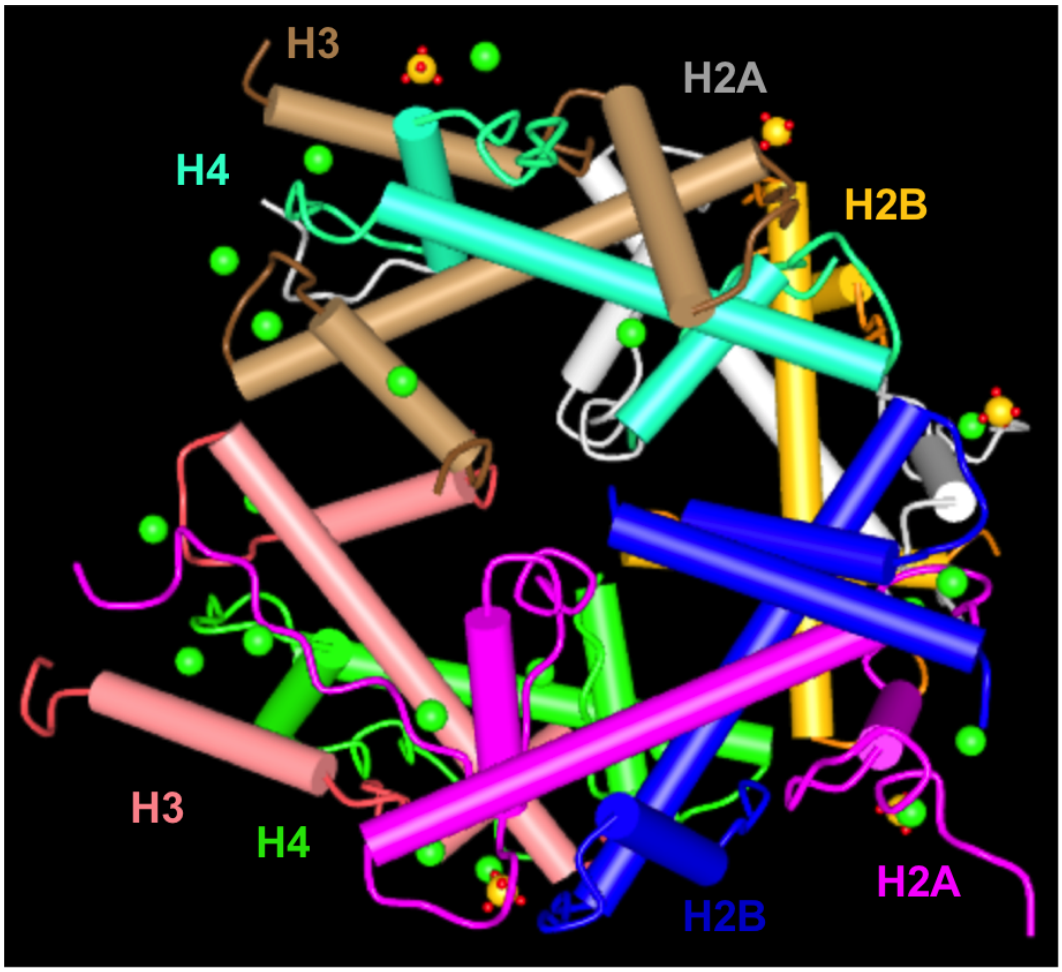

Figure 1.3: Core Histone Octomer (PDB 1TZY)

Core histone octomer at 1.9 angstrom resolution (PDB Accession 1TZY). Composed two H2A:H2B dimers and two H3:H4 dimers. Each histone that makes up the core octamer is labeled with corresponding colors. Protein structure is visualized using Cn3D.

The basic nature of histone proteins facilitates their interaction with the negatively charged DNA backbone in the nucleosome core. Each core histone is composed of a globular domain, responsible for histone-histone and histone-DNA interactions, and a mostly unstructured N-terminal tail that protrudes out from the nucleosome core (Davey et al., 2002; Richmond and Davey, 2003). Although the globular domains can be modified (Feng et al., 2002; Ng et al., 2002; van Leeuwen et al., 2002; Zhang et al., 2002), the histone tails are more eas-

ily accessible and can be extensively modified with diverse chemical groups. Of these, the most commonly studied histone post-translational modifications (PTMs) are arginine methylation, lysine methylation, acetylation, ubiquitination, and sumoylation and serine and threonine phosphorylation, although more novel modifications such has lysine crotonylation and tyrosine hydroxylation, have recently been identified (Tan et al., 2011). In addition, the number of histone PTMs has only increased with advances in mass spectrometry methods to include over 125 uniquely modified sites (Tan et al., 2011).

Histone PTMs are thought to act in two ways (1) to change the local chemical environment, which determines how strong the interaction is between the histones and DNA and (2) recruit proteins that reorganize chromatin and initiate or repress translation, thus providing a mechanism for gene regulation (Musselman et al., 2012). Since every cell in an organism contains the exact same genetic code, histones and their PTMs are believed to make up a histone code−a second set of instructions eukaryotic cells use to maintain their unique identities (Strahl and Allis, 2000; Jenuwein and Allis, 2001).

1.3 Histone Methylation and Demethylation

Histones can be methylated at the basic residues lysine, arginine, and histidine. In addition, lysine can be mono-, di-, or trimethylated and arginine can be mono-methylated, or symmetrically or asymmetrically dimethylated (histidine methylation has yet to be characterized). Histone methyltransferases (HMTs) are the "writers" of methylation marks on histones. All HMTs utilize the metabolic derived universal methyl donor, S-adenosylmethionine (SAM) to

methylate histones, releasing S-adenosylhomocysteine (SAH) in the process.

In addition to histone methyltransferases, "erasers", or histone demethylases exist to remove methylation marks from histones and other proteins. Many believed that histone methylation was permanent until LSD1 (renamed KDM1), the first histone demethylase, was described by Shi et al. (2004). The mechanism of demethylation involves a deimination reaction to remove the methyl groups from lysine and arginine. Currently, two types of histone demethylases have been described–Flavin adenine dinucleotide (FAD) dependent and Jumonji (JmjC) Histone demethylases–and are categorized by the metabolite co-factors utilized in the demethylation reaction. Flavin adenine dinucleotide (FAD) dependent demethylases are able to demethylate mono- and dimethylated histones through an amine oxidase reaction.

1.4 The Link Between Metabolism and Epigenetics

Once controversial, it has become appreciated that histone methylation is a dynamic process that allows for addition and removal of methyl groups from histones in response to the environment (Schneider et al., 2002; Zee et al., 2010). Shyh-Chang et al. (2013) observed decreased H3K4me2 and H3K4me3 after threonine restriction in mouse embryonic stem cells causing decreased SAM pools. This was followed by experiments showing over-expression of Nicotinamide N-methyltransferase (NNMT) sequesters SAM away from histone methyltransferase reactions, creating a "methyl sink" and reduces H3K4 methylation among others (Ulanovskaya et al., 2013). Shiraki et al. (2014) followed up on the original observation by performing similar experiments in hu-

man embryonic stem cells showing methionine restriction reduces SAM availability and decreases histone methylation, again with H3K4 methylation being the most affected. Although in this case, p53 and other stress response pathways, which are known to down regulate HMT gene expression, were activated (Tang et al., 2004). More links were drawn by Tang et al. (2015) that showed arginine and polyamine synthesis were required for the methionine restriction response in MCF7 cells and blocking creatine synthesis restored H3K4me3 levels.

1.5 Scope of this Thesis

The link between metabolism and epigenetics is an interesting one that has garnered the attention of many over the past few years, deservedly so. However, this thesis and current research only scratches the surface of our understanding. Determining the effects of changes in nutrient availability on metabolism and epigenetics could finally provide a strong link between between the environment and our genes and progress in this field could lead to treatments for diseases, like cancer.

In the following chapter, I explain one potential link between cell metabolism and epigenetics via one carbon metabolism and histone methylation. The theory details the hypotheses that can be tested; mainly that decreases in nutrient availability of methionine will decrease SAM availability and thus alter histone methylation due to the biochemical properties of these reactions.

In chapter 3, these hypotheses are tested using high throughput metabolomics and NGS sequencing technologies for the first time to detail the

metabolic, epigenetic, and transcriptional changes in response to decreased methionine. We provide evidence that one-carbon metabolism is altered in response to methionine deprivation in vitro and in vivo and these alterations lead to decreased H3K4me3. This relationship has the potential to alter key genes that are important in one carbon metabolism and cancer pathogenesis.

The final appendices detail the scripts used to process the ChIP-seq and RNA-seq data for reproducibility purposes.

LITERATURE CITED

Davey, C. A., Sargent, D. F., Luger, K., Maeder, A. W., and Richmond, T. J. (2002). Solvent mediated interactions in the structure of the nucleosome core particle at 1.9 a resolution. *J. Mol. Biol.*, 319(5):1097–1113.

Feng, Q., Wang, H., Ng, H. H., Erdjument-Bromage, H., Tempst, P., Struhl, K., and Zhang, Y. (2002). Methylation of H3-lysine 79 is mediated by a new family of HMTases without a SET domain. *Curr. Biol.*, 12(12):1052–1058.

Finkelstein, J. D. (1990). Methionine metabolism in mammals. *J. Nutr. Biochem.*, 1(5):228–237.

Finkelstein, J. D. and Martin, J. J. (1984). Methionine metabolism in mammals. Distribution of homocysteine between competing pathways. *J. Biol. Chem.*, 259(15):9508–9513.

Hoffman, D. R., Marion, D. W., Cornatzer, W. E., and Duerre, J. A. (1980). S-Adenosylmethionine and S-adenosylhomocystein metabolism in isolated rat liver. Effects of L-methionine, L-homocystein, and adenosine. *J. Biol. Chem.*, 255(22):10822–10827.

Jenuwein, T. and Allis, C. D. (2001). Translating the histone code. *Science*, 293(5532):1074–1080.

Kornberg, R. D. (1977). Histone composition of nucleosomes isolated from cultured Chinese hamster cells. *Biochemistry*, 16(22):4940–4944.

Mato, J. M., Martinez-Chantar, M. L., and Lu, S. C. (2008). Methionine metabolism and liver disease. *Annu. Rev. Nutr.*, 28:273–293.

Musselman, C. A., Lalonde, M. E., Cote, J., and Kutateladze, T. G. (2012). Perceiving the epigenetic landscape through histone readers. *Nat. Struct. Mol. Biol.*, 19(12):1218–1227.

Ng, H. H., Feng, Q., Wang, H., Erdjument-Bromage, H., Tempst, P., Zhang, Y., and Struhl, K. (2002). Lysine methylation within the globular domain of histone H3 by Dot1 is important for telomeric silencing and Sir protein association. *Genes Dev.*, 16(12):1518–1527.

Richmond, T. J. and Davey, C. A. (2003). The structure of DNA in the nucleosome core. *Nature*, 423(6936):145–150.

Schneider, R., Bannister, A. J., and Kouzarides, T. (2002). Unsafe SETs: histone lysine methyltransferases and cancer. *Trends Biochem. Sci.*, 27(8):396–402.

Shi, Y., Lan, F., Matson, C., Mulligan, P., Whetstine, J. R., Cole, P. A., Casero, R. A., and Shi, Y. (2004). Histone demethylation mediated by the nuclear amine oxidase homolog LSD1. *Cell*, 119(7):941–953.

Shiraki, N., Shiraki, Y., Tsuyama, T., Obata, F., Miura, M., Nagae, G., Aburatani, H., Kume, K., Endo, F., and Kume, S. (2014). Methionine metabolism regulates maintenance and differentiation of human pluripotent stem cells. *Cell Metab.*, 19(5):780–794.

Shyh-Chang, N., Locasale, J. W., Lyssiotis, C. A., Zheng, Y., Teo, R. Y., Ratanasirintrawoot, S., Zhang, J., Onder, T., Unternaehrer, J. J., Zhu, H., Asara, J. M., Daley, G. Q., and Cantley, L. C. (2013). Influence of threonine metabolism on S-adenosylmethionine and histone methylation. *Science*, 339(6116):222–226.

Strahl, B. D. and Allis, C. D. (2000). The language of covalent histone modifications. *Nature*, 403(6765):41–45.

Tan, M., Luo, H., Lee, S., Jin, F., Yang, J. S., Montellier, E., Buchou, T., Cheng, Z., Rousseaux, S., Rajagopal, N., Lu, Z., Ye, Z., Zhu, Q., Wysocka, J., Ye, Y., Khochbin, S., Ren, B., and Zhao, Y. (2011). Identification of 67 histone marks and histone lysine crotonylation as a new type of histone modification. *Cell*, 146(6):1016–1028.

Tang, X., Keenan, M. M., Wu, J., Lin, C. A., Dubois, L., Thompson, J. W., Freedland, S. J., Murphy, S. K., and Chi, J. T. (2015). Comprehensive profiling of amino acid response uncovers unique methionine-deprived response dependent on intact creatine biosynthesis. *PLoS Genet.*, 11(4):e1005158.

Tang, X., Milyavsky, M., Shats, I., Erez, N., Goldfinger, N., and Rotter, V. (2004). Activated p53 suppresses the histone methyltransferase EZH2 gene. *Oncogene*, 23(34):5759–5769.

Townsend, D. M., Tew, K. D., and Tapiero, H. (2004). Sulfur containing amino acids and human disease. *Biomed. Pharmacother.*, 58(1):47–55.

Ulanovskaya, O. A., Zuhl, A. M., and Cravatt, B. F. (2013). NNMT promotes epigenetic remodeling in cancer by creating a metabolic methylation sink. *Nat. Chem. Biol.*, 9(5):300–306.

van Leeuwen, F., Gafken, P. R., and Gottschling, D. E. (2002). Dot1p modulates silencing in yeast by methylation of the nucleosome core. *Cell*, 109(6):745–756.

Wood, C. M., Nicholson, J. M., Lambert, S. J., Chantalat, L., Reynolds, C. D., and Baldwin, J. P. (2005). High-resolution structure of the native histone octamer. *Acta Crystallogr. Sect. F Struct. Biol. Cryst. Commun.*, 61(Pt 6):541–545.

Zee, B. M., Levin, R. S., Xu, B., LeRoy, G., Wingreen, N. S., and Garcia, B. A.

(2010). In vivo residue-specific histone methylation dynamics. *J. Biol. Chem.*, 285(5):3341–3350.

Zhang, K., Tang, H., Huang, L., Blankenship, J. W., Jones, P. R., Xiang, F., Yau, P. M., and Burlingame, A. L. (2002). Identification of acetylation and methylation sites of histone H3 from chicken erythrocytes by high-accuracy matrix-assisted laser desorption ionization-time-of-flight, matrix-assisted laser desorption ionization-postsource decay, and nanoelectrospray ionization tandem mass spectrometry. *Anal. Biochem.*, 306(2):259–269.

CHAPTER 2

ONE CARBON METABOLISM: UNDERSTANDING THE SPECIFICITY[1]

2.1 Summary

One carbon metabolism is a metabolic network that integrates nutrient status from the environment to yield multiple biological functions. Composed of the folate and methionine cycle, it generates S-adenosylmethionine (SAM), which is the universal methyl donor for methylation reactions, including histone and DNA methylation. Histone methylation is a crucial part of the epigenetic code and plays diverse roles in the establishment of chromatin states that mediate the regulation of gene expression. The activities of histone methyltransferases (HMTs) are dependent on intracellular levels of SAM, which fluctuate based on cellular nutrient availability, providing a link between cell metabolism and histone methylation. Here we discuss the biochemical properties of and gene regulation by histone methyltransferases and the connection to cellular metabolism. Our emphasis is on understanding the specificity of this intriguing link.

2.2 Introduction

Studies in a variety of organisms, including humans, have suggested roles for nutrient metabolism in regulating the epigenetic state in normal and disease states. Chronic diseases such as diabetes, obesity, cancer, heart disease and ag-

[1]This chapter has been adapted from our recent publication, Mentch & Locasale, *NYAS*, (2016). (Mentch and Locasale, 2016)

ing all have been linked to metabolic and epigenetic factors that play a role in pathogenesis (Grandison et al., 2009; Yun et al., 2012; Kraus et al., 2014; Cabreiro et al., 2013; Ordovás and Smith, 2010; Benayoun et al., 2015). The maintenance of cellular homeostasis requires that alterations in nutrient availability be met by appropriate adaptations. An example is the case of cell proliferation when nutrient availability is limiting (Wellen and Thompson, 2010). These adaptations necessitate sensing mechanisms that can be modulated by nutrient availability in the environment and communicate metabolic status to affect cellular physiology.

One carbon metabolism utilizes a variety of nutrients such as glucose, vitamins and amino acids to fuel a variety of metabolic pathways that utilize these one carbon units. These pathways include nucleotide metabolism, maintenance of cellular redox status, lipid biosynthesis and methylation metabolism (Locasale, 2013). Two major components of one carbon metabolism comprise the folate and methionine cycles (Figure 2.1), that function to transfer single carbon units to acceptor substrates. Importantly, the methionine cycle provides a link to histone methylation through the generation of S-adenosylmethionine (SAM).

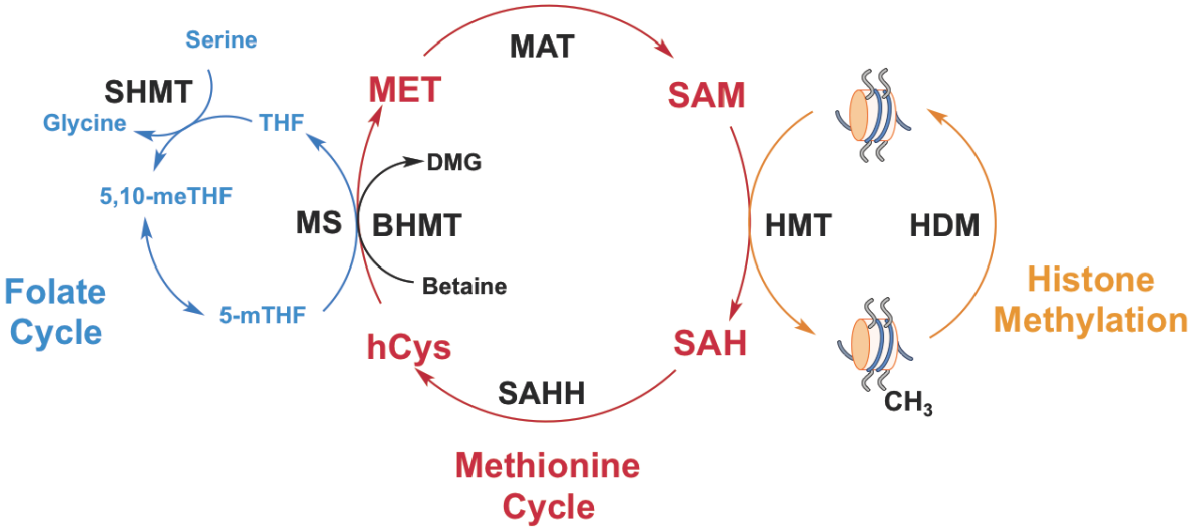

Figure 2.1: The Methionine Cycle

One carbon metabolism and histone methylation. S-adenosylmethionine (SAM) is produced from methionine (MET) by Methionine Adenosyltransferase (MAT). Histone methyltransferases (HMT) utilize SAM to donate a methyl group to their histone substrate producing S-adenosylhomocysteine (SAH). Histone demethylases (HDM) remove the methyl group from histones returning them to an unmethylated state. SAH is converted to homocysteine (hCys) via s-adenosylhomocysteine hydrolase (SAHH). To complete the cycle, SAH can be remethylated to regenerate MET by donation of a methyl group from the 5-methyltetrahydrafolate (5-mTHF) via methionine synthase (MS) or from betaine via betaine-homocysteine S-methyltransferase (BHMT).

Histones can be mono-, di-, or trimethylated at lysines and arginines by histone methyltransferases (HMTs), which transfer the methyl group from SAM to the histone substrate generating SAH (Figure 2.1). Histone methyltransferases (HMTs) are the "writers" of methylation marks on histones. Although histone methylation was discovered in 1964 (Murray, 1964), bona fide HMTs were not described until 45 years later in 1999 and 2000 with the characterization of Coactivator Arginine Methyltransferase1 (CARM1) (Chen et al., 1999) and Su-var

3-9 Homologue 1 (SUV39H1) (Rea et al., 2000), respectively. Currently, there are over 30 characterized HMTs with different methylation capacities and specificities that fall into two families–lysine methyltransferases (KMTs) and protein arginine methyltransferases (PRMTs).

Methyltransferase activity depends on substrate concentration, as is the case with all enzymes. However in contrast to phosphorylation kinetics, where adenine triphosphate (ATP) is present in cellular concentrations far greater than the enzyme K_M values (concentration of metabolite at half maximum velocity of enzyme-mediated reaction), cellular concentrations of SAM are similar to HMT K_M values (Figure 2.2). In addition, SAH is a known inhibitor of HMTs (Deguchi and Barchas, 1971), suggesting the SAM/SAH ratio may also play a role in the regulation of HMT activity (Hoffman et al., 1979). Based solely on the biochemical characteristics of HMTs, small fluctuations in SAM concentration could significantly affect HMT activity, either increasing or decreasing histone methylation activity as has been proposed (Locasale and Cantley, 2011). This suggests a direct link from cell metabolism to histone methylation status exists which could be tested (Teperino et al., 2010).

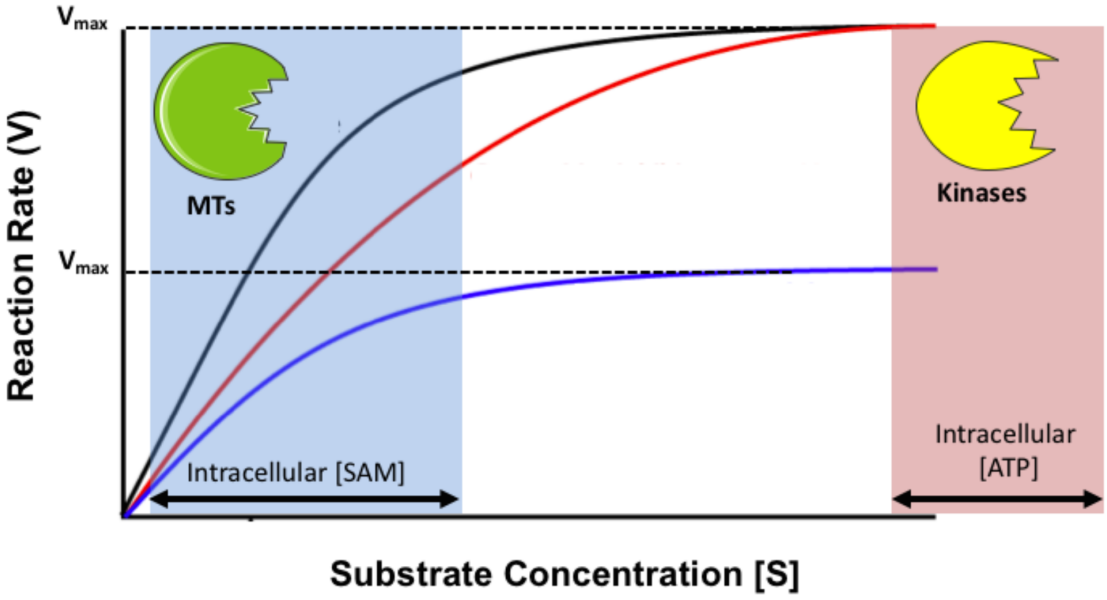

Figure 2.2: Methyltransferase Kinetics

Illustrative example comparing methyltransferase (MT) and kinase kinetics. Methyltransferase activity depends heavily on fluctuations of intracellular concentrations of S-adenosylmethionine (SAM) since MT K_M values (concentration of SAM at half maximum velocity (1/2 V_{max}) of the methyltransferase reaction) lie within the range of possible intracellular SAM concentrations. This is in contrast to kinases, in which activity is independent of intracellular adenosine triphosphate (ATP) concentration due to high intracellular concentrations of ATP.

Recent work has shown that altered metabolism does have an effect on histone methylation (Shiraki et al., 2014; Ulanovskaya et al., 2013; Tang et al., 2015), but the direct mechanistic details have yet to be fully understood. In mouse embryonic stem cells (mESC), threonine depletion contributed to decreases in the SAM/SAH ratio and histone H3 lysine 4 trimethylation (H3K4me3). However, this was observed with many other alterations such as effects on acetyl-coA metabolism indicating an indirect pathway (Shyh-Chang et al., 2013; Wang et al., 2009). Additional work on Nicotinamide N-methyltransferase (NNMT),

a SAM-consuming enzyme demonstrated over expression decreased SAM and increased SAH, overall decreasing the SAM/SAH ratio and decreasing histone methylation at H3K9me2 and H3K27me3 (Ulanovskaya et al., 2013). Further, methionine deprivation in human stem cells decreased H3K4me3 but the observation was due in part to indirect mechanisms involving an activation of a stress response, apoptotic, and differentiation pathways (Shiraki et al., 2014). Despite these advances in our understanding, the precise molecular mechanisms and specific effects on gene expression have been largely uncharacterized.

In this review we will focus on methionine metabolism as an essential regulator of histone methylation and the possibility for specific gene regulation determined by the biochemical properties, specificities of HMTs and the availability of the cofactor SAM. We will concentrate on histone lysine methylation because of its importance in epigenetics and its dysregulation in disease states.

2.3 Methionine and One Carbon Metabolism

The methionine cycle is essential for the generation of SAM through the adenylation of methionine by methionine adenosyltransferase (MAT) (Finkelstein, 1990; Cantoni, 1953; De La Haba and Cantoni, 1959). SAM is considered the universal methyl donor and is used by methyltransferases to methylate metabolites, RNA, DNA, and proteins, including histones. After the methyl group is transferred from SAM to an acceptor substrate, S-adenosylhomocysteine (SAH) is produced. In turn, SAH is hydrolyzed to adenine and homocysteine. In vivo, the reaction kinetics proceed forward in this direction, as long as the products are being removed through other metabolic pathways. Otherwise,

the reverse reaction is more favorable increasing the pool of SAH (De La Haba and Cantoni, 1959). Homocysteine can enter the transulfuration pathway and condense with serine to generate cystathionine in an irreversible reaction catalyzed by cystathionine-β-synthase (CBS). In addition, two enzymes can utilize homocysteine to regenerate methionine. Betaine-homocysteine methyltransferases (BHMT) transfers a methyl group from betaine, an intermediate in choline metabolism, to regenerate methionine and produce dimethylglycine. 5-methyltetrahydrofolate-homocysteine methyltransferase (MS) regenerates methionine by the transfer of the 5-methyltetrahydrofolate methyl moiety to homocysteine producing tetrahydrofolate (THF).

The amount of intracellular SAM depends largely on the availability of methionine, an essential amino acid sourced from the diet. The concentration of methionine circulating throughout the body in the serum is around 30μM in adults but may vary widely and change with disease (Cynober, 2002; Psychogios et al., 2011). It was recently found that methionine was observed to be the most variable serum amino acid with dietary factors being a major source of the variation (Mentch et al., 2015). SAM concentration, on the other hand, is very low in the serum (<0.5μM) (Melnyk et al., 2000) and is contained mostly in intracellular pools ranging from below 10μM up to 90μM under normal conditions and is dependent on tissue type (Duncan et al., 2013).

2.4 Histone Methyltransferases and Their Biochemical Properties

Histones can be methylated at basic residues, most notably, lysine and arginine. In addition, lysine can be mono-, di-, or trimethylated and arginine can be mono-methylated, or symmetrically or asymmetrically dimethylated. All characterized lysine-specific methyltransferases contain a SET (Su(var), Enhancer of Zeste and Trithorax) domain except Disruptor of Telomeric Silencing-like 1 (DOT1L), which methylates the globular domain of H3 at Lysine 79 (H3K79) putatively only when the nucleosome is intact (Feng et al., 2002). The SET domain spans 130 amino acids forming a tunnel that connects the cofactor binding site to the substrate binding site on the opposite side. This lysine access channel determines the number of methyl groups that can be transferred during a reaction for a given HMT and depends on the position of the methylated lysine (Figure 2.3) (Xiao et al., 2003; Dolinsky et al., 2004).

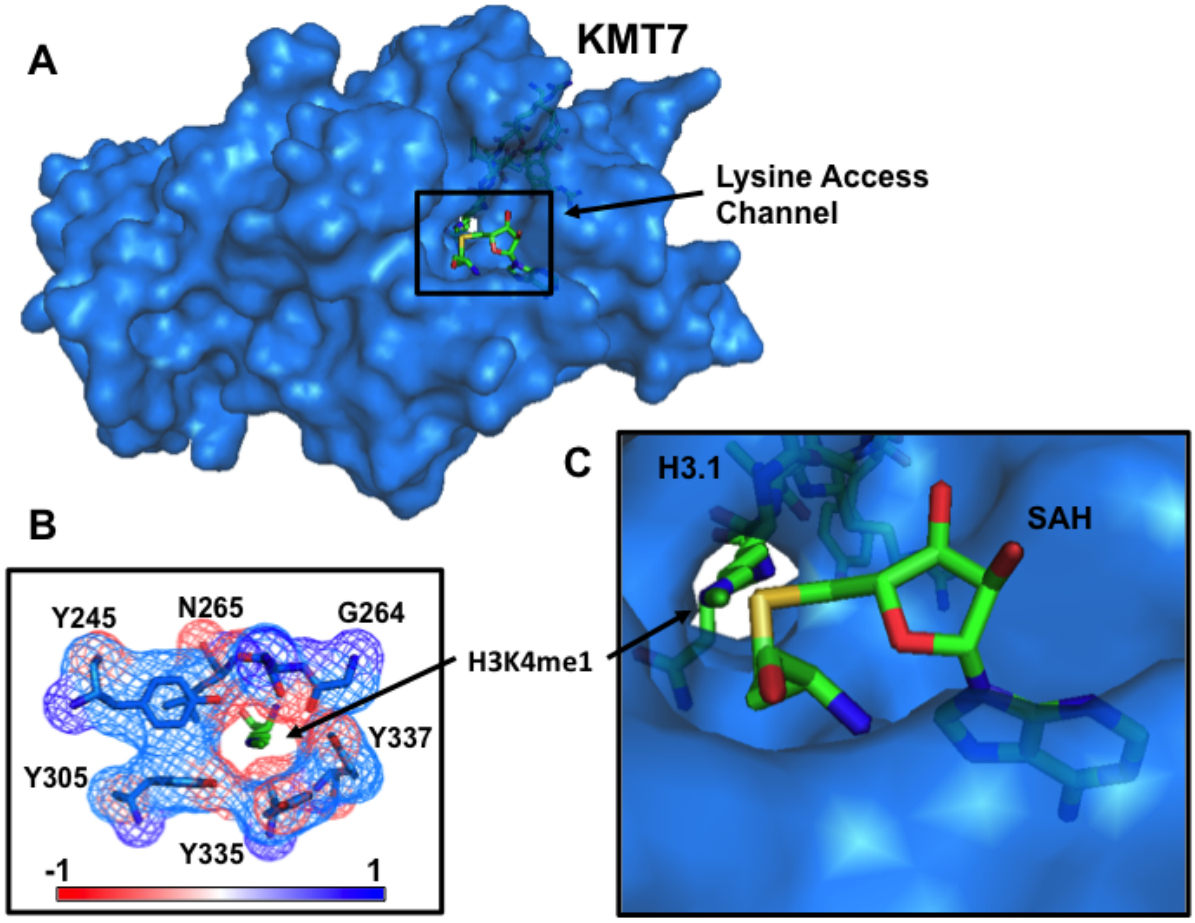

Figure 2.3: Histone Methyltransferase Structure and Binding

(A) Surface model demonstrates SAH binding and the lysine access channel with a methylated H3 tail within the SET domain of KMT730 (RCSB 1O9S) (B) The lysine access channel colored according to its electrostatic potential calculated by PDB2PQR 2.031 (C) Surface view of active site; Lysine 4 of the H3 tail enters through the lysine access channel approaching the active site containing SAH

Before transfer, the ϵ-amino group on the lysine substrate is deprotonated and points towards the SAM methyl group at 180° suggesting an S_N2 reaction mechanism of transfer. No matter the type of HMT, they utilize the universal methyl donor, S-adenosylmethionine (SAM) to methylate histones releasing S-adenosylhomocysteine (SAH) in the process allowing for regulation by cell metabolism.

The regulation of HMT activity would depend on the processing of methionine to form SAM, SAM availability to HMTs, and the concentration of HMTs in the cell. Many HMTs have been carefully studied and characterized (Summarized in Table 2.4). Interestingly, the K_M, SAM for the methylation reactions performed by HMTs falls within the range of observed intracellular SAM concentrations. Notably, there is also range of kinetic parameters across the family of HMTs suggesting that a change in metabolic flux would affect only select HMT activity.

Table 2.1: Kinetic Properties of Histone Methyltransferases

Residue	HMT	Modification	K_M(SAM) [μM]	References
H3K4	KMT2A (MLL1)	me1/2/3	10.4 ± 3.1	(Patel et al., 2014)
	KMT2B (MLL2)	me1/2/3	4.5 ± 0.82	(Horiuchi et al., 2013)
	KMT2C (MLL3)	me1/2/3	0.85 ± 0.19	(Horiuchi et al., 2013)
	KMT7 (SET7/9)	me3	6.0 ± 1.4	(Xiao et al., 2003)
H3K9	KMT1A (SUV39H1)	me1/2	12.3 ± 0.6	(Chin et al., 2005)
	KMT1B (SUV39H2)	me1/2	0.74 ± 0.23	(Horiuchi et al., 2013)
	KMT1C (EHMT2)	me2/3	1.8 ± 0.2	(Patnaik et al., 2004)
H3K27	EZH1	me1/2/3	1.24 ± 0.15	(Horiuchi et al., 2013)
	KMT6 (EZH2)	me1/2/3	1.64 ± 0.26	(Horiuchi et al., 2013)

2.5 Histone Methylation Readers, Chromatin Organization, and Gene Expression

Lysine methylation does not significantly alter the local chemical environment and leads to modest if not insignificant changes in DNA and gene accessibility, in contrast to acetylation and phosphorylation. Therefore, ”readers” of histone methylation are important since they are able to bind specific histone methylation marks to propagate their effects to gene expression (Musselman et al., 2012). Several conserved histone methyl binding motifs are categorized broadly into two groups, those containing Chromodomains and those that are part of the Royal superfamily (Musselman et al., 2012; Taverna et al., 2007). These domains are present in ”reader” proteins that bind histone methylation sites, like CHD1 (chromodomain helices DNA-bnding protein 1) (Pray-Grant et al., 2005), HP1 (heterochromatin protein 1) (Bannister et al., 2001), PC (polycomb protein) (Cao et al., 2002), and p53BP1 (p53-binding protein 1) (Huyen et al., 2004) which allow HMTs to regulate a range of cellular processes including, transcription, RNA processing, and DNA methylation, all of which affect gene expression by chromatin remodeling and transcriptional machinery recruitment.

With the advances in sequencing and chromatin immunoprecipitation (ChIP), we now have a vast repository of data showing the genomic locations of associated proteins including modified histones (Koch et al., 2007; Roadmap et al., 2015; Birney et al., 2007; Barski et al., 2007). H3K4me3 has been shown to correlate well with active gene transcription and is concentrated around transcriptional start sites (Noma and Grewal, 2002; Bernstein et al., 2002). ChIP-seq has confirmed earlier studies and consistently identifies H3K4me3 at promoters

as a predictive mark of actively transcribed genes (Birney et al., 2007). Recent analyses have also identified the shape of the peak around the transcriptional start site to be a major feature of genes involved in key biological processes such as aging and tumor suppression (Chen et al., 2015; Benayoun et al., 2014). H3K4me3 is recognized by TAF3 (TATA Box Binding Protein (TBP) Associated Factor, 140kD) a subunit of TFIID (Transcription Factor II D) suggesting a broad role in RNAP II dependent gene transcription (van Ingen et al., 2008). In addition, H3K4me1 has been implicated in marking enhancer regions and depletion at enhancers abolishes long range effects on gene regulation (Herz et al., 2012).

H3K9 methylation, participates in both constitutive and facultative heterochromatin formation and maintenance (Nakayama et al., 2001; Noma et al., 2001; Peters et al., 2002, 2001). HP1 is recruited to sites of H3K9me3 by interactions with the trimethyl moiety on H3K9 and SUV39H1 (Stewart et al., 2005). HP1 then forms a multimeric complex as SUV39H1 methylates more H3K9 recruiting more HP1 in a positive feedback loop that continues to maintain these heterochromatin regions (Lachner et al., 2001).

In addition, H3K27me is correlated with gene inactivation and silencing (Barski et al., 2007). In contrast to other histone methylation events, only two enzymes (EZH1 and EZH2) methylate H3K27 and both are associated with the Polycomb Repressive Complexes (PRCs) (Abel et al., 1996). The PRC is responsible for transcriptional repression by ubiquitination of Histone H2A Lysine 119 (H2A119ub1) (Wang et al., 2004), recruitment of DNA methyltransferases (DNMTs) (Viré et al., 2006) and chromatin compaction (Francis et al., 2004). Thus with each of these types of regulation by different histone methylation events, metabolism offers several selective modes of interaction to mediate hi-

stone methylation and downstream consequences. For instance, a change in SAM levels could trigger a cascade that would propagate through the activity of the HMTs to the recruitment of readers to reach the end point of differential gene expression.

2.6 Histone Methyltransferases and Their Target Genes

Genetic studies in Drosophila identified two groups of genes that suppress and enhance the position-effect variegation phenotype, referred to as the trithorax (trx) and Polycomb (Pc) genes, respectively (Stassen et al., 1995; Tschiersch et al., 1994). Many of these genes encode proteins, which contain a SET domain. SET1, the first identified HMT with a SET domain was characterized in yeast and further studies identified the Complex of Proteins Associated with SET1 (COMPASS) (Miller et al., 2001; Krogan et al., 2002). In humans there are two homologous complexes that associate with SET1a and SET1b in addition to four COMPASS-like complexes that associate with MLL1-4 (Shilatifard, 2012).

SET1 is recruited to actively transcribed genes by an interaction at the C-terminal Domain (CTD) of RNAPII during elongation and is responsible for broader H3K4me3 marking across the gene (Ng et al., 2003; Wu et al., 2008). In humans, SET1a and SET1b localize to different euchromatic structures within the nucleus suggesting distinct roles in regulating gene expression (Lee et al., 2007). RNAi-mediated knockdown of Set1a decreased promoter H3K4me2 accompanied by decreased expression of oncogenes, Myc and BRCA1 (Nguyen et al., 2008).

The MLL family of histone methyltransferases was identified in humans be-

cause of their significant role in Leukemias (Krivtsov and Armstrong, 2007). MLL-1 is present at active promoters with 90% overlap with RNAPII suggesting a broad role in regulating active transcription (Guenther et al., 2005). In addition, ChIP-chip experiments suggest a specific role in regulating miRNAs and the late HoxA cluster (HoxA7, HoxA9, HoxA10, HoxA11, and HoxA13) (Guenther et al., 2005). In contrast, MLL-2 and MLL-3 do not alter bulk H3K4me3 after more than 80% knockdown (Hu et al., 2013). Instead, MLL-2 seems to functions at developmentally regulated genes with characteristic bivalent promoters marked by H3K27me3 and H3K4me3 including all four Hox gene clusters (Hu et al., 2013). ChIP-seq analysis of MLL4 demonstrated a unique subset of enhancers that are dynamically regulated by MLL4 mono- and dimethylation at different points during differentiation (Lee et al., 2013). MLL4 co-localizes with transcription factors (PPARγ and C/EBPs) that determine cell lineage during adipogenesis. In addition, deletion of MLL4 decreases H3K4me1, H3K4me2, RNAPII and Mediator occupancy at active enhancers.

H3K9 methyltransferases belong to the KMT1 family with the exception of PRDM2 (KMT8). Supressor of Variegation 3-9 Homolog 1 (SUV39H1) and 2 (SUV39H2) have redundant function and methylate pericentric regions to maintain chromatin organization (Peters et al., 2001). On the other hand, H3K9 Euchromatic Histone-Lysine N-Methyltransferase 2 (EHMT2/KMT1C) ChIP-seq data shows enrichment at developmental genes and co-localization with PRC2 at a subset of genes suggesting cross talk between H3K9me and H3K27me. Interestingly, co-localization of EHMT2 and PRC2 subunits are enriched at genes important in neuronal development. (Mozzetta et al., 2014) Lastly, H3K27 methylation occurs via EZH1 or EZH2. In mouse hair follicle, single mutants EZH1-/- or EZH2-/- showed no phenotypic difference, suggesting functional

redundancy as concluded by the authors. However a group of genes associated with cell cycle progression, cell death and regulation of biological/cellular processes had increased expression and decreased H3K27me2/3 after knockdown of EZH2 by siRNA (McCabe et al., 2012).

The activity of each of these enzymes is affected differently by the availability of methionine and status of one carbon metabolism. In each of the genetic studies, it is tempting to speculate that the observed phenotypes that demonstrate the requirements of each HMT would depend on the nutritional environment and metabolic status of the experimental background. For example, in conditions of SAM levels, one might observe different dependencies of different MLL enzymes with differential requirements on the maintenance of histone methylation. Furthermore, the target list of genes mediated by these enzymes may be grossly different in conditions of different one carbon metabolism since it is likely that the marks surrounding a given gene would not be altered in an identical manner to what would be observed in a neighboring gene. Comparative ChIP-seq analysis is likely to reveal new principles into how this specificity would be maintained.

2.7 Conclusions

While some HMTs appear to exhibit regulation of broad chromatin regions (ex. MLL1), most have demonstrated a preference for a subset of genes that are specifically regulated. Since the activity of each HMT is also governed by substrate availability (SAM or histone), gene specific regulation is likely altered under different metabolic conditions. For example, if the SAM concentration is

suppressed due to insufficient amounts of methionine and choline in the diet, this change in the intracellular concentration of SAM would in turn decrease the activity of a subset of methyltransferases based on SAM K_M values and other relevant kinetic parameters. In this regard, KMT2A (MLL1), with a K_M, SAM of 12.3μM, should be more affected by decreases in SAM than EZH1, with a K_M,SAM of 1.24μM. This could have specific consequences on gene expression. Since MLL1 is a general H3K4me3 methyltransferase, one might hypothesize an overall decrease in H3K4me3 deposition across the genome specifically at promoter regions while H3K27me3 is largely unaffected. The loss of H3K4me3 at promoters has been linked to decreases in Transcription Factor II D (TFIID) binding, an important player in Pol II recruitment, through its TAF3 subunit, ultimately leading to decreased gene expression (Vermeulen et al., 2007). Although there are many factors to consider in this regulation, mathematical modeling allows one to parse many simultaneous interactions and would be a useful tool to determine the contribution of each HMT to the regulation of global and specific gene expression. It will be important to determine how methionine metabolism is altered in different physiological states, (dieting, cancer, etc.), and the consequences on histone methylation and gene expression to determine the specificity of this sensing mechanism. Future work providing deeper mechanistic connections between metabolism and epigenetics will provide insight into the link between metabolic status, histone methylation and the effect on gene expression–whether transient or permanent–providing a molecular basis for how environmental factors, such as diet, can influence gene expression via cell metabolism.

LITERATURE CITED

Abel, K. J., Brody, L. C., Valdes, J. M., Erdos, M. R., Mckinley, D. R., Castilla, L. H., Merajver, S. D., Couch, F. J., Friedman, L. S., Ostermeyer, E. A., et al. (1996). Characterization ofezh1, a human homolog ofdrosophila enhancer of zestenearbrca1. *Genomics*, 37(2):161–171.

Bannister, A. J., Zegerman, P., Partridge, J. F., Miska, E. A., Thomas, J. O., Allshire, R. C., and Kouzarides, T. (2001). Selective recognition of methylated lysine 9 on histone h3 by the hp1 chromo domain. *Nature*, 410(6824):120–124.

Barski, A., Cuddapah, S., Cui, K., Roh, T.-Y., Schones, D. E., Wang, Z., Wei, G., Chepelev, I., and Zhao, K. (2007). High-resolution profiling of histone methylations in the human genome. *Cell*, 129(4):823–837.

Benayoun, B. A., Pollina, E. A., and Brunet, A. (2015). Epigenetic regulation of ageing: linking environmental inputs to genomic stability. *Nature Reviews Molecular Cell Biology*, 16(10):593–610.

Benayoun, B. A., Pollina, E. A., Ucar, D., Mahmoudi, S., Karra, K., Wong, E. D., Devarajan, K., Daugherty, A. C., Kundaje, A. B., Mancini, E., et al. (2014). H3k4me3 breadth is linked to cell identity and transcriptional consistency. *Cell*, 158(3):673–688.

Bernstein, B. E., Humphrey, E. L., Erlich, R. L., Schneider, R., Bouman, P., Liu, J. S., Kouzarides, T., and Schreiber, S. L. (2002). Methylation of histone h3 lys 4 in coding regions of active genes. *Proceedings of the National Academy of Sciences*, 99(13):8695–8700.

Birney, E., Stamatoyannopoulos, J. A., Dutta, A., Guigó, R., Gingeras, T. R., Margulies, E. H., Weng, Z., Snyder, M., Dermitzakis, E. T., Thurman, R. E., et al.

(2007). Identification and analysis of functional elements in 1% of the human genome by the encode pilot project. *Nature*, 447(7146):799–816.

Cabreiro, F., Au, C., Leung, K.-Y., Vergara-Irigaray, N., Cochemé, H. M., Noori, T., Weinkove, D., Schuster, E., Greene, N. D., and Gems, D. (2013). Metformin retards aging in c. elegans by altering microbial folate and methionine metabolism. *Cell*, 153(1):228–239.

Cantoni, G. L. (1953). S-adenosylmethionine; a new intermediate formed enzymatically from l-methionine and adenosinetriphosphate. *The Journal of biological chemistry*, 204(1):403–416.

Cao, R., Wang, L., Wang, H., Xia, L., Erdjument-Bromage, H., Tempst, P., Jones, R. S., and Zhang, Y. (2002). Role of histone h3 lysine 27 methylation in polycomb-group silencing. *Science*, 298(5595):1039–1043.

Chen, D., Ma, H., Hong, H., Koh, S. S., Huang, S.-M., Schurter, B. T., Aswad, D. W., and Stallcup, M. R. (1999). Regulation of transcription by a protein methyltransferase. *Science*, 284(5423):2174–2177.

Chen, K., Chen, Z., Wu, D., Zhang, L., Lin, X., Su, J., Rodriguez, B., Xi, Y., Xia, Z., Chen, X., et al. (2015). Broad h3k4me3 is associated with increased transcription elongation and enhancer activity at tumor-suppressor genes. *Nature genetics*.

Chin, H. G., Pradhan, M., Esteve, P. O., Patnaik, D., Evans, T. C., and Pradhan, S. (2005). Sequence specificity and role of proximal amino acids of the histone H3 tail on catalysis of murine G9A lysine 9 histone H3 methyltransferase. *Biochemistry*, 44(39):12998–13006.

Cynober, L. A. (2002). Plasma amino acid levels with a note on membrane transport: characteristics, regulation, and metabolic significance. *Nutrition*, 18(9):761–766.

De La Haba, G. and Cantoni, G. (1959). The enzymatic synthesis of s-adenosyl-l-homocysteine from adenosine and homocysteine. *Journal of Biological Chemistry*, 234(3):603–608.

Deguchi, T. and Barchas, J. (1971). Inhibition of transmethylations of biogenic amines by s-adenosylhomocysteine enhancement of transmethylation by adenosylhomocysteinase. *Journal of Biological Chemistry*, 246(10):3175–3181.

Dolinsky, T. J., Nielsen, J. E., McCammon, J. A., and Baker, N. A. (2004). Pdb2pqr: an automated pipeline for the setup of poisson–boltzmann electrostatics calculations. *Nucleic acids research*, 32(suppl 2):W665–W667.

Duncan, T. M., Reed, M., Nijhout, H. F., et al. (2013). The relationship between intracellular and plasma levels of folate and metabolites in the methionine cycle: A model. *Molecular nutrition & food research*, 57(4):628–636.

Feng, Q., Wang, H., Ng, H. H., Erdjument-Bromage, H., Tempst, P., Struhl, K., and Zhang, Y. (2002). Methylation of h3-lysine 79 is mediated by a new family of hmtases without a set domain. *Current Biology*, 12(12):1052–1058.

Finkelstein, J. D. (1990). Methionine metabolism in mammals. *The Journal of nutritional biochemistry*, 1(5):228–237.

Francis, N. J., Kingston, R. E., and Woodcock, C. L. (2004). Chromatin compaction by a polycomb group protein complex. *Science*, 306(5701):1574–1577.

Grandison, R. C., Piper, M. D., and Partridge, L. (2009). Amino-acid imbalance

explains extension of lifespan by dietary restriction in drosophila. *Nature*, 462(7276):1061–1064.

Guenther, M. G., Jenner, R. G., Chevalier, B., Nakamura, T., Croce, C. M., Canaani, E., and Young, R. A. (2005). Global and hox-specific roles for the mll1 methyltransferase. *Proceedings of the National Academy of Sciences of the United States of America*, 102(24):8603–8608.

Herz, H.-M., Mohan, M., Garruss, A. S., Liang, K., Takahashi, Y.-h., Mickey, K., Voets, O., Verrijzer, C. P., and Shilatifard, A. (2012). Enhancer-associated h3k4 monomethylation by trithorax-related, the drosophila homolog of mammalian mll3/mll4. *Genes & development*, 26(23):2604–2620.

Hoffman, D. R., Cornatzer, W. E., and Duerre, J. A. (1979). Relationship between tissue levels of s-adenosylmethionine, s-adenosylhomocysteine, and transmethylation reactions. *Canadian journal of biochemistry*, 57(1):56–64.

Horiuchi, K. Y., Eason, M. M., Ferry, J. J., Planck, J. L., Walsh, C. P., Smith, R. F., Howitz, K. T., and Ma, H. (2013). Assay development for histone methyltransferases. *Assay Drug Dev Technol*, 11(4):227–236.

Hu, D., Garruss, A. S., Gao, X., Morgan, M. A., Cook, M., Smith, E. R., and Shilatifard, A. (2013). The mll2 branch of the compass family regulates bivalent promoters in mouse embryonic stem cells. *Nature structural & molecular biology*, 20(9):1093–1097.

Huyen, Y., Zgheib, O., DiTullio Jr, R. A., Gorgoulis, V. G., Zacharatos, P., Petty, T. J., Sheston, E. A., Mellert, H. S., Stavridi, E. S., and Halazonetis, T. D. (2004). Methylated lysine 79 of histone h3 targets 53bp1 to dna double-strand breaks. *Nature*, 432(7015):406–411.

Koch, C. M., Andrews, R. M., Flicek, P., Dillon, S. C., Karaöz, U., Clelland, G. K., Wilcox, S., Beare, D. M., Fowler, J. C., Couttet, P., et al. (2007). The landscape of histone modifications across 1% of the human genome in five human cell lines. *Genome research*, 17(6):691–707.

Kraus, D., Yang, Q., Kong, D., Banks, A. S., Zhang, L., Rodgers, J. T., Pirinen, E., Pulinilkunnil, T. C., Gong, F., Wang, Y.-c., et al. (2014). Nicotinamide n-methyltransferase knockdown protects against diet-induced obesity. *Nature*, 508(7495):258–262.

Krivtsov, A. V. and Armstrong, S. A. (2007). Mll translocations, histone modifications and leukaemia stem-cell development. *Nature Reviews Cancer*, 7(11):823–833.

Krogan, N. J., Dover, J., Khorrami, S., Greenblatt, J. F., Schneider, J., Johnston, M., and Shilatifard, A. (2002). Compass, a histone h3 (lysine 4) methyltransferase required for telomeric silencing of gene expression. *Journal of biological chemistry*, 277(13):10753–10755.

Lachner, M., O'Carroll, D., Rea, S., Mechtler, K., and Jenuwein, T. (2001). Methylation of histone h3 lysine 9 creates a binding site for hp1 proteins. *Nature*, 410(6824):116–120.

Lee, J.-E., Wang, C., Xu, S., Cho, Y.-W., Wang, L., Feng, X., Baldridge, A., Sartorelli, V., Zhuang, L., Peng, W., et al. (2013). H3k4 mono-and di-methyltransferase mll4 is required for enhancer activation during cell differentiation. *Elife*, 2:e01503.

Lee, J.-H., Tate, C. M., You, J.-S., and Skalnik, D. G. (2007). Identification and

characterization of the human set1b histone h3-lys4 methyltransferase complex. *Journal of Biological Chemistry*, 282(18):13419–13428.

Locasale, J. W. (2013). Serine, glycine and one-carbon units: cancer metabolism in full circle. *Nature Reviews Cancer*, 13(8):572–583.

Locasale, J. W. and Cantley, L. C. (2011). Metabolic flux and the regulation of mammalian cell growth. *Cell metabolism*, 14(4):443–451.

McCabe, M. T., Ott, H. M., Ganji, G., Korenchuk, S., Thompson, C., Van Aller, G. S., Liu, Y., Graves, A. P., Diaz, E., LaFrance, L. V., et al. (2012). Ezh2 inhibition as a therapeutic strategy for lymphoma with ezh2-activating mutations. *Nature*, 492(7427):108–112.

Melnyk, S., Pogribna, M., Pogribny, I. P., Yi, P., and James, S. J. (2000). Measurement of plasma and intracellular s-adenosylmethionine and s-adenosylhomocysteine utilizing coulometric electrochemical detection: alterations with plasma homocysteine and pyridoxal 5?-phosphate concentrations. *Clinical Chemistry*, 46(2):265–272.

Mentch, S. J. and Locasale, J. W. (2016). One-carbon metabolism and epigenetics: understanding the specificity. *Ann. N. Y. Acad. Sci.*, 1363:91–98.

Mentch, S. J., Mehrmohamadi, M., Huang, L., Liu, X., Gupta, D., Mattocks, D., Padilla, P. G., Ables, G., Bamman, M. M., Thalacker-Mercer, A. E., et al. (2015). Histone methylation dynamics and gene regulation occur through the sensing of one-carbon metabolism. *Cell metabolism*, 22(5):861–873.

Miller, T., Krogan, N. J., Dover, J., Erdjument-Bromage, H., Tempst, P., Johnston, M., Greenblatt, J. F., and Shilatifard, A. (2001). Compass: a complex of pro-

teins associated with a trithorax-related set domain protein. *Proceedings of the National Academy of Sciences*, 98(23):12902–12907.

Mozzetta, C., Pontis, J., Fritsch, L., Robin, P., Portoso, M., Proux, C., Margueron, R., and Ait-Si-Ali, S. (2014). The histone h3 lysine 9 methyltransferases g9a and glp regulate polycomb repressive complex 2-mediated gene silencing. *Molecular cell*, 53(2):277–289.

Murray, K. (1964). The occurrence of iε-n-methyl lysine in histones. *Biochemistry*, 3(1):10–15.

Musselman, C. A., Lalonde, M.-E., Côté, J., and Kutateladze, T. G. (2012). Perceiving the epigenetic landscape through histone readers. *Nature structural & molecular biology*, 19(12):1218–1227.

Nakayama, J.-i., Rice, J. C., Strahl, B. D., Allis, C. D., and Grewal, S. I. (2001). Role of histone h3 lysine 9 methylation in epigenetic control of heterochromatin assembly. *Science*, 292(5514):110–113.

Ng, H. H., Robert, F., Young, R. A., and Struhl, K. (2003). Targeted recruitment of set1 histone methylase by elongating pol ii provides a localized mark and memory of recent transcriptional activity. *Molecular cell*, 11(3):709–719.

Nguyen, P., Bar-Sela, G., Sun, L., Bisht, K. S., Cui, H., Kohn, E., Feinberg, A. P., and Gius, D. (2008). Bat3 and set1a form a complex with ctcfl/boris to modulate h3k4 histone dimethylation and gene expression. *Molecular and cellular biology*, 28(21):6720–6729.

Noma, K.-i., Allis, C. D., and Grewal, S. I. (2001). Transitions in distinct histone h3 methylation patterns at the heterochromatin domain boundaries. *Science*, 293(5532):1150–1155.

Noma, K.-i. and Grewal, S. I. (2002). Histone h3 lysine 4 methylation is mediated by set1 and promotes maintenance of active chromatin states in fission yeast. *Proceedings of the National Academy of Sciences*, 99(suppl 4):16438–16445.

Ordovás, J. M. and Smith, C. E. (2010). Epigenetics and cardiovascular disease. *Nature Reviews Cardiology*, 7(9):510–519.

Patel, A., Vought, V. E., Swatkoski, S., Viggiano, S., Howard, B., Dharmarajan, V., Monteith, K. E., Kupakuwana, G., Namitz, K. E., Shinsky, S. A., Cotter, R. J., and Cosgrove, M. S. (2014). Automethylation activities within the mixed lineage leukemia-1 (MLL1) core complex reveal evidence supporting a "two-active site" model for multiple histone H3 lysine 4 methylation. *J. Biol. Chem.*, 289(2):868–884.

Patnaik, D., Chin, H. G., Esteve, P. O., Benner, J., Jacobsen, S. E., and Pradhan, S. (2004). Substrate specificity and kinetic mechanism of mammalian G9a histone H3 methyltransferase. *J. Biol. Chem.*, 279(51):53248–53258.

Peters, A. H., Mermoud, J. E., O'Carroll, D., Pagani, M., Schweizer, D., Brockdorff, N., and Jenuwein, T. (2002). Histone h3 lysine 9 methylation is an epigenetic imprint of facultative heterochromatin. *Nature genetics*, 30(1):77–80.

Peters, A. H., O'Carroll, D., Scherthan, H., Mechtler, K., Sauer, S., Schöfer, C., Weipoltshammer, K., Pagani, M., Lachner, M., Kohlmaier, A., et al. (2001). Loss of the suv39h histone methyltransferases impairs mammalian heterochromatin and genome stability. *Cell*, 107(3):323–337.

Pray-Grant, M. G., Daniel, J. A., Schieltz, D., Yates, J. R., and Grant, P. A. (2005). Chd1 chromodomain links histone h3 methylation with saga-and slik-dependent acetylation. *Nature*, 433(7024):434–438.

Psychogios, N., Hau, D. D., Peng, J., Guo, A. C., Mandal, R., Bouatra, S., Sinelnikov, I., Krishnamurthy, R., Eisner, R., Gautam, B., et al. (2011). The human serum metabolome. *PloS one*, 6(2):e16957.

Rea, S., Eisenhaber, F., O'Carroll, D., Strahl, B. D., Sun, Z.-W., Schmid, M., Opravil, S., Mechtler, K., Ponting, C. P., Allis, C. D., et al. (2000). Regulation of chromatin structure by site-specific histone h3 methyltransferases. *Nature*, 406(6796):593–599.

Roadmap, E., Kundaje, A., Meuleman, W., Ernst, J., Bilenky, M., Yen, A., Heravi-Moussavi, A., Kheradpour, P., Zhang, Z., Wang, J., et al. (2015). Integrative analysis of 111 reference human epigenomes. *Nature*, 518:317–330.

Shilatifard, A. (2012). The compass family of histone h3k4 methylases: mechanisms of regulation in development and disease pathogenesis. *Annual review of biochemistry*, 81:65.

Shiraki, N., Shiraki, Y., Tsuyama, T., Obata, F., Miura, M., Nagae, G., Aburatani, H., Kume, K., Endo, F., and Kume, S. (2014). Methionine metabolism regulates maintenance and differentiation of human pluripotent stem cells. *Cell metabolism*, 19(5):780–794.

Shyh-Chang, N., Locasale, J. W., Lyssiotis, C. A., Zheng, Y., Teo, R. Y., Ratanasirintrawoot, S., Zhang, J., Onder, T., Unternaehrer, J. J., Zhu, H., et al. (2013). Influence of threonine metabolism on s-adenosylmethionine and histone methylation. *Science*, 339(6116):222–226.

Stassen, M. J., Bailey, D., Nelson, S., Chinwalla, V., and Harte, P. J. (1995). The drosophila trithorax proteins contain a novel variant of the nuclear receptor

type dna binding domain and an ancient conserved motif found in other chromosomal proteins. *Mechanisms of development*, 52(2):209–223.

Stewart, M. D., Li, J., and Wong, J. (2005). Relationship between histone h3 lysine 9 methylation, transcription repression, and heterochromatin protein 1 recruitment. *Molecular and cellular biology*, 25(7):2525–2538.

Tang, X., Keenan, M. M., Wu, J., Lin, C.-A., Dubois, L., Thompson, J. W., Freedland, S. J., Murphy, S. K., and Chi, J.-T. (2015). Comprehensive profiling of amino acid response uncovers unique methionine-deprived response dependent on intact creatine biosynthesis. *PLoS Genetics*, 11(4):e1005158.

Taverna, S. D., Li, H., Ruthenburg, A. J., Allis, C. D., and Patel, D. J. (2007). How chromatin-binding modules interpret histone modifications: lessons from professional pocket pickers. *Nature structural & molecular biology*, 14(11):1025–1040.

Teperino, R., Schoonjans, K., and Auwerx, J. (2010). Histone methyl transferases and demethylases; can they link metabolism and transcription? *Cell metabolism*, 12(4):321–327.

Tschiersch, B., Hofmann, A., Krauss, V., Dorn, R., Korge, G., and Reuter, G. (1994). The protein encoded by the drosophila position-effect variegation suppressor gene su (var) 3-9 combines domains of antagonistic regulators of homeotic gene complexes. *The EMBO journal*, 13(16):3822.

Ulanovskaya, O. A., Zuhl, A. M., and Cravatt, B. F. (2013). Nnmt promotes epigenetic remodeling in cancer by creating a metabolic methylation sink. *Nature chemical biology*, 9(5):300–306.

van Ingen, H., van Schaik, F. M., Wienk, H., Ballering, J., Rehmann, H., Dechesne, A. C., Kruijzer, J. A., Liskamp, R. M., Timmers, H. T. M., and Boelens, R. (2008). Structural insight into the recognition of the h3k4me3 mark by the tfiid subunit taf3. *Structure*, 16(8):1245–1256.

Vermeulen, M., Mulder, K. W., Denissov, S., Pijnappel, W. P., van Schaik, F. M., Varier, R. A., Baltissen, M. P., Stunnenberg, H. G., Mann, M., and Timmers, H. T. M. (2007). Selective anchoring of tfiid to nucleosomes by trimethylation of histone h3 lysine 4. *Cell*, 131(1):58–69.

Viré, E., Brenner, C., Deplus, R., Blanchon, L., Fraga, M., Didelot, C., Morey, L., Van Eynde, A., Bernard, D., Vanderwinden, J.-M., et al. (2006). The polycomb group protein ezh2 directly controls dna methylation. *Nature*, 439(7078):871–874.

Wang, H., Wang, L., Erdjument-Bromage, H., Vidal, M., Tempst, P., Jones, R. S., and Zhang, Y. (2004). Role of histone h2a ubiquitination in polycomb silencing. *Nature*, 431(7010):873–878.

Wang, J., Alexander, P., Wu, L., Hammer, R., Cleaver, O., and McKnight, S. L. (2009). Dependence of mouse embryonic stem cells on threonine catabolism. *Science*, 325(5939):435–439.

Wellen, K. E. and Thompson, C. B. (2010). Cellular metabolic stress: considering how cells respond to nutrient excess. *Molecular cell*, 40(2):323–332.

Wu, M., Wang, P. F., Lee, J. S., Martin-Brown, S., Florens, L., Washburn, M., and Shilatifard, A. (2008). Molecular regulation of h3k4 trimethylation by wdr82, a component of human set1/compass. *Molecular and cellular biology*, 28(24):7337–7344.

Xiao, B., Jing, C., Wilson, J. R., Walker, P. A., Vasisht, N., Kelly, G., Howell, S., Taylor, I. A., Blackburn, G. M., and Gamblin, S. J. (2003). Structure and catalytic mechanism of the human histone methyltransferase set7/9. *Nature*, 421(6923):652–656.

Yun, J., Johnson, J. L., Hanigan, C. L., and Locasale, J. W. (2012). Interactions between epigenetics and metabolism in cancers. *Frontiers in oncology*, 2:163.

CHAPTER 3

REGULATION OF HISTONE METHYLATION VIA METHIONINE METABOLISM[1]

3.1 Summary

S-adenosylmethionine (SAM) and S-adenosylhomocysteine (SAH) link one carbon metabolism to methylation status. However, it is unknown whether regulation of SAM and SAH by nutrient availability can be directly sensed to alter the kinetics of key histone methylation marks. We provide evidence that the status of methionine metabolism is sufficient to determine levels of histone methylation by modulating SAM and SAH. This dynamic interaction led to rapid changes in H3K4me3, altered gene transcription, provided feedback regulation to one carbon metabolism, and could be fully recovered upon restoration of methionine. Modulation of methionine in diet led to changes in metabolism and histone methylation in the liver. In humans, methionine variability in fasting serum was commensurate with concentrations needed for these dynamics and could be partly explained by diet. Together these findings demonstrate that flux through methionine metabolism and the sensing of methionine availability may allow direct communication to the chromatin state in cells.

[1]This chapter has been adapted from our recent publication, Mentch, et al., *Cell Metabolism*, (2015). (Mentch et al., 2015)

3.2 Introduction

Alterations in the methylation status of proteins, nucleic acids, and metabolites contribute to the pathogenesis of many of the major human pathophysiological conditions including cancer, obesity, and aging (Bergman and Cedar, 2013; Greer and Shi, 2012; Kraus et al., 2014). When these changes affect the methylation of histones and nucleic acids that determine the epigenetic status in cells, they can affect the expression of thousands of genes (Barth and Imhof, 2010). Changes in methylation status occur due to differences in the enzyme activity of methyltransferases and demethylases. Genes that encode these enzymes are frequently altered in pathological states leading to alterations in methylation (Chi et al., 2010; Dawson and Kouzarides, 2012). It has also been long established that S-adenosylmethionine (SAM) is the universal methyl donor for these enzymes that transfer its methyl group to yield S-adenosylhomocysteine (SAH) and a methylated substrate (Finkelstein, 1990). The methylation of this substrate provides a link between the metabolism that regulates SAM and SAH, which may act through product inhibition of a methyltransferase, and the epigenetic status of cells (Gut and Verdin, 2013; Katada et al., 2012; Teperino et al., 2010).

SAM and SAH are intermediate metabolites in a metabolic pathway that is a subset of a larger network collectively referred to as one carbon metabolism (Locasale, 2013). One carbon metabolism integrates nutrients from diverse sources such as glucose, serine, threonine, methionine, and choline and processes them into distinct outputs that achieve diverse biological functions. Whether the concentrations of SAM and SAH or their ratio ever reach physiological values that could affect methyltransferase activity has been controversial. Some studies

have concluded that their concentrations do not reach limiting values (Hoffman et al., 1979). Recent studies however have provided evidence that under pathological conditions aberrant expression of NNMT, an enzyme that metabolizes SAM, has profound biological consequences resulting from changes in histone methylation (Kraus et al., 2014; Ulanovskaya et al., 2013). Others have found that only the levels of SAH correlated with methylation status including a recent finding that investigated threonine metabolism in mouse pluripotent stem cells that demonstrated threonine catabolism affected both pyruvate and glycine metabolism and altered histone methylation (Shyh-Chang et al., 2013). Although this study was the first to our knowledge to document the influence of an amino acid on histone methylation, this effect was shown to occur through indirect pathways involving energy production and acetyl-coA metabolism. Further studies have demonstrated in human pluripotent stem cells that a depletion of methionine that is the precursor to SAM could lead to changes in histone methylation (Shiraki et al., 2014). However, these changes are also accompanied by widespread induction of stress response pathways and cell death confounding the interpretation of whether the changes in histone methylation occurred directly through the sensing of SAM/SAH status.

Given these previous findings, we hypothesized that there exists a direct mechanism whereby the status of one carbon metabolism could alter the concentrations of SAM and SAH to confer, through their interaction with methyltransferases, the output of a defined methylation state. We focused on histones since key methylation modifications on their tails such as trimethylation at Lysine 4 are known to be required for the maintenance of defined cellular states (Benayoun et al., 2014; Ruthenburg et al., 2007) and have been shown to be modulated by metabolism (Shiraki et al., 2014; Shyh-Chang et al., 2013). We

provide evidence in cells and mice that both SAM levels and the SAM/SAH ratio can be quantitatively tuned through changes in the metabolic flux of the methionine cycle to affect a critical component of chromatin status. This regulation occurred at physiologically relevant concentrations and appeared to control numerous physiological processes including direct feedback regulation for the maintenance of homeostasis in one carbon metabolism and the activity of genes involved in cancer and cell fate. Together these findings are consistent with a model whereby the status of one carbon metabolism is in communication with the chromatin state of cells through its ability to modify the kinetics of enzymes that mediate histone methylation.

3.3 Results

3.3.1 Methionine Metabolism Quantitatively Affects Histone Methylation

Since methionine is the closest substrate in the methionine cycle and one carbon metabolism that affects SAM levels, we therefore tested whether cells depleted of methionine have alterations in the methionine cycle and whether this would confer effects on the methylation of histones. We generated a media formulation in which methionine was restricted from the culture media. HCT116 cells were placed in this methionine restricted (3μM) media for 24 hours. We then utilized a liquid chromatography, high-resolution mass spectrometry (LC-HRMS) metabolomics technology we have recently developed (Liu et al., 2014a,b) to generate a quantitative profile of over 300 metabolites in response to methion-

ine restriction that is visualized in a volcano plot (Figure 3.1A). It was found that metabolites in the methionine cycle exhibited dramatic changes in their concentrations with only moderate compensation from other pathways that fuel the one carbon cycle (Figure 3.1B).

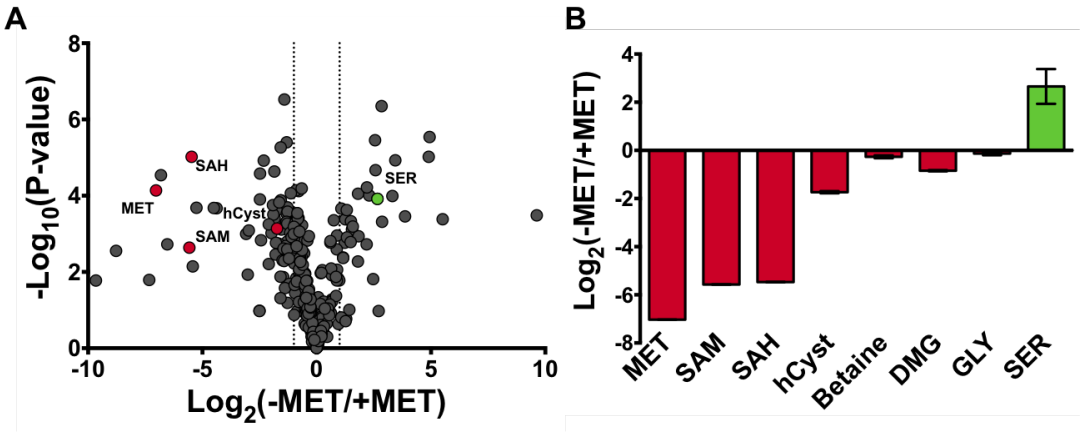

Figure 3.1: Metabolic Alterations After Methionine Restriction

(A) Metabolomics profile of HCT116 cells after 24 hours of methionine restriction. Log_2 change versus -log_10(p-value), Student's two-tailed t-test, n=3. (B) Effects of methionine restriction on one carbon cycle metabolism.

Notably, both SAM and SAH are depleted under these conditions.

To test whether these alterations were sufficient to induce changes in histone methylation, we considered the relative levels of several histone methylation marks involving trimethylation at lysines 4,9, 27 that are each known to have substantial roles defining chromatin states, most notably at active and inactive genes, and mediating gene expression (Shilatifard, 2006) (Figure 3.2).

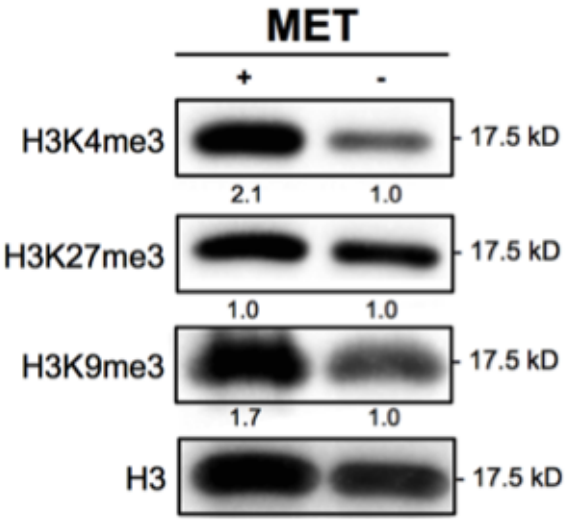

Figure 3.2: Histone Methylation Depleted After Methionine Restriction

Nuclear extracts from methionine restricted HCT116 cells were blotted for H3K4me3, H3K9me3, and H3K27me3 and imaged using a ChemiDoc. Band intensities are normalized to total H3 and fold change was calculated.

In addition, the kinetic properties, such as SAM binding affinity (K_M), of these histone methyltransferases (An et al., 2011; Chin et al., 2005; Horiuchi et al., 2013; Obianyo et al., 2008; Patnaik et al., 2004; Xiao et al., 2003) suggests SAM concentration may play a role in their regulation and directly affect the rate of histone methylation reactions in the cell (Figure 3.3).

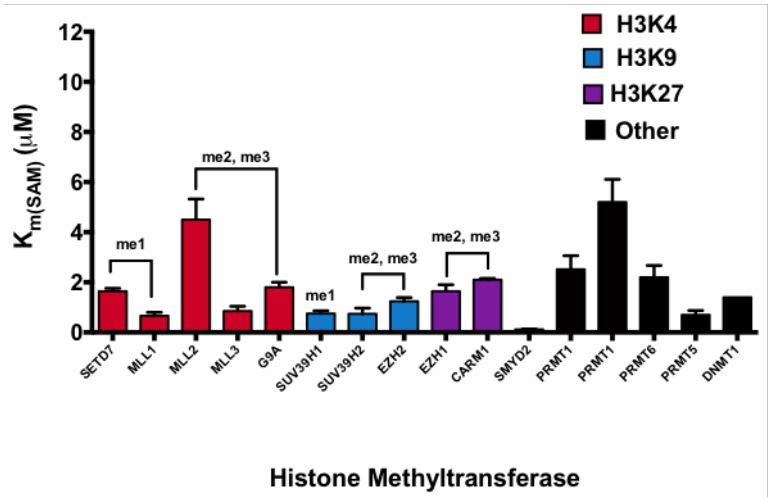

Figure 3.3: Published Histone Methyltransferase K_M Parameters

Published histone methyltransferase kinetic parameters from several sources categorized by histone substrate (H3K4, H3K9, and H3K27) or other.

Each modification exhibited decreased methylation with trimethylation at lysine 4 on histone H3 (H3K4me3) exhibiting the largest change. To investigate whether these changes were specific to methionine restriction, we considered the removal of several other amino acids (W, Q, K, H, L) that include essential amino acids and glutamine that has been shown to be essential for cell proliferation (Figure 3.4).

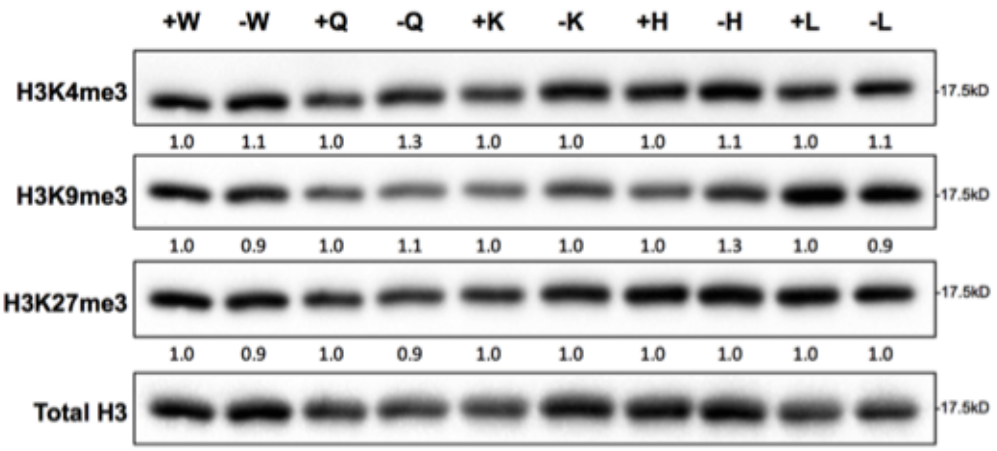

Figure 3.4: No Significant Changes in Histone Methylation after Individual Essential Amino Acid Restriction

HCT116 cells were grown in conditional media lacking one of five essential amino acids (W, Q, K, H, or L) and western blot was used to determine the change in histone methylation. Bands were normalized to total H3 protein and a fold change was calculated for each amino acid deprivation experiment.

We found that in each case no change in histone methylation was observed. To further test the generality of this observation, we considered the response of H3K4me3 to methionine restriction on a panel of six human cell lines subjected to methionine restriction for 24 hours (Figure 3.5A). Metabolomics across the cell panel revealed methionine cycle metabolism and purine and pyrimidine metabolism decreased significantly for all cell lines (Figure 3.5B). In addition, fatty acid metabolism and serine/glycine metabolism significantly increased across all cell lines tested (Figure 3.5C).

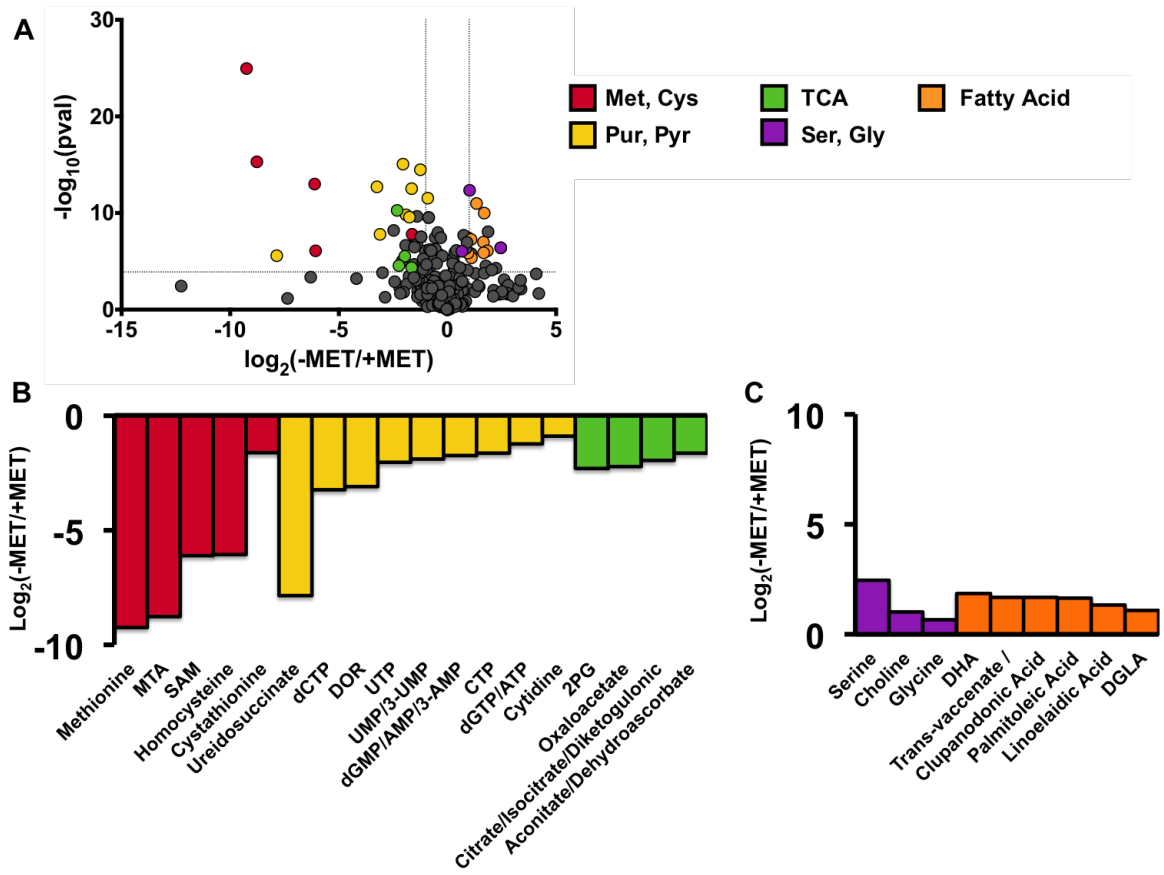

Figure 3.5: Metabolic Response to Methionine Restriction in Colon Cancer Cell Line Panel

After 24 hours of methionine restriction, metabolites were collected from a panel of colon cancer cell lines (SQ620, SW480, HCT8, HT29, HCT116, NCI-H5087) and metabolomics was performed. (A) Volcano plot highlighting metabolic modules that are significantly altered after methionine restriction. Log_2 change versus -Log_{10}(p-value), Student's two-tailed t-test using Holm-Sidak multiple testing correction procedure, $\alpha = 0.5$, n = 18. Significant pathway enrichment determined using MetaboAnalyst. (B) Metabolites that are significantly decreased after methionine restriction. (C) Metabolites that are significantly increased after methionine restriction. Methionine & Cysteine Metabolism (Met, Cys); Tricarboxylic Acid Cycle (TCA); Purine & Pyrimidine Metabolism (Pur, Pyr); Serine & Glycne Metabolism (Ser, Gly).

Next, we tested how H3K4me3 responded to methionine restriction across the cell line panel. In each case, H3K4me3 was responsive to methionine restriction (Figure 3.6).

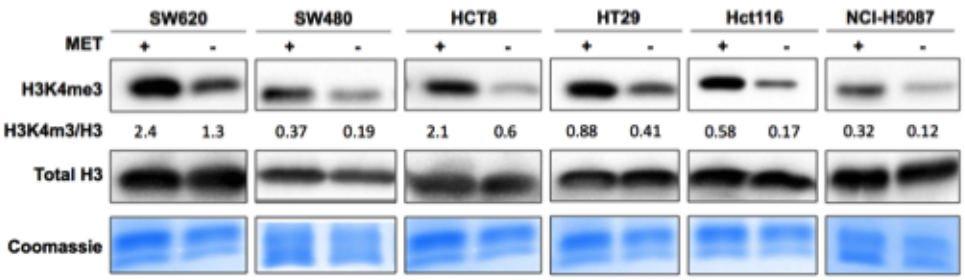

Figure 3.6: Colon Cancer Cell Line Panel Response to Methionine Restriction

After 24 hours of methionine restriction, histone lysates from a panel of colon cancer cell lines were collected and blotted for histone methylation marks and imaged using a ChemiDoc. Band intensities were normalized to total H3. Coomassie staining of total protein input is shown as a loading control.

Having shown that extreme restriction of methionine is sufficient to alter histone methylation, we investigated the concentration of methionine needed to achieve this effect. We considered a titration of differing concentrations of methionine in the culture media ranging from 3 to 500 μM. The relative levels of the methionine cycle and one carbon metabolism-related metabolites including methionine, SAM, SAH, homocysteine, betaine, and dimethylglycine (DMG) were measured (Figure 3.7A). It was found that the levels of these intermediates exhibited a graded response to changes in methionine concentration in the media. SAM and SAH were altered at concentrations below 25 μM - concentrations well below those present in typical culture media. We next investigated the dose response of changes in histone methylation to changes in methionine availability (Figure 3.7B). Histone methylation responded differently to differing concentrations of methionine. H3K4me3 was affected at concentrations between 10 and 25 μM consistent with concentrations needed to deplete SAM and SAH in the methionine cycle.

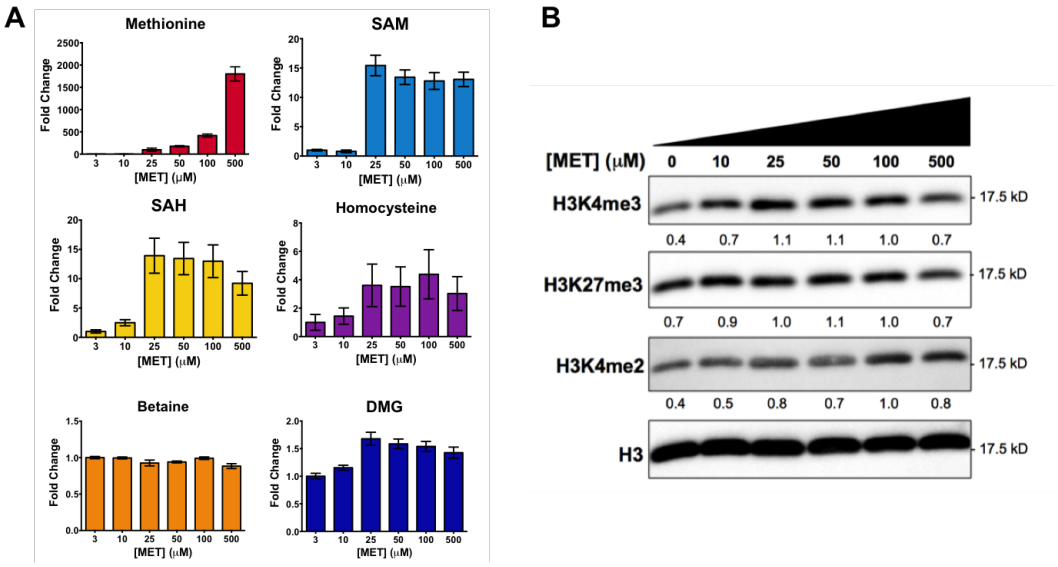

Figure 3.7: The Effects of Methionine Concentration on the Methionine Cycle and Histone Methylation

(A). Relative concentrations of methionine cycle metabolites in cells cultured at different concentrations of methionine. (B) Concentration-dependent effects of methionine restriction on histone methylation. Data are normalized to the 100μM condition.

One possibility is that these changes were due to non-specific effects on cell proliferation. We therefore considered the effects of methionine restriction on cell proliferation over a course of three days (Figure 3.8A, 3.8B). At low concentrations of methionine, there were marked defects in cell morphology and cell proliferation but no activation of p53 when H3K4me3 is changing (Figure 3.8B, 3.8C) indicating that H3K4me3 dynamics occur before a cellular stress response. At 10 μM, cells remained viable with no gross alterations in morphology and only a modest decrease in cell proliferation that was fully recoverable at 25 μM confirming that the changes in histone methylation are not likely due to defects in cell proliferation. Together these findings demonstrate that methionine affects histone methylation and the dynamics of the methionine cycle.

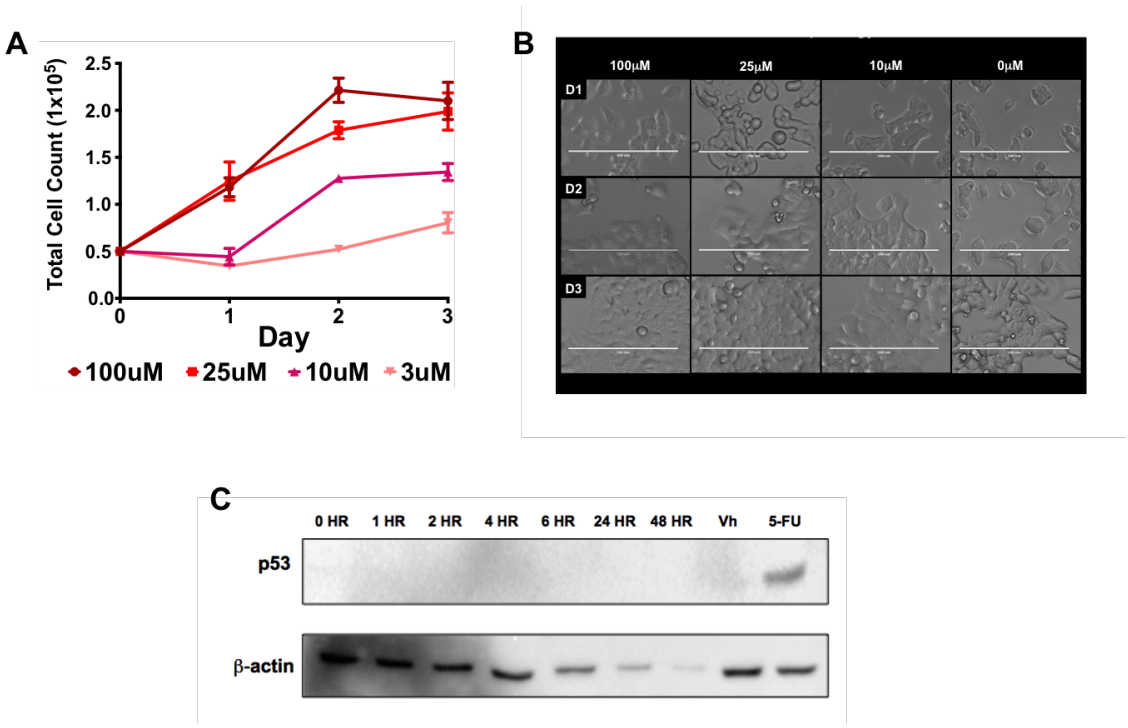

Figure 3.8: The Effects of Methionine Concentration on Cell Growth and Morphology

(A) HCT116 cell proliferation at different levels of methionine. All error bars are computed from standard error of measurement (n=3).(B) Cell morphology in response to different levels of methionine restriction at different days. (C) p53 response after methionine restriction or 5-FU treatment in HCT116 cells.

3.3.2 Methionine Cycle and Histone Methylation Dynamics in Response to Methionine Restriction

Having observed alterations in the methionine cycle and concomitant changes in histone methylation, we sought to understand the dynamics of the process and its connection to cellular metabolism. We reasoned that the kinetics could provide further insights into how changes in metabolism alter histone methylation. We considered the metabolic dynamics of methionine restriction across

twelve time points (0, 5, 15, 30, 60, 90, 120, 240, 360, 540, 720, and 1440 minutes) from very early time up to times leading to cell death (Figure 3.9A). At each of these time points, we profiled over 300 metabolites spanning pathways across central carbon and secondary metabolism. A hierarchical clustering of the time course revealed coordinated dynamics across the metabolome in response to methionine restriction. Waves of coordinated changes that involve different metabolic pathways were observed.

We utilized a recently developed algorithm for assessing the contribution to different pathways (i.e. pathway impact) defined by the Kyoto Encyclopedia of Genes and Genomes (KEGG) (Xia and Wishart, 2010) (Figure 3.9B). Pathway impact is computed by considering a weighted score of each metabolite with greater weights being assigned to metabolites that are centrally located in a given metabolic pathway. At early times, a module related to cysteine and methionine metabolism exhibited decreasing dynamics that were sustained across the time course. At intermediate times alterations in metabolites belonging to phenylalanine, tryptophan, and lysine metabolism were observed. At later times arginine and proline metabolism appeared altered together suggesting that a complex compensatory amino acid response at later times occurs after the primary response to methionine restriction.

A further inspection of the module related to methionine cycle dynamics revealed that within minutes of methionine restriction, methionine is depleted within cells (Figure 3.9C). SAM levels exhibited a decay that occurred within an hour (Figure 3.9D). SAH levels exhibited more complex behavior involving a fast decrease, a recovery at two hours and a later decrease (Figure 3.9E). These dynamics are likely due to additional pathways such as remethylation from one

carbon metabolism, methionine salvage, and flux into the transsulfuration pathway. These changes contributed to complicated dynamics of the SAM/SAH ratio that decreased at two hours (Figure 3.9F).

We next monitored the dynamics of histone methylation to assess its interaction with metabolic dynamics. We considered the dynamics of the levels of H3K4/9/27 in response to methionine restriction (Figure 3.9G,H). Surprisingly, it was found that within two to four hours, a depletion of histone methylation was observed. These kinetics exhibited only a one to two hour lag between depletion of the methionine cycle and the subsequent changes in histone methylation. These dynamics are generally too short for a transcriptional or translational regulatory response. Together these findings conclude that the dynamics of methionine metabolism result primarily in amino acid compensatory responses and not general features that result in disruption of cell proliferation. They also indicate that methionine dynamics can be coordinately sensed by histones to determine the levels of histone methylation.

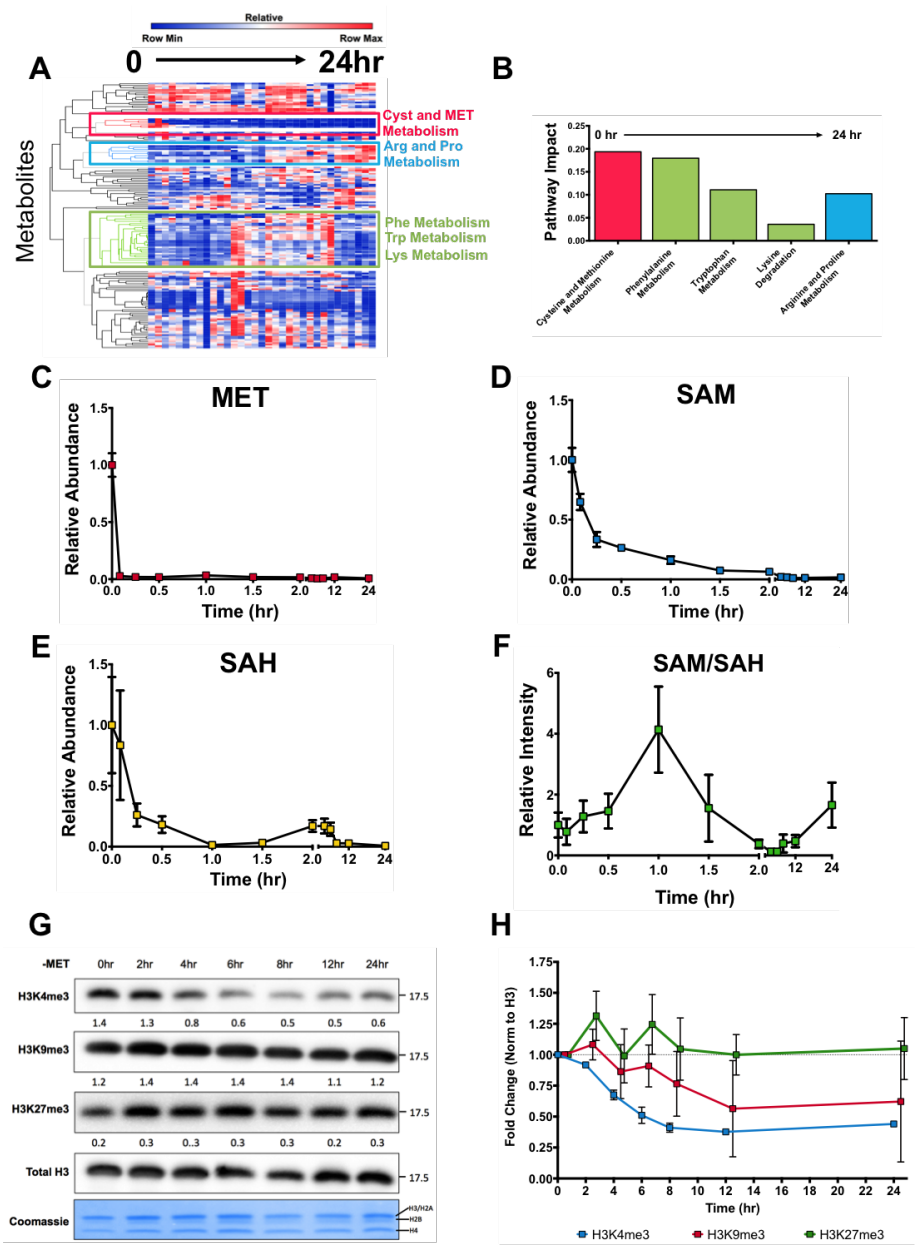

Figure 3.9: Histone Methylation is Dynamically Regulated by Methionine Metabolism

(A) Global metabolic dynamics in response to methionine restriction over a 24 hour time course. (B) Pathway analysis of methionine cycle dynamics show in (A). (C) Dynamics of methionine over 24 hours of methionine restriction. (D) Dynamics of SAM over 24 hours of methionine restriction. (E) Dynamics of SAH over 24 hours of methionine restriction. (F) Dynamics of the SAM/SAH ratio over 24 hours of methionine restriction. (G) Dynamics of histone methylation in response to methionine restriction over 24 hours. (H) Quantification of results in (G) and two other independent experiments. Integrated intestines are normalized to total H3, and the fold change represents the differences compared with 24 hours. All error bars are computed from SEM (n=3).

3.3.3 Methionine Metabolism and Histone Methylation Dynamics Are Reversible

Thus far we have shown that methionine metabolism can induce alterations in histone methylation levels and that this effect is dynamic and occurs on time scales consistent with that of a direct sensing mechanism. Another necessary requirement of such a signal transduction mechanism is that the dynamics are reversible. We therefore questioned whether metabolism and histone methylation can be recovered after methionine restriction. Cells were subjected to methionine restriction for 24 hours (between day 1 and day 2) at which point we allowed the cells to be cultured for an additional 24 hours in media containing the full concentration of methionine (between day 2 and day 3) (Figure 3.10).

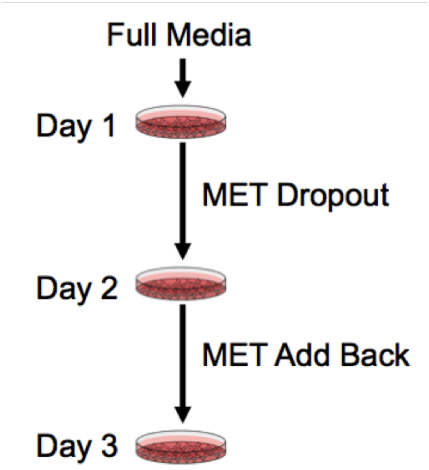

Figure 3.10: Methionine Cycle Rescue

Experimental setup of methionine restriction and recovery. HCT116 cells were grown in -MET media for 24 hours then switched to +MET media for an additional 24 hours. Samples were collected on day 1, day 2 (MET dropout), and day 3 (MET rescue).

We carried out metabolomics at each time point as considered previously (Figure 3.11A). Hierarchical clustering of each profile revealed marked changes

across the metabolic network at days 1, 2, and 3. The gross measured differences in metabolism from day 1 and day 3 revealed that overall metabolism is not reversible under these conditions. An assessment of the pathways involved indicated that several amino acid metabolism pathways were not recoverable at 3 days (Figure 3.11B). Of the pathways recovered after reincorporation of methionine into the culture media, cysteine and methionine metabolism was one of three pathways shown to be reversible. This effect is illustrated in Figure 3.11C where the methionine cycle is plotted and for each metabolite in the cycle, some recovery of its concentration and the concentration of the metabolites in its salvage and the transsulfuration pathways (Figure 3.11D, E) was observed. To investigate whether these dynamics correlate with histone methylation we measured histone methylation levels (Figure 3.11F) and found that methylation levels exhibited a concomitant recovery back to levels observed in the original culture conditions.

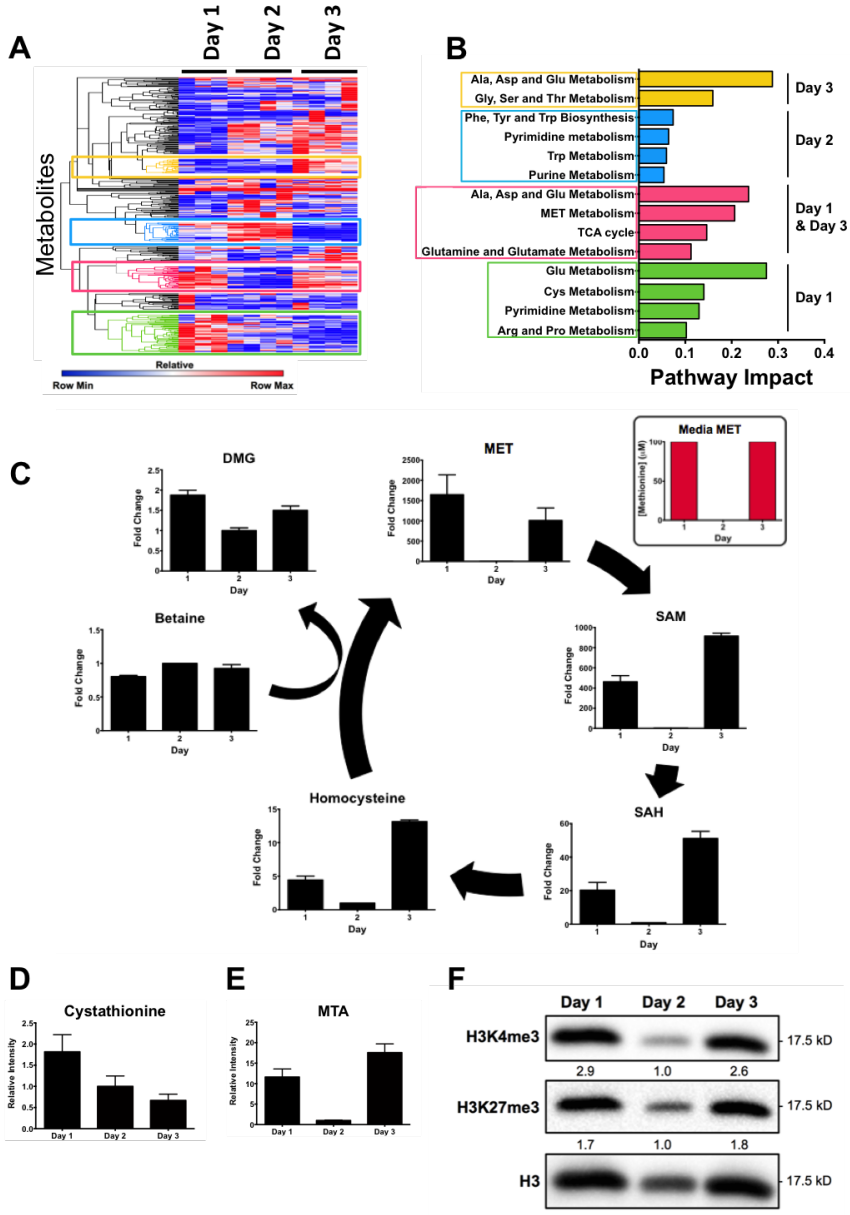

Figure 3.11: Histone Methylation and Methionine Cycle Dynamics are Reversible

(A) Effects of methionine restriction and recovery on global metabolism. (B) Metabolic pathway analysis of methionine restriction and recovery. (C) Effects of methionine restriction and recovery on methionine cycle metabolism. (D) Effects of methionine restriction and recovery on the methionine salvage pathway (MTA). (E) Effects of methionine restriction and recovery on the transsulfuration pathway (cystathionine). (F) Response of histone methylation to methionine restriction and recovery. Integrated intensities are normalized to total H3 and fold change was calculated. All error bars are computed from the SEM (n=3).

Together these findings indicate that the methionine cycle is reversible even when the remainder of global metabolism is altered. Furthermore, these results show that the recovery of the levels of the metabolites in the methionine cycle is sufficient to restore the levels of histone methylation.

3.3.4 Methionine Restriction Decreases H3K4me3 Signature Peaks and Alters Gene Expression

Although results from immunoblotting identified global alterations in histone methylation after methionine restriction, it remained unclear whether methionine metabolism affected specific marks on the genome to mediate gene expression. We therefore sought to determine the precise location H3K4me3 on the genome using chromatin immunoprecipation with sequencing (ChIP-seq) and the consequences on gene expression using RNA-sequencing (RNA-seq). The sensitivity was first confirmed using serial titrations of H3K4me3 peptides (Figure 3.12A) and the specificity of the H3K4me3 antibody was tested with modified histone peptide array (Figure 3.12B, C) as suggested in the ENCODE guidelines (Bailey et al., 2013). From these results we conclude that the H3K4me3 antibody is sensitive and specific for H3K4me3. There was little off target reactivity and binding was not significantly altered when H3K4me3 was present on H3 peptides with other post-translational modifications (except phosphorylation).

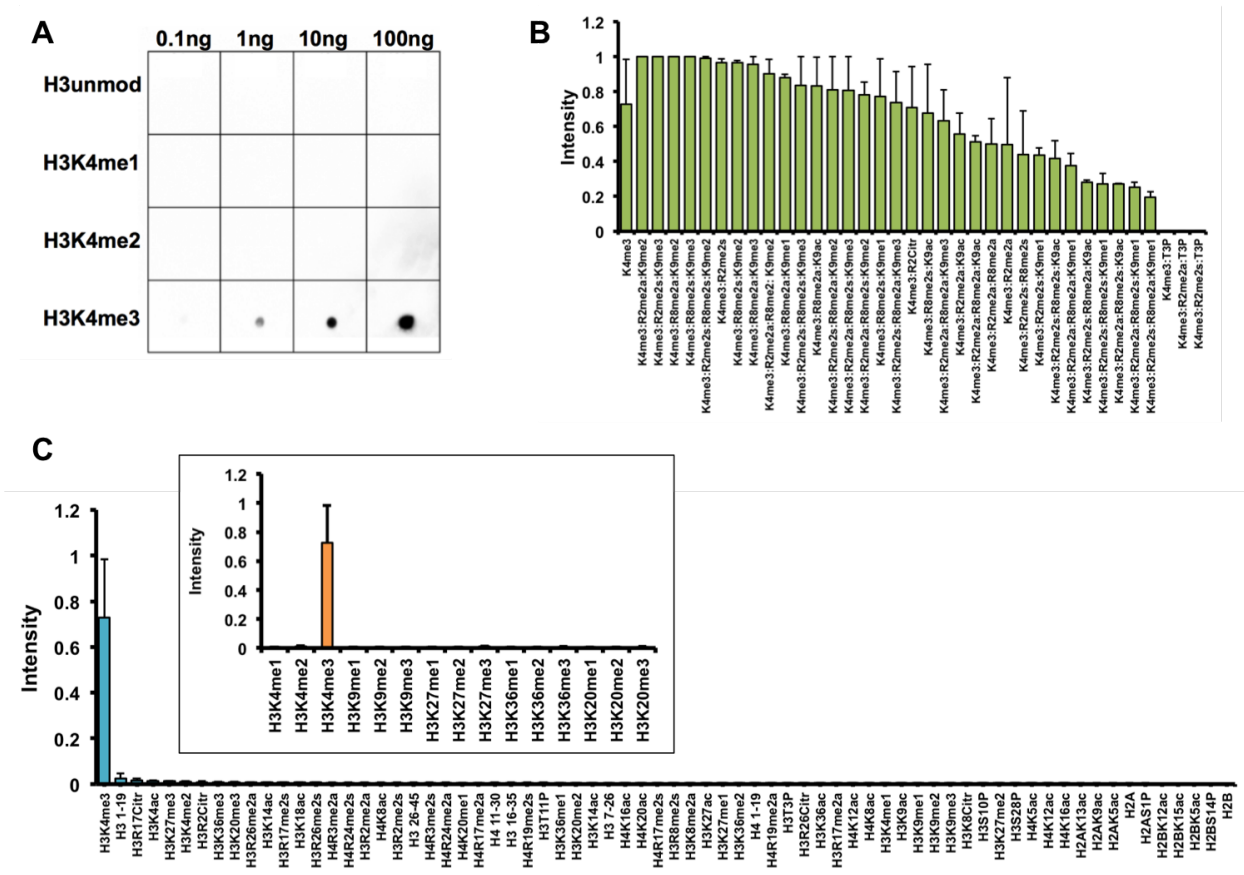

Figure 3.12: H3K4me3 Antibody Specificity

(A) Dot blot using H3K4me3 ChIP-seq antibody with unmodified and modified histone peptides at varying concentrations. (B) H3K4me3 ChIP-seq antibody reactivity ranked high to low for peptides with H3K4me3 plus up to three additional modifications on the same peptide. (C) H3K4me3 ChIP-seq antibody reactivity ranked high to low for individual histone modifications. Inset shows ChIP-seq antibody reactivity for H3K4me1/2/3, H3K9me1/2/3 and H3K27me1/2/3. ChIP-seq antibody reactivity was measured using the Active Motif MODified Histone Peptide Array (cat #13001).

Cells were subjected to methionine restriction (-MET) or normal methionine (+MET) conditions for 24 hours and cross-linked chromatin was collected for H3K4me3 ChIP-seq analysis with total RNA collected for RNA-seq in parallel. After peak calling (methods), replicate samples for the +MET and -MET conditions cluster together suggesting the genome-wide profile of H3K4me3 marks

are similar between replicates but vastly different between the conditions (Figure 3.13).

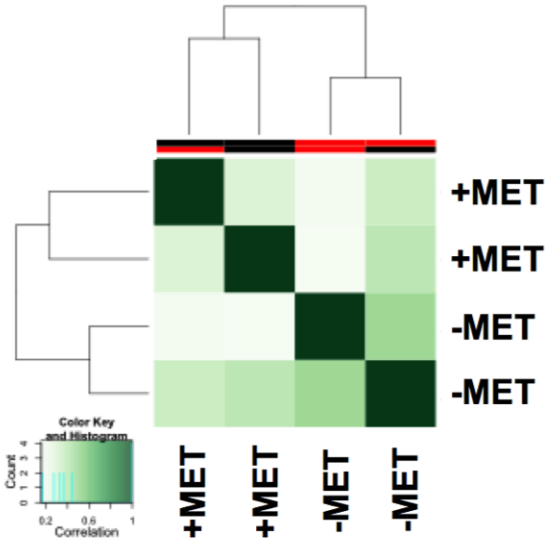

Figure 3.13: Replicates Cluster Together Based on MACS2 H3K4me3 Called Peaks

H3K4me3 ChIP-seq was performed in +MET and -MET conditions after 24 hours. Hierarchical clustering was performed on replicates using peaks called from MACS2.

Next, we investigated the change in H3K4me3 peaks at the transcription start site (TSS) of genes, since H3K4me3 at gene promoters has been associated with gene transcription. Overall, we found that the H3K4me3 peaks around the TSS are bimodal and decrease, on average, after methionine restriction (Figure 3.14A). In addition, H3K4me3 peaks decreased breadth after methionine restriction (Figure 3.14B) but no significant change in H3K4me3 binding site distribution around the TSS was observed (Figure 3.14C). Next, peak counts were plotted for each chromosome showing H3K4me3 peak distribution across the genome is relatively consistent (Figure 3.14D). Closer inspection of individual chromosomes revealed that particular genomic regions are differentially marked by H3K4me3.

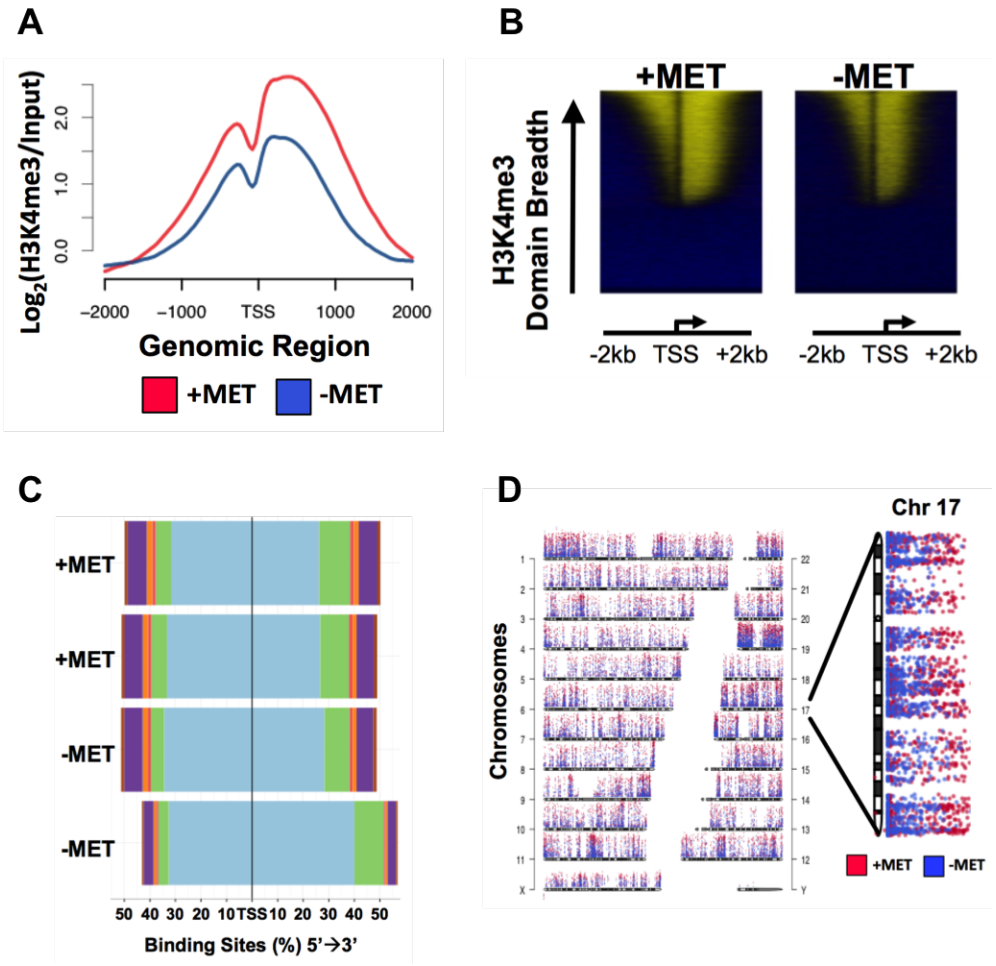

Figure 3.14: ChIP-seq Reveals Global Reductions in H3K4me3 at TSSs

(A) Change in H3K4me3 distribution around the TSS after 24 hours of methionine restriction. (B) Change in H3K4me3 TSS domain breadth after 24 hours of methionine restriction. (C) Genome-wide binding site affinity from the TSS after methionine restriction. (D) Genome-wide distribution of H3K4me3 peaks in +MET (red) and -MET (blue) conditions with an enlargement of chromosome 17.

To determine those H3K4me3 peaks that were lost or gained in response to methionine restriction, peaks from both replicates in each condition were used to make a consensus peak set containing all peaks in both +MET or -MET (see Appendix B). This method removed peaks that were only present in one replicate. Overall, a total of 27,235 peaks were identified (Figure 3.15A). Out of all the peaks identified, most peaks, not surprisingly, were found in introns (Fig-

ure 3.15B), since introns make up 37% of the human genome. Taking the distribution of genomic features into consideration, H3K4me3 peaks were enriched at the beginning of genes at the promoter and 5'UTR (Figure 3.15C). Finally, we investigated where peaks were lost or gained in response to methionine deprivation. A total of 6,457 peaks were lost after methionine restriction and 184 peaks were gained. Of these, most peaks were lost at promoters (33%) (Figure 3.15D). Those peaks that appeared after methionine restriction were found at intergenic regions (57%) (Figure 3.15E).

For each peak, the closest gene was identified using the Homer Software Suite (see Appendix B). No significant gene set enrichment was observed for genes closest to H3K4me3 peaks gained after methionine restriction. Note though most peaks gained after methionine restriction occur in the intergenic regions. For peaks lost during methionine restriction in HCT116 cells we focused on loss at the promoter regions. Gene enrichment analysis confirmed promoters of genes that lost H3K4me3 after methionine restriction in our study overlapped well with known genes with H3K4me3 present at the promoter in HCT116 cells from ENCODE (adjusted $p = 2.5 \times 10^{-38}$). In addition, many peaks were lost at genes involved in Wnt signaling, GTPase activity, and CTCF binding.

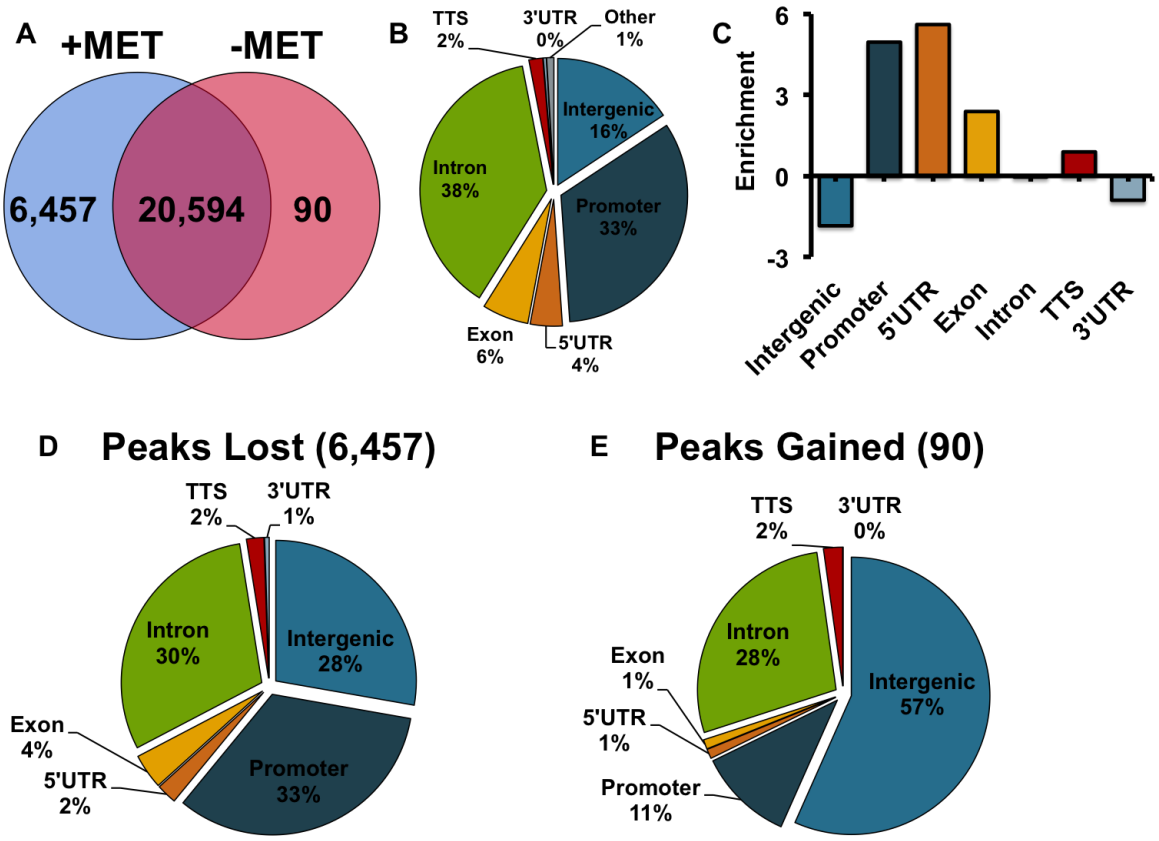

Figure 3.15: Genomic Distribution of H3K4me3 in Response to Methionine Restriction

(A) H3K4me3 peaks called by MACS2 before and after methionine restriction. (B) Percent of all H3K4me3 peaks found in each genomic region. (C) Enrichment of H3K4me3 peaks in each genomic region. (D) Percent of H3K4me3 peaks lost after methionine restriction found in each genomic region. (E) Percent of H3K4me3 peaks gained after methionine restriction found in each genomic region.

Since promoter H3K4me3 is a signature for active transcription we further investigated how decreased H3K4me3 at promoters affects gene transcription. To this end we performed RNA-seq (Figure 3.16) under methionine-restricted conditions in HCT116 cells and compared these results to our ChIP-seq analysis.

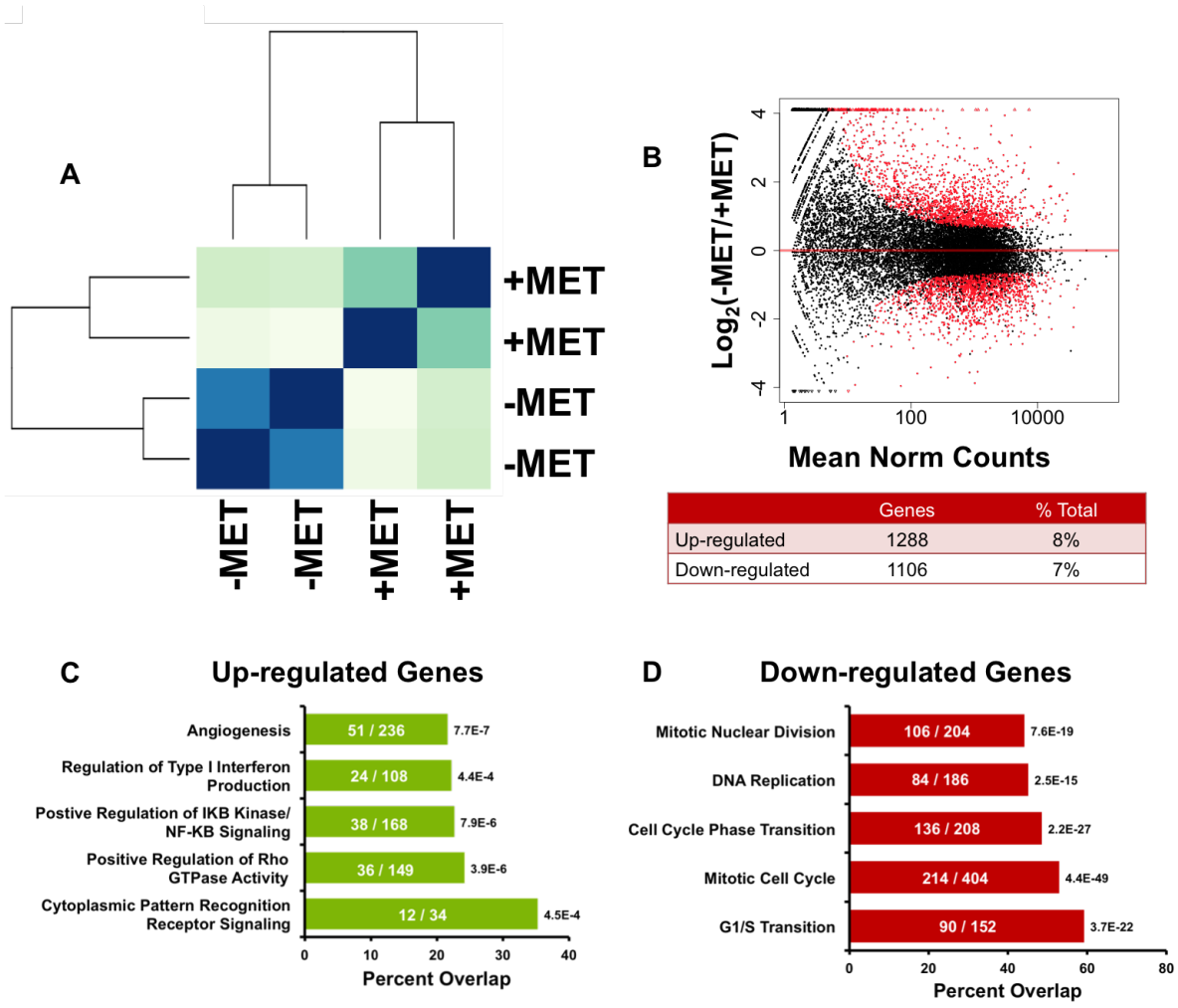

Figure 3.16: Global Effects on Transcription After Methionine Restriction

RNA-seq was performed in +MET and -MET after 24 hours in parallel with ChIP-seq experiments. (A) Hierarchical cluster was performed on replicates using normalized counts from DESeq2. (B) RNA-seq identifies differentially expressed (FDR < 0.05) genes (red) after methionine restriction. (C) Pathway enrichment analysis for genes significantly up-regulated after methionine restriction. (D) Pathway enrichment analysis for genes significantly down regulated after methionine restriction. Percent overlap is calculated as the number of hits divided by the number of genes in the list. The number of hits out of total number of genes in the list is shown in each bar. The corrected p-value is shown to the right of each bar.

Hierarchical clustering revealed strong correlation between replicate experiments (Figure 3.16A). Using DESeq2, 5,375 significantly differentially expressed

genes were identified (Figure 3.16B). Genes with significantly up-regulated expression were enriched for pathways involved in angiogenesis, Interferon production, NF-KB signaling and Rho GTPase activity (Figure 3.16C). Genes with significantly decreased expression were enriched for pathways involved in the mitotic cell cycle and DNA replication (Figure 3.16D).

Interestingly, we found that colorectal cancer (CRC)-associated genes were enriched for loss of H3K4me3 at promoters with resulting decreased expression ($p = 0.02$, Fisher's Exact Test). Notably the cancer-associated genes AKT1, MYC, and MAPK, among others are responsive to decreases in promoter H3K4me3 (Figure 3.17A). In addition, CRC genes that have significant decreases in gene expression also show significant decreases in H3K4me3 over the promoter region when compared to genome wide loss of H3K4me3 (Figure 3.17B). Overall, these results suggest that nutrient status, has a dramatic effect on the chromatin state and gene regulation in cells with likely effects on pathophysiological outcomes.

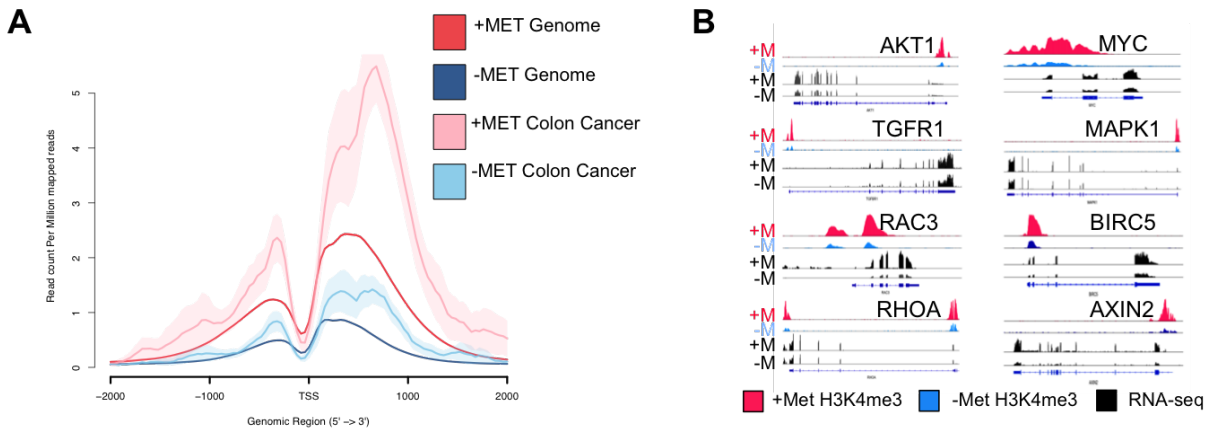

Figure 3.17: Methionine Restriction Decreases H3K4me3 at Colon Cancer Genes and Alters Gene Expression

(A) Distribution of H3K4me3 at the TSS of colon cancer genes with significantly reduced expression after methionine restriction compared to the average genome distribution. (B) Changes in H3K4me3 ChIP-seq signal with corresponding changes in gene expression form RNA-seq for colon cancer genes.

To further evaluate specific physiological consequences of this mechanism, we identified a network of enzymes involved in one carbon metabolism that show decreased H3K4me3 with concomitant decreases in expression (Figure 3.18) suggesting a feedback mechanism that decreases consumption of SAM by alternate pathways and an attempt to maintain H3K4me3 by regulation of JARID1B (KDM5B), H3K4me3 demethylase that is deregulated in cancer (Yamane et al., 2007). MAT2A, the predominant SAM producer in these cells, is significantly up-regulated under methionine restricted conditions, whereas, AHCY, responsible for the conversion of SAH to homocysteine is significantly down regulated (Figure 3.18B). In addition, many of the enzymes involved in pathways connected to methionine metabolism are downregulated (methionine salvage, folate cycle).

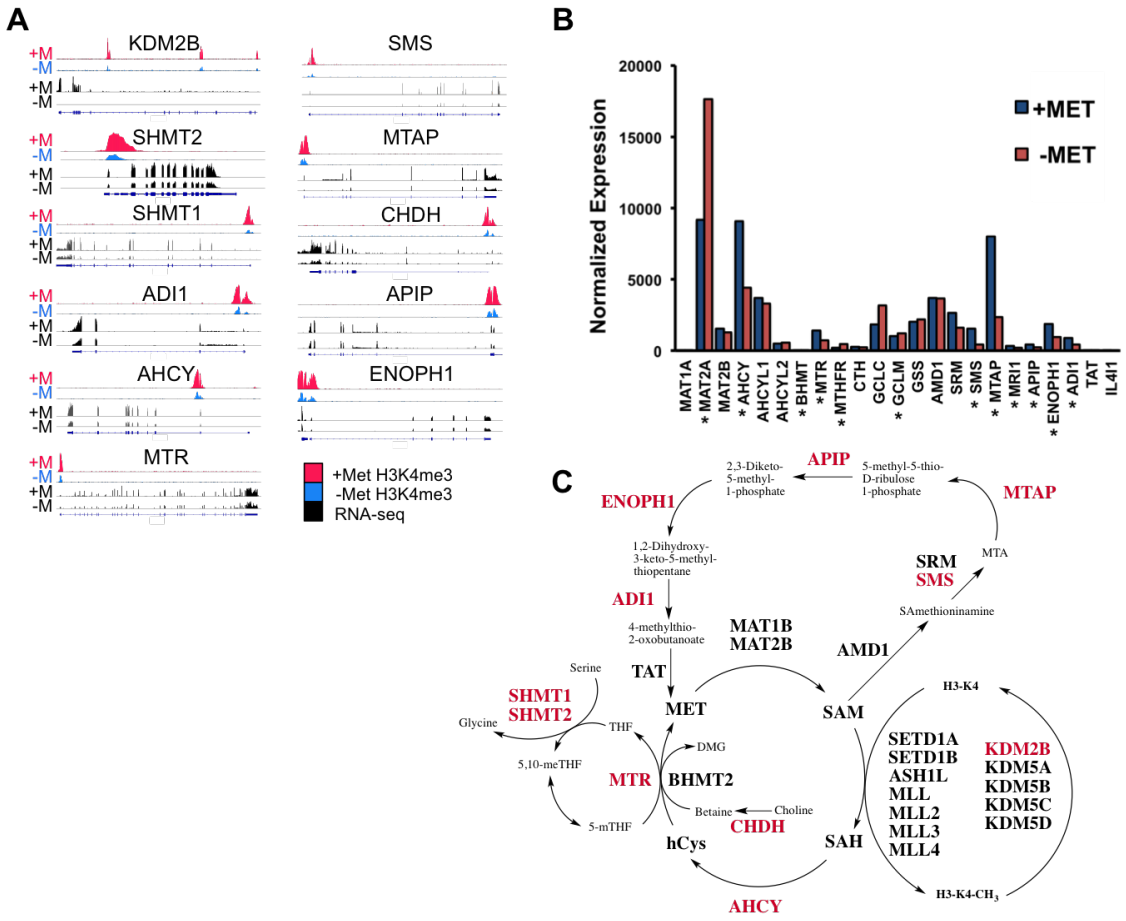

Figure 3.18: Methionine Restriction Decreases H3K4me3 at One Carbon Genes and Alters Gene Expression

(A) Changes in H3K4me3 ChIP-seq signal with corresponding changes in gene expression form RNA-seq for methionine cycle genes. (B) Normalized expression of methionine cycle genes before and after methionine restriction. (C) Schematic highlighting enzymes (from A) in red with decreased H3K4me3 and gene expression essential in one carbon metabolism and related pathways.

This finding is indicative of a signal transduction mechanism by which alterations in H3K4me3 directly feedback to one carbon metabolism and methylation-related enzymes to maintain physiological homeostasis.

3.3.5 Methionine Cycle Alterations Can Be Sustained by Diet In Vivo

We next questioned whether changes in methionine can occur through and are maintained in response to alterations in nutrient availability in a longer-term physiological setting. We considered an analysis of the effects of methionine restriction in vivo at a concentration that has been shown to have health-promoting effects (Ables et al., 2012). Seven-week-old C57Bl6 mice were randomized into two groups and one arm was fed a standard diet consisting of 0.84% (w/w) methionine and the other a methionine-restricted (MR) diet consisting of seven times less methionine (0.12%, w/w) (Figure 3.19).

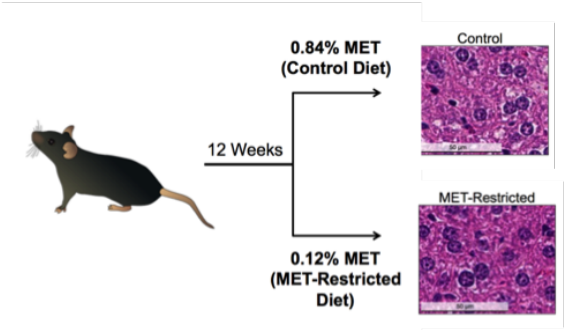

Figure 3.19: Methionine Restriction in Mice

Mice were fed a control or methionine restricted (MR) diet for 12 weeks. Representative liver histology from each group is shown at 40x with hematoxylin and eosin (H&E) staining.

We first confirmed that the MR diet specifically decreased serum methionine levels compared to the levels of all other amino acids (Figure 3.20). In addition to significantly reduced methionine, a significant increase in serine levels was also observed mirroring the effects in vitro.

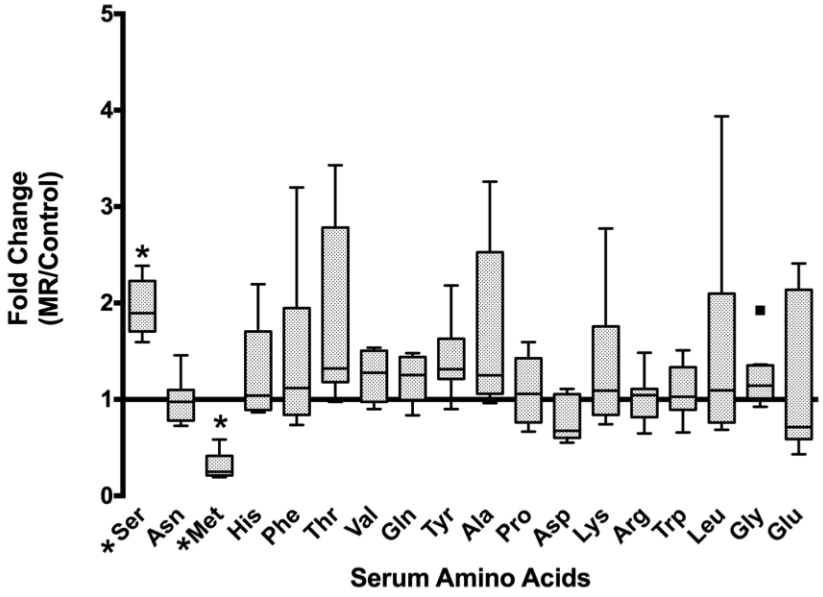

Figure 3.20: Change in Serum Amino Acid Levels After MR in Mice

Fold change of serum amino acids in mice fed control compared with methionine restricted (MR) diet, measured by LC-MS (*p< 0.001).

At twelve weeks, mice were sacrificed and no gross phenotypic alterations were observed as measured by liver histology and as previously described (Ables et al., 2012) (Figure 3.19). An examination of the metabolite profile in fasting serum and liver by carrying out unsupervised hierarchical clustering revealed global alterations in metabolism in liver and plasma (Figure 3.21A) with a pathway analysis revealing that cysteine and methionine metabolites were predominantly altered in plasma (Figure 3.21B). Other amino acid metabolism pathways to a lesser extent exhibited alterations. Inspection of metabolism in liver exhibited sustained alterations in cysteine and methionine along with alterations in taurine metabolism and other amino acid metabolism pathways (Figure 3.21C).

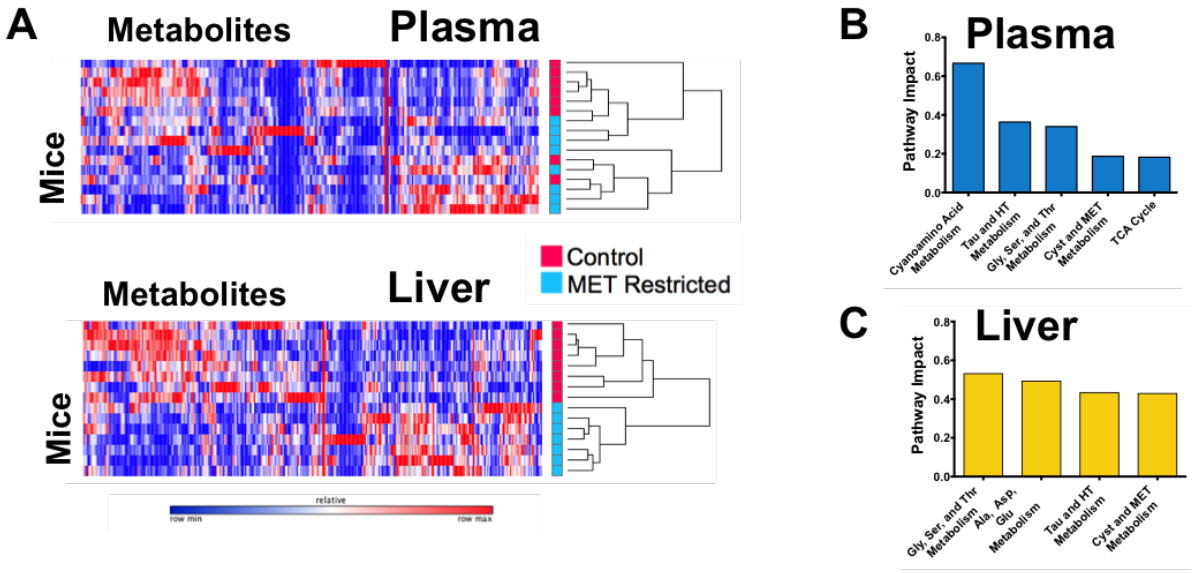

Figure 3.21: MR in Mice Produces Distinct Metabolic Profile in Liver and Plasma

(A) Global effects on metabolism in mouse serum and liver due to methionine restriction (MR). (B) Pathway analysis on serum metabolites shows significantly different profiles between control and MR groups. (C) Pathway analysis on liver metabolites shows significantly different profiles between control and MR groups.

Globally, an analysis of the quantile-quantile (Q-Q) plot showed skewness towards more changes being observed in liver but with more significant changes occurring in the serum (Figure 3.22A). These differences were further exemplified by comparing correlations of metabolite levels between liver and plasma (Figure 3.22B) with metabolites related to beta oxidation such as acylcarnitines, amino acid metabolism, and one carbon metabolism found to correlate with the extent of methionine levels in the plasma (Figure 3.22C).

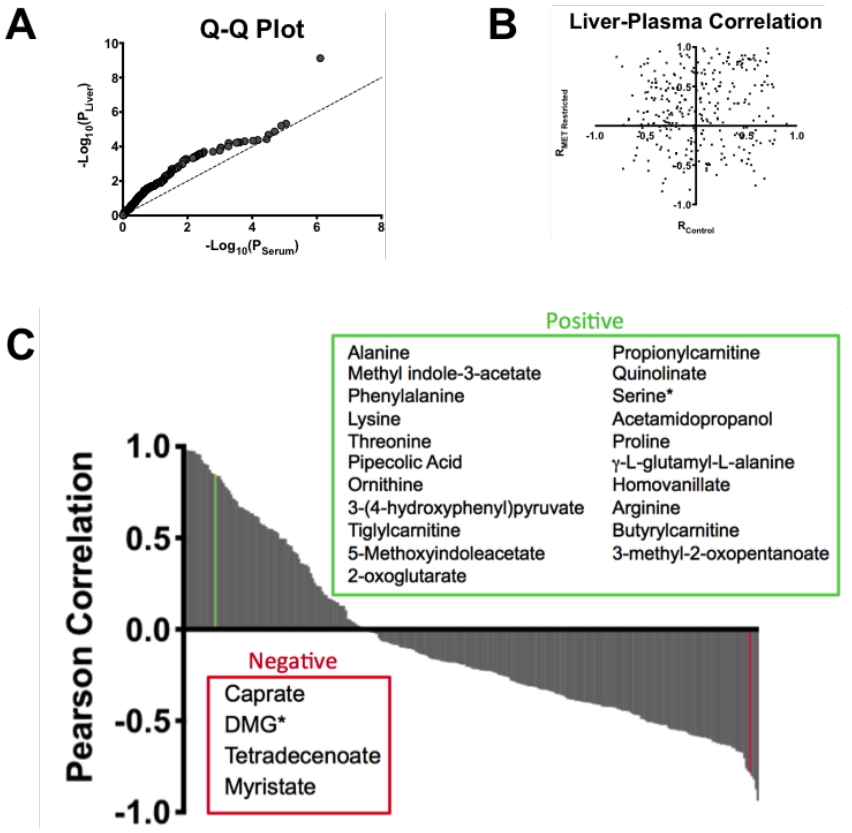

Figure 3.22: Comparing the Metabolic Changes in Mice After MR in Liver Versus Plasma

(A) Quantile-quantile plot of the differences in serum and liver. (B) Correlation analysis of the metabolism in the liver and plasma. (C) Correlation analysis of methionine levels and metabolites in plasma of MR animals. Significantly correlated metabolites are identified. All statistical analyses performed were student's t-tests, n=8, two-tailed, α<0.05.

Together these findings indicate that the regions of the metabolic network that are altered in response to sustained methionine-restriction in vivo are comparable to those aspects of the metabolic network that are dynamic in response to acute methionine restriction in cells. Furthermore, the metabolic state of fasting liver is different in the animals that were maintained on different diets for the long term.

3.3.6 Methionine Restriction In Vivo Sustains Altered Methionine Cycle and Histone Methylation

Having demonstrated that cysteine and methionine metabolism exhibit sustainable alterations in mice, we then asked whether these changes led to differences in the methionine cycle. In liver (Figure 3.23A), methionine concentrations exhibited no significant changes suggesting that compensatory fluxes involving its consumption or intake are occurring. These changes in fluxes resulted in decreases in SAM, SAH, the SAM/SAH ratio, cystathionine, and methylthioadenosine (MTA) and increases in the methyl donors dimethylglycine (DMG) and betaine. However, in plasma (Figure 3.23B), methionine levels were maintained at lower levels in response to MR diet. In addition, cystathionine and 2-keto-4-methylthiobutyrate (KMTB) a component of the methionine salvage pathway were also significantly decreased. Conversely, betaine and DMG each exhibited increases suggestive of their possibility as plasma biomarkers. Methionine cycle metabolites SAM and SAH did not show changes in plasma. This observation was expected since cells are not thought to secrete these metabolites at appreciable concentrations (Agrimi et al., 2004).

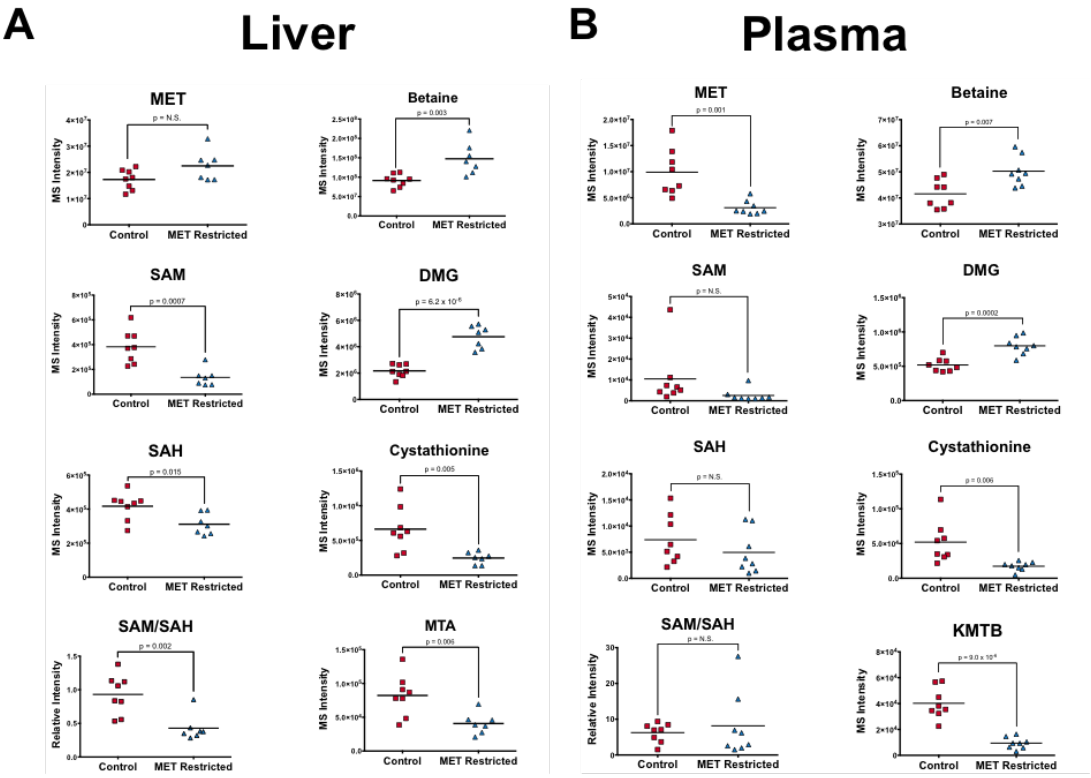

Figure 3.23: Changes in Methionine Cycle Metabolism Are Sustained by Diet in Vivo

(A) Methionine cycle metabolites in liver of mice fed Control or MR diet. (B) Methionine cycle metabolites in plasma of mice fed Control or MR diet.

We next asked whether these sustained changes in the methionine cycle were sufficient to induce changes in histone methylation. We observed decreases in H3K4me3 in the methionine restricted liver (Figure 3.24A) that we quantified (Figure 3.24B) indicating that the alterations in SAM and SAH levels observed in the liver are sufficient to induce global changes in histone methylation.

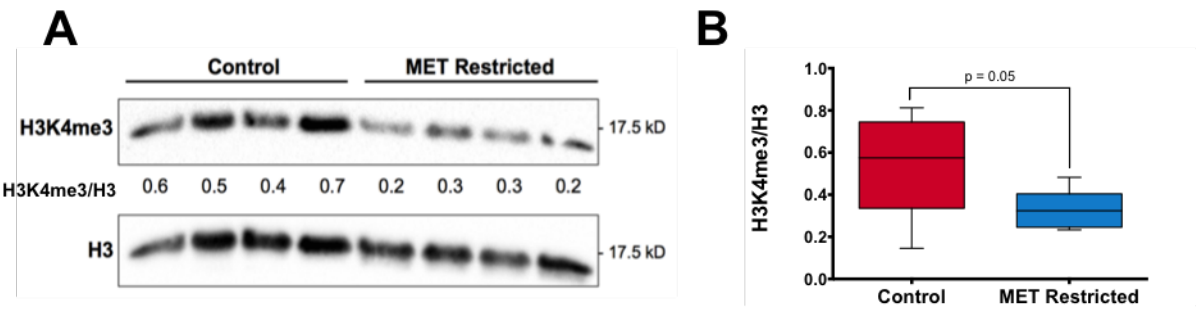

Figure 3.24: Decreased H3K4me3 In Liver or MID3 after MR

(A) Histone methylation (H3K4me3) in liver of MR mice. Integrated intensities were normalized to total H3. (B) Quantitation of results in (A) from n=8 mice in each cohort. P-value was obtained from a Student's t-test with equal variance.

We found that SAM, the SAM/SAH ratio, cystathionine positively correlated with H3K4me3 levels and methionine, betaine, and DMG negatively correlated with H3K4me3 levels (Figure 3.25A, B). In plasma, the levels of methionine and cystathionine were positively correlated and betaine and DMG were negatively correlated (Figures 3.25C, D). Together these findings provide evidence that the levels of SAM and SAM/SAH ratio in the liver are predictive of histone methylation levels, that plasma metabolites in methionine cycle metabolism are predictive of histone methylation in liver and that these levels can be directly modulated by diet in mice.

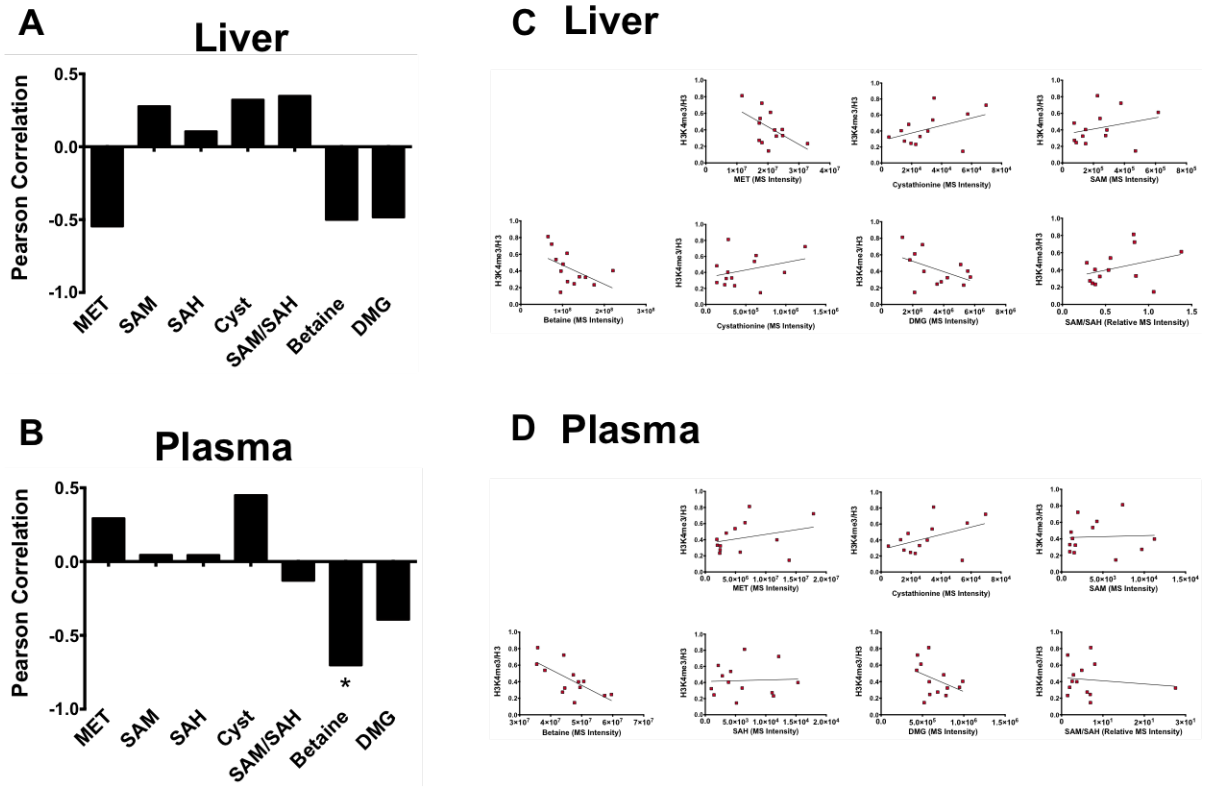

Figure 3.25: Correlation of Histone Methylation and Methionine Cycle Metabolites

(A) Correlation of histone methylation and methionine cycle metabolites in the liver. (B) Correlation of one carbon related metabolites and H3K4me3 in the plasma. (C) Correlation of changes in histone methylation and methionine cycle metabolites in plasma. (D) Correlation of other one carbon related metabolites and H3K4me3 in the plasma.

3.3.7 Humans Exhibit Variability in Methionine Levels

We next questioned whether variability in methionine metabolism exists in humans and how it can be regulated. Standard clinical parameters and a record of dietary intake over four days was considered to reflect variations in habitual diet as is standard practice in clinical nutrition (Levine et al., 2014) across a cohort of healthy human subjects. Fasting serum was collected graciously by

Anna Thalacker-Mercer and subjected to metabolomics performed by Xiaojing Liu. Then an analysis was performed to determine the metabolic profiles observed and the absolute concentration of metabolites . (Figure 3.26A, B).

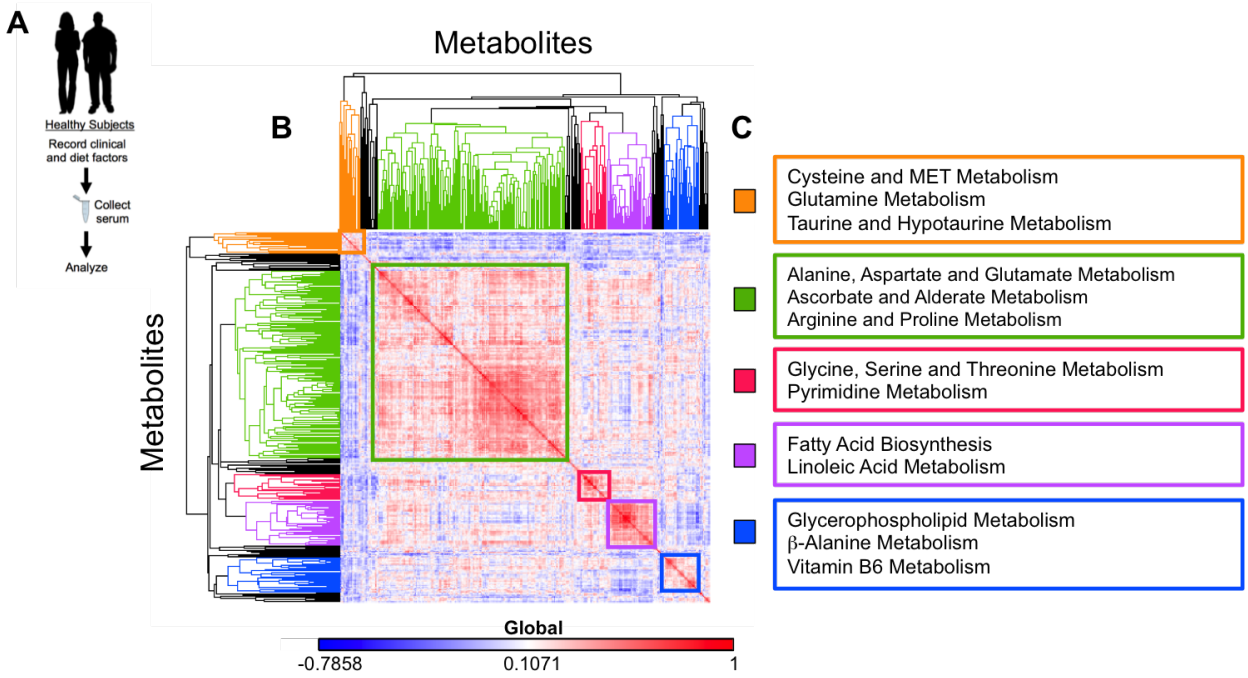

Figure 3.26: Methionine and Metabolic Variation in Human Subjects

(A) Measurement of serum methionine and clinical and dietary variable in human subjects. (B) Measurement of a metabolomics profile across the human cohort (N=38). Results of unsupervised clustering of a distance matrix for metabolites is shown. (C) Pathways that correspond to clusters observed in (B). Pathways were identified by considering the highest pathway impacts of all the metabolites contained in the specified cluster denoted by the different colored boxes and nodes.

In addition to this, other analyses performed by Mahya Mehrmohamadi and Lei Huang determined nutrient intake for each subject could be defined into modules that classified subjects into discrete dietary behavior groups (such as diets high in fruits and vegetables or carbohydrates)(Mentch et al., 2015).

We next measured the concentration of methionine along with a panel of

amino acids in these subjects (Figure 3.27A). Strikingly, the concentration of methionine exhibits substantial variation with values ranging from 3 to 30 μM (Figure 3.27B) with methionine exhibiting the largest variation (Figure 3.27C). This variation in concentration is on the same order as that needed to induce changes in histone methylation in cells and in mice. In addition, methionine in the serum correlates with N,N,N-trimethyllysine and N-methylglycine (sarcosine), both of which are methylated by the transfer of methyl groups from SAM, suggesting that methionine levels in the serum are indicative of cellular methylation status (Figure 3.27D, E).

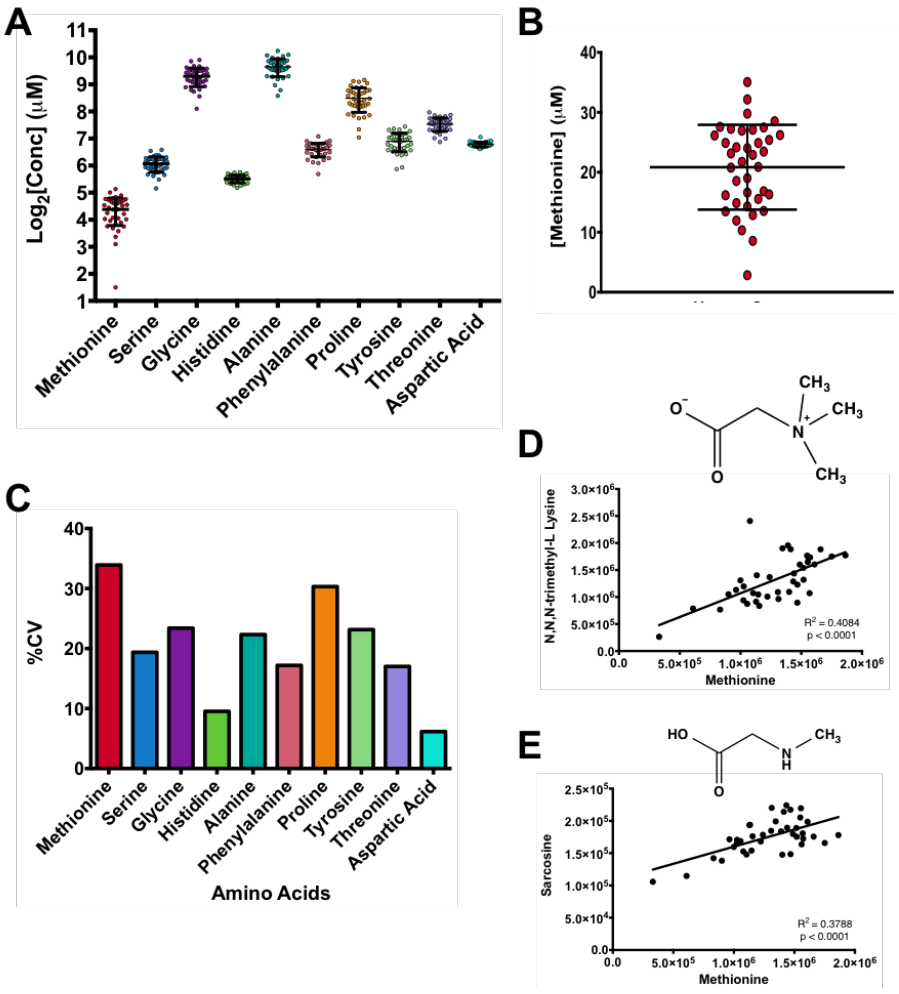

Figure 3.27: Methionine is the Most Variable Serum Amino Acid in a Cohort of Healthy Subjects

(A) Absolute concentrations of amino acids in fasting serum were measured in 38 human subjects. (B) Absolute concentration of methionine in fasting serum. (C) Coefficients of variation of amino acids in fasting serum. (D) Correlation of methionine in the serum with methylated serum metabolite N,N,N-trimethyllysine. (E) Correlation of methionine in serum with methylated serum metabolite sarcosine.

Taken together, these findings demonstrate that the variability in methionine concentration in humans is on the same scale as that needed to induce alterations in histone methylation and that these differences correlate with changes in diet and health status.

3.4 Discussion

These findings together provide evidence for a dynamic regulatory mechanism whereby the status of the methionine component of one carbon metabolism is sensed by histones to determine the levels of methylation on critical residues that mediate cellular epigenetic status. We first demonstrated that methionine deprivation and subsequent depletion of SAM and SAH induce changes in histone methylation. Furthermore, we tested and confirmed that these dynamics occurred in a manner consistent with a signal transduction mechanism. Necessarily, we found that changes in histone methylation occurred at quantitatively relevant concentrations of methionine. The kinetics of turnover of histone methylation in response to SAM and SAH availability were found to occur within hours and thus are much shorter than times corresponding to changes in cell cycle progression or global stress responses that also affect histone methylation. Importantly these dynamics were found to be reversible as the depletion of histone methylation could be recovered upon restoration of methionine availability even when the remainder of cellular metabolism was not recovered. Each of these properties is consistent with a mechanism whereby the status of key histone marks such as H3K4me3 that mediate chromatin structure, gene expression, and cell identity directly sense the metabolic status of one carbon metabolism.

In vivo, the dynamic response to methionine restriction further provided support of such a mechanism since alterations in SAM and SAH could be sustained in liver and these changes were sufficient to induce changes in histone methylation. Interestingly, although this dietary intervention maintained reduced methionine levels in the serum, the levels in the liver were not altered

suggesting that compensatory adaptations in methionine fluxes occurred, likely through other remethylation pathways for example from Folate metabolism. These metabolic adaptations likely serve to maintain other essential processes involved in methionine metabolism possibly providing a basis for why methionine restriction can be sustained in healthy animals even when changes in histone methylation are observed. Notably, methylation status and metabolism were measured in fasting conditions where methionine restriction was shown to alter histone methylation. This fasted condition we expect sets a lower bound on the extent that the methionine cycle can be depleted with feeding contributing to increases in methionine levels. Given this observation, it is tempting to speculate that feeding or a diurnal rhythm might regulate this effect, perhaps raising methionine levels to recover depletions in histone methylation.

In humans, the variation of methionine in healthy individuals was found to be largest across a panel of serum amino acids. Although these measurements are by no means exhaustive of human population dynamics, concentrations in many individuals were found to be far lower than the concentration required to induce changes in methylation levels. Computational modeling of diet and clinical variables performed by Mehrmohamadi & Huang (Mentch et al., 2015) found that about thirty percent of the variation could be due to fundamental clinical variables such as age, body composition, and gender, and about thirty percent was modulated by diet. In the future the results from these models could further be integrated with genomics data to specifically define the genetic contributions as have been identified to associate with serum metabolite levels (Suhre et al., 2011). Nevertheless it is tempting to speculate that basic dietary factors such as vegetable and fat intake could mediate human epigenetics through modulation of methionine metabolism.

3.4.1 One Carbon Metabolism as a Metabolic Signal Transduction Mechanism

Cellular decision-making occurs through signal transduction that utilizes post-translation modifications. For example, protein kinases establish networks of protein phosphorylation with multiple layers of nonlinear regulation that control almost all aspects of physiology. Despite the ubiquitous importance of histone and other macromolecular methylation, relatively little is known about how methylation is regulated. In contrast to protein kinases where the substrate, ATP, is in vast excess, the concentrations of SAM or SAH are on the order of the kinetic parameters that determine enzyme activity. Thus much of histone and other methylation could be regulated in large part by the status of methionine metabolism and one carbon cycle flux consistent with relatively few numbers of methyltransferases compared to the over 500 protein kinases that exist. This type of regulation by virtue of its biochemistry would have fundamentally different control properties and information capacity than that of protein kinase-mediated signaling. This regulation is evident in the feedback control observed in genes in one carbon metabolism whose expression and H3K4me3 signature is modulated in response to a decrease in SAM and SAH levels, likely as a specific mechanism to maintain homeostasis in one carbon metabolism. In particular, enzymes important in regenerating methionine by utilizing SAM are some of the most down regulated genes with loss of H3K4me3 at their promoters.

3.4.2 Methionine Metabolism in Pathophysiology through Its Modulation of Chromatin State

Numerous studies have documented a contribution of methionine metabolism and its restriction to beneficial metabolic health including the extension of mammalian life span, the acquisition of resistance to diet-induced obesity, and the therapeutic efficacy of ketogenic diets (Kraus et al., 2014; Malloy et al., 2006; Orentreich et al., 1993; Pissios et al., 2013). In each of these cases, the biological mechanisms contributing to these outcomes are largely unknown. Although alterations in methylation status are likely not accounting for all of these effects, it is possibly if not likely that the alterations in gene expression of key genes important for the relevant physiological effect in each of these cases. Indeed chronic diseases including obesity, diabetes, and cancer often stem from the inability of the organism to adapt to the demands of their nutritional load (Hotamisligil, 2010; Laplante and Sabatini, 2012). These adaptations require signal transduction mechanisms that integrate nutritional status to achieve the desired physiological demand. There are numerous signal transduction pathways that sense nutritional status and it is likely that the sensing of one carbon metabolism by histones is one of these mechanisms. Interestingly, this mechanism affected gene regulation of several cancer-promoting genes. Many cancers are vulnerable to disruptions in one carbon metabolism (Locasale, 2013), and our results demonstrate the necessity of methionine metabolism for the maintenance of histone methylation and the consequences for expression of oncogenic programs. Thus it is tempting to speculate that some of the anti-tumor effects of targeting one carbon metabolism may occur through changes in cancer epigenetics and further studies could more deeply elaborate these mechanisms.

3.5 Experimental Procedures

3.5.1 Methionine Restriction in Cell Culture

For methionine deprivation, RPMI 1640 lacking amino acids, glucose, and glutamine was supplemented with Minimal Essential Media Non-Essential Amino Acids (MEM NEAA), 5mM glucose, 2 μM glutamine, 10% FBS, 100 U/mL penicillin, and 100 mg/mL streptomycin. Essential amino acids, except methionine, were added back at the same concentrations found in MEM Amino Acids Solution for minus methionine (-MET) media. For plus methionine (+MET) media, methionine was added to -MET media to a final concentration of 100μM. For titration experiments, methionine was added at the respective concentrations to the -MET media. Each additional amino acid dropout media was prepared in a similar manner but with concentrations supplemented to the respective condition in the plus amino acid condition. At the start of each experiment, cells were seeded at a density of 2.2 x 10^6 cells for 10cm plates for protein collection or 3 x 10^5 cells/well in a 6-well plate for metabolite collection and allowed to adhere for 24 hours. After a 24 hour incubation, cells were washed once with PBS and placed in respective media for 24 hours unless otherwise noted

3.5.2 Mouse Feeding and Tissue and Plasma Analysis

Seven week-old C57BL/6J mice were purchased from Jackson Laboratories (Bar Harbor, ME) and housed in a conventional animal facility maintained at 202C, 5010% relative humidity and a 12 h light: 12 h dark light cycle. All animal procedures were approved by the Institutional Animal Care and Use Committee of

the Orentreich Foundation for the Advancement of Science, Inc. (Permit Number: 0511MB). Food and water were provided ad libitum. Upon arrival, the mice were acclimated for one week and fed Rodent Chow 5001 (Purina LabDiets) and water ad libitum. After one week, the mice were randomized and fed either an isocaloric 0.84% (w/w) methionine (control-fed; CF, N=8) diet or 0.12% (w/w) methionine (methionine-restricted; MR, N=8) diet from Research Diets. After 12 weeks of feeding, mice were fasted for 4 hours at the beginning of the light cycle to establish a physiological baseline and then sacrificed. Blood was collected from the retro-orbital plexus and plasma was collected, flash frozen and stored at -80C until analyzed. The liver was harvested, flash frozen and stored at -80C until processed. Liver tissues samples were fixed in 10% formalin solution (Thermo Scientific) and paraffin embedded. Hematoxylin and eosin (H & E) staining and imaging was carried out at Histowiz, high resolution slide scanning was carried out using Leica SCN400 and image analysis was conducted using Image-pro software (Media Cybernetics).

3.5.3 Immunoblotting

Samples were homogenized in Triton Extraction Buffer (TEB: 0.5% Triton X 100, 2mM phenylmethylsulfonyl fluoride (PMSF), 0.02% NaN3 in PBS) and centrifuged at 2000rpm for 10 min at 4C. Pellets were resuspended in 0.2N HCl and histones were acid extracted overnight at 4C. Histone extracts were loaded onto 12% SDS-PAGE gels and transferred to polyvinylidene difluoride (PVDF) membranes. Membranes were blocked in 5% dry milk in TBST and incubated with anti-H3K4me3 (Millipore, cat #07-473) 1:2000, anti-H3K9me3 (Millipore, cat #05-1250) 1:2000, anti-H3K27me3 (Millipore, cat #05-1951) 1:10000,

or anti-H3 (Millipore, cat #07-690) 1:10000. Horseradish-peroxidase-conjugated anti-rabbit (Rockland cat #611-7302) or anti-mouse (Rockland, cat #611-4302), 1:10,000, were used as secondary antibodies. Chemiluminescent signals were detected with Clarity Western ECL Detection Kit (Bio-Rad) and imaged using a ChemiDoc MP System (Bio-Rad). All western blots are normalized to the total H3 signal before relative quantification was calculated.

3.5.4 Metabolite Extraction and LC-HRMS Analysis

For culture from adherent cells, the media was quickly aspirated and cells were washed with cold PBS then placed on dry ice. Then, 1mL of extraction solvent (80% methanol/water) cooled to -80C was added immediately to each well, and the dishes were transferred to -80C for 15 min. Plates were removed and cells were scraped into the extraction solvent on dry ice. For tissue, the sample was homogenized in liquid nitrogen and then 5 to 10 mg was weighed in a new Eppendorf tube. Ice-cold extraction solvent (250μL) was added to each tissue sample and homogenized using a tissue homogenizer. The homogenate was incubated on ice for 10 min. For plasma or serum, 20μL was transferred to a new Eppendorf tube containing 80μL HPLC grade water. Next, 400μL of ice-cold methanol was added to the sample for a final methanol concentration of 80% (v/v). Samples were incubated on ice for 10 min. All metabolite extracts were centrifuged at 20,000g at 4C for 10 min. Finally the solvent in each sample was evaporated in a Speed Vacuum for metabolomics analysis. For polar metabolite analysis, the cell extract was dissolved in 15μL water and 15μL methanol/acetonitrile (1:1 v/v) (LC-MS optima grade, Thermo Scientific). Samples were centrifuged at 20,000g for 10min at 4C and the supernatants were transferred to

Liquid Chromatography (LC) vials. The injection volume for polar metabolite analysis was 5μL.

3.5.5 Liquid Chromatography

An Xbridge amide column (100 x 2.1 mm i.d., 3.5 ?m; Waters) is employed on a Dionex (Ultimate 3000 UHPLC) for compound separation at room temperature. The mobile phase A is 20 mM ammonium acetate and 15 mM ammonium hydroxide in water with 3% acetonitrile, pH 9.0 and mobile phase B is acetonitrile. Linear gradient as follows: 0 min, 85% B; 1.5 min, 85% B, 5.5 min, 35% B; 10min, 35% B, 10.5 min, 35% B, 14.5 min, 35% B, 15 min, 85% B, and 20 min, 85% B. The flow rate was 0.15 ml/min from 0 to 10 min and 15 to 20 min, and 0.3 ml/min from 10.5 to 14.5 min. All solvents are LC-MS grade and purchased from Fisher Scientific.

3.5.6 Mass Spectrometry

The Q Exactive MS (Thermo Scientific) is equipped with a heated electrospray ionization probe (HESI), and the relevant parameters are as listed: evaporation temperature, 120 C; sheath gas, 30; auxiliary gas, 10; sweep gas, 3; spray voltage, 3.6 kV for positive mode and 2.5 kV for negative mode. Capillary temperature was set at 320C, and S-lens was 55. A full scan range from 60 to 900 (m/z) was used. The resolution was set at 70 000. The maximum injection time was 200 ms. Automated gain control (AGC) was targeted at 3,000,000 ions.

3.5.7 Metabolomics and Data Analysis

Raw data collected from LC-Q Exactive MS is processed on Sieve 2.0 (Thermo Scientific). Peak alignment and detection are performed according to the protocol described by Thermo Scientific. For a targeted metabolite analysis, the method "peak alignment and frame extraction" is applied. An input file of theoretical m/z and detected retention time of 263 known metabolites is used for targeted metabolites analysis with data collected in positive mode, while a separate input file of 197 metabolites is used for negative mode. M/Z width is set at 10 ppm. The output file including detected m/z and relative intensity in different samples is obtained after data processing. Dot plots and other quantitation and statistics were calculated and visualized with the Graphpad prism software package.

3.5.8 RNA Sequencing

Total RNA was extracted using the PARIS kit (Life Technologies, cat #AM1921), polyA selected before library generation, and prepared according to a standard protocol provided by Illumina by the Weill Cornell Medical College Epigenomics Core. Samples were pooled into one lane on the Illumina HiSEQ2500 and sequenced. Reads were mapped to the reference genome (hg19) using TopHat2.0.7 in the Galaxy software suite (https://usegalaxy.org). For the analysis, we generated a counts table from accepted hits bam files using HTseq ((Anders et al., 2015)) with the following parameters: htseq-count -f bam -s yes [input bam] [hg19genes.gtf]. Differential expression was calculated from the counts table using the edgeR package in R (Nikolayeva and Robinson, 2014; Robinson

et al., 2010) and DEseq2 (Love et al., 2014).

3.5.9 Chromatin Immunoprecipation and Sequencing

HCT116 cells were cultured in 15cm plates resulting in $3x10^7$ cells at 80% confluency. Cells were cross-linked for 5 minutes at room temperature by addition of 1% formaldehyde to the cell culture media. The reaction was quenched for 5 minutes by the addition of 2.5M glycine. Cells were collected and lysed in FA buffer (50mM HEPES/KOH pH 7.5, 1mM EDTA, 1% Triton X-100, 0.1% sodium deoxycholate, 1M NaCl) with protease inhibitors. Cross-linked chromatin was resuspended in LB3 (10mM Tris-HCl, pH 8.0, 200mM NaCl, 1mM EDTA, pH 8.0, 0.5mM EGTA, pH 8.0, 0.1% Sodium deoxycholate, 0.5% N-lauroylsarcosine) and samples were sheared using the Covaris M2 ultrasonicator (Covaris) . Each IP was performed as previously described, (Ercan et al., 2007; Landt et al., 2012) (Ercan et al., 2007; Landt et al., 2012) using 1.5x107 cells and the Millipore ChIPAb+ H3K4me3 antibody (cat #17-614, lot #2196044) with Protein A Agarose beads (Millipore, cat #16-125, lot #2444123). Libraries were made and pooled according to Illumina instructions, then sequenced on an Illumina HiSEQ 2500 Rapid Run sequencer. Reads were mapped to the reference genome (hg19) using Bowtie2.2.4. H3K4me3 ChIP peaks were called using MACS2.08 with the broad setting. Alignment and peak calling were performed on the Galaxy platform (Blankenberg et al., 2010; Giardine et al., 2005; Goecks et al., 2010). H3K4me3 distribution was visualized using the ngsplot package (Shen et al., 2014) and ChIPseeker in R (Yu et al., 2015).

3.5.10 Analysis of ChIP-seq Results for Differentially Bound Chromosome Regions

We used the R package "DiffBind" (Stark and Brown, 2011) to find regions with a significant difference in H3K4me3 between the minus-Methionine and the plus-Methionine conditions. In summary, peaks were first called by MACS2 (see Appendix B) to generate a consensus peak-set which we defined as a set of peaks called in at least 2 samples. Then using the original read files, we generated the counts table including the number of reads corresponding to each consensus peak in each sample. Finally using edgeR and DESeq2 we performed differential binding analysis on all of the consensus peaks and reported the significantly differentially bound regions (FDR¡0.1). Finally, the "quantsmooth" package in R (Oosting et al., 2014; Ross-Innes et al., 2012) was used to overlay counts onto the human chromosomal ideograms.

3.5.11 Clinical Nutrition Studies

A four-day diet record was collected according to previous standards of recording diet to reflect habitual behaviors as has been previously described (Levine et al., 2014). Surveys were converted into nutritional variables according to previously described procedures using standard software (Levine et al., 2014). Nutrition data system for research (NDSR) dietary analysis software (University of Minnesota), a comprehensive food and nutrient database, was used to determine the average macro- and micronutrients consumed over the four-day period as previously described (Thalacker-Mercer et al., 2009). Before serum was collected, each subject was subjected to overnight fasting. Metabolites

from serum were extracted using a previously described protocol (Shestov et al., 2014) (Shestov et al., 2014). All additional clinical variables were recorded according to previously described methods (Thalacker-Mercer et al., 2013, 2009). The computational model of the factors contributing to methionine concentration variation is described in detail later.

3.5.12 Statistical Analysis

Error bars represent standard error of the measurement (SEM). Significance reported are results from Student's t-test unless otherwise noted.

LITERATURE CITED

Ables, G., Perrone, C., Orentreich, D., and Orentreich, N. (2012). Methionine-restricted c57bl/6j mice are resistant to diet-induced obesity and insulin resistance but have low bone density. *PLoS ONE*, 7(12). cited By 45.

Agrimi, G., Di Noia, M., Marobbio, C., Fiermonte, G., Lasorsa, F., and Palmieri, F. (2004). Identification of the human mitochondrial s-adenosylmethionine transporter: Bacterial expression, reconstitution, functional characterization and tissue distribution. *Biochemical Journal*, 379(1):183–190. cited By 76.

An, S., Yeo, K., Jeon, Y., and Song, J.-J. (2011). Crystal structure of the human histone methyltransferase ash1l catalytic domain and its implications for the regulatory mechanism. *Journal of Biological Chemistry*, 286(10):8369–8374. cited By 32.

Anders, S., Pyl, P. T., and Huber, W. (2015). HTSeq–a Python framework to work with high-throughput sequencing data. *Bioinformatics*, 31(2):166–169.

Bailey, T., Krajewski, P., Ladunga, I., Lefebvre, C., Li, Q., Liu, T., Madrigal, P., Taslim, C., and Zhang, J. (2013). Practical guidelines for the comprehensive analysis of chip-seq data. *PLoS Computational Biology*, 9(11). cited By 48.

Barth, T. and Imhof, A. (2010). Fast signals and slow marks: the dynamics of histone modifications. *Trends in Biochemical Sciences*, 35(11):618–626. cited By 105.

Benayoun, B., Pollina, E., Ucar, D., Mahmoudi, S., Karra, K., Wong, E., Devarajan, K., Daugherty, A., Kundaje, A., Mancini, E., Hitz, B., Gupta, R., Rando, T., Baker, J., Snyder, M., Cherry, J., and Brunet, A. (2014). H3k4me3 breadth

is linked to cell identity and transcriptional consistency. *Cell*, 158(3):673–688. cited By 52.

Bergman, Y. and Cedar, H. (2013). Dna methylation dynamics in health and disease. *Nature Structural and Molecular Biology*, 20(3):274–281. cited By 130.

Blankenberg, D., Von Kuster, G., Coraor, N., Ananda, G., Lazarus, R., Mangan, M., Nekrutenko, A., and Taylor, J. (2010). Galaxy: a web-based genome analysis tool for experimentalists. *Curr Protoc Mol Biol*, Chapter 19:1–21.

Chi, P., Allis, C., and Wang, G. (2010). Covalent histone modifications-miswritten, misinterpreted and mis-erased in human cancers. *Nature Reviews Cancer*, 10(7):457–469. cited By 497.

Chin, H., Pradhan, M., Estve, P.-O., Patnaik, D., Evans Jr., T., and Pradhan, S. (2005). Sequence specificity and role of proximal amino acids of the histone h3 tail on catalysis of murine g9a lysine 9 histone h3 methyltransferase. *Biochemistry*, 44(39):12998–13006. cited By 19.

Dawson, M. and Kouzarides, T. (2012). Cancer epigenetics: From mechanism to therapy. *Cell*, 150(1):12–27. cited By 653.

Ercan, S., Giresi, P., Whittle, C., Zhang, X., Green, R., and Lieb, J. (2007). X chromosome repression by localization of the c. elegans dosage compensation machinery to sites of transcription initiation. *Nature Genetics*, 39(3):403–408. cited By 70.

Finkelstein, J. (1990). Methionine metabolism in mammals. *The Journal of Nutritional Biochemistry*, 1(5):228–237. cited By 781.

Giardine, B., Riemer, C., Hardison, R. C., Burhans, R., Elnitski, L., Shah, P., Zhang, Y., Blankenberg, D., Albert, I., Taylor, J., Miller, W., Kent, W. J., and

Nekrutenko, A. (2005). Galaxy: a platform for interactive large-scale genome analysis. *Genome Res.*, 15(10):1451–1455.

Goecks, J., Nekrutenko, A., Taylor, J., Afgan, E., Ananda, G., Baker, D., Blankenberg, D., Chakrabarty, R., Coraor, N., Goecks, J., Von Kuster, G., Lazarus, R., Li, K., Nekrutenko, A., Taylor, J., and Vincent, K. (2010). Galaxy: a comprehensive approach for supporting accessible, reproducible, and transparent computational research in the life sciences. *Genome Biol.*, 11(8):R86.

Greer, E. and Shi, Y. (2012). Histone methylation: A dynamic mark in health, disease and inheritance. *Nature Reviews Genetics*, 13(5):343–357. cited By 436.

Gut, P. and Verdin, E. (2013). The nexus of chromatin regulation and intermediary metabolism. *Nature*, 502(7472):489–498. cited By 94.

Hoffman, D., Cornatzer, W., and Duerre, J. (1979). Relationship between tissue levels of s-adenosylmethionine, s-adenosylhomocysteine, and transmethylation reactions. *Canadian Journal of Biochemistry*, 57(1):56–65. cited By 134.

Horiuchi, K., Eason, M., Ferry, J., Planck, J., Walsh, C., Smith, R., Howitz, K., and Ma, H. (2013). Assay development for histone methyltransferases. *Assay and Drug Development Technologies*, 11(4):227–236. cited By 16.

Hotamisligil, G. (2010). Endoplasmic reticulum stress and the inflammatory basis of metabolic disease. *Cell*, 140(6):900–917. cited By 995.

Katada, S., Imhof, A., and Sassone-Corsi, P. (2012). Connecting threads: Epigenetics and metabolism. *Cell*, 148(1-2):24–28. cited By 100.

Kraus, D., Yang, Q., Kong, D., Banks, A., Zhang, L., Rodgers, J., Pirinen, E., Pulinilkunnil, T., Gong, F., Wang, Y.-C., Cen, Y., Sauve, A., Asara, J., Peroni,

O., Monia, B., Bhanot, S., Alhonen, L., Puigserver, P., and Kahn, B. (2014). Nicotinamide n-methyltransferase knockdown protects against diet-induced obesity. *Nature*, 508(7495):258–262. cited By 55.

Landt, S. G., Marinov, G. K., Kundaje, A., Kheradpour, P., Pauli, F., Batzoglou, S., Bernstein, B. E., Bickel, P., Brown, J. B., Cayting, P., Chen, Y., DeSalvo, G., Epstein, C., Fisher-Aylor, K. I., Euskirchen, G., Gerstein, M., Gertz, J., Hartemink, A. J., Hoffman, M. M., Iyer, V. R., Jung, Y. L., Karmakar, S., Kellis, M., Kharchenko, P. V., Li, Q., Liu, T., Liu, X. S., Ma, L., Milosavljevic, A., Myers, R. M., Park, P. J., Pazin, M. J., Perry, M. D., Raha, D., Reddy, T. E., Rozowsky, J., Shoresh, N., Sidow, A., Slattery, M., Stamatoyannopoulos, J. A., Tolstorukov, M. Y., White, K. P., Xi, S., Farnham, P. J., Lieb, J. D., Wold, B. J., and Snyder, M. (2012). ChIP-seq guidelines and practices of the ENCODE and modENCODE consortia. *Genome Res.*, 22(9):1813–1831.

Laplante, M. and Sabatini, D. (2012). Mtor signaling in growth control and disease. *Cell*, 149(2):274–293. cited By 2120.

Levine, M., Suarez, J., Brandhorst, S., Balasubramanian, P., Cheng, C.-W., Madia, F., Fontana, L., Mirisola, M., Guevara-Aguirre, J., Wan, J., Passarino, G., Kennedy, B., Wei, M., Cohen, P., Crimmins, E., and Longo, V. (2014). Low protein intake is associated with a major reduction in igf-1, cancer, and overall mortality in the 65 and younger but not older population. *Cell Metabolism*, 19(3):407–417. cited By 101.

Liu, X., Ser, Z., Cluntun, A., Mentch, S., and Locasale, J. (2014a). A strategy for sensitive, large scale quantitative metabolomics. *Journal of Visualized Experiments*, (87). cited By 2.

Liu, X., Ser, Z., and Locasale, J. (2014b). Development and quantitative eval-

uation of a high-resolution metabolomics technology. *Analytical Chemistry*, 86(4):2175–2184. cited By 35.

Locasale, J. (2013). Serine, glycine and one-carbon units: Cancer metabolism in full circle. *Nature Reviews Cancer*, 13(8):572–583. cited By 154.

Love, M. I., Huber, W., and Anders, S. (2014). Moderated estimation of fold change and dispersion for RNA-seq data with DESeq2. *Genome Biol.*, 15(12):550.

Malloy, V., Krajcik, R., Bailey, S., Hristopoulos, G., Plummer, J., and Orentreich, N. (2006). Methionine restriction decreases visceral fat mass and preserves insulin action in aging male fischer 344 rats independent of energy restriction. *Aging Cell*, 5(4):305–314. cited By 88.

Mentch, S. J., Mehrmohamadi, M., Huang, L., Liu, X., Gupta, D., Mattocks, D., Padilla, P. G., Ables, G., Bamman, M. M., Thalacker-Mercer, A. E., et al. (2015). Histone methylation dynamics and gene regulation occur through the sensing of one-carbon metabolism. *Cell metabolism*, 22(5):861–873.

Nikolayeva, O. and Robinson, M. D. (2014). edgeR for differential RNA-seq and ChIP-seq analysis: an application to stem cell biology. *Methods Mol. Biol.*, 1150:45–79.

Obianyo, O., Osborne, T., and Thompson, P. (2008). Kinetic mechanism of protein arginine methyltransferase. *Biochemistry*, 47(39):10420–10427. cited By 47.

Oosting, J., Eilers, P., and Menezes, R. (2014). quantsmooth: Quantile smoothing and genomic visualization of array data.

Orentreich, N., Matias, J., DeFelice, A., and Zimmerman, J. (1993). Low methionine ingestion by rats extends life span. *Journal of Nutrition*, 123(2):269–274. cited By 213.

Patnaik, D., Hang, G., Estve, P.-O., Benner, J., Jacobsen, S., and Pradhan, S. (2004). Substrate specificity and kinetic mechanism of mammalian g9a histone h3 methyltransferase. *Journal of Biological Chemistry*, 279(51):53248–53258. cited By 78.

Pissios, P., Hong, S., Kennedy, A., Prasad, D., Liu, F.-F., and Maratos-Flier, E. (2013). Methionine and choline regulate the metabolic phenotype of a ketogenic diet. *Molecular Metabolism*, 2(3):306–313. cited By 10.

Robinson, M. D., McCarthy, D. J., and Smyth, G. K. (2010). edgeR: a Bioconductor package for differential expression analysis of digital gene expression data. *Bioinformatics*, 26(1):139–140.

Ross-Innes, C. S., Stark, R., Teschendorff, A. E., Holmes, K. A., Ali, H. R., Dunning, M. J., Brown, G. D., Gojis, O., Ellis, I. O., Green, A. R., Ali, S., Chin, S. F., Palmieri, C., Caldas, C., and Carroll, J. S. (2012). Differential oestrogen receptor binding is associated with clinical outcome in breast cancer. *Nature*, 481(7381):389–393.

Ruthenburg, A., Allis, C., and Wysocka, J. (2007). Methylation of lysine 4 on histone h3: Intricacy of writing and reading a single epigenetic mark. *Molecular Cell*, 25(1):15–30. cited By 607.

Shen, L., Shao, N., Liu, X., and Nestler, E. (2014). ngs.plot: Quick mining and visualization of next-generation sequencing data by integrating genomic databases. *BMC Genomics*, 15:284.

Shestov, A. A., Liu, X., Ser, Z., Cluntun, A. A., Hung, Y. P., Huang, L., Kim, D., Le, A., Yellen, G., Albeck, J. G., and Locasale, J. W. (2014). Quantitative determinants of aerobic glycolysis identify flux through the enzyme GAPDH as a limiting step. *Elife*, 3.

Shilatifard, A. (2006). Chromatin modifications by methylation and ubiquitination: Implications in the regulation of gene expression. *Annual Review of Biochemistry*, 75:243–269. cited By 681.

Shiraki, N., Shiraki, Y., Tsuyama, T., Obata, F., Miura, M., Nagae, G., Aburatani, H., Kume, K., Endo, F., and Kume, S. (2014). Methionine metabolism regulates maintenance and differentiation of human pluripotent stem cells. *Cell Metabolism*, 19(5):780–794. cited By 45.

Shyh-Chang, N., Locasale, J., Lyssiotis, C., Zheng, Y., Teo, R., Ratanasirintrawoot, S., Zhang, J., Onder, T., Unternaehrer, J., Zhu, H., Asara, J., Daley, G., and Cantley, L. (2013). Influence of threonine metabolism on s-adenosylmethionine and histone methylation. *Science*, 339(6116):222–226. cited By 135.

Stark, R. and Brown, G. (2011). DiffBind: differential binding analysis of ChIP-Seq peak data.

Suhre, K., Shin, S.-Y., Petersen, A.-K., Mohney, R., Meredith, D., Wgele, B., Altmaier, E., Deloukas, P., Erdmann, J., Grundberg, E., Hammond, C., De Angelis, M., Kastenmller, G., Kttgen, A., Kronenberg, F., Mangino, M., Meisinger, C., Meitinger, T., Mewes, H.-W., Milburn, M., Prehn, C., Raffler, J., Ried, J., Rmisch-Margl, W., Samani, N., Small, K., Erich Wichmann, H., Zhai, G., Illig, T., Spector, T., Adamski, J., Soranzo, N., and Gieger, C. (2011). Human

metabolic individuality in biomedical and pharmaceutical research. *Nature*, 477(7362):54–62. cited By 359.

Teperino, R., Schoonjans, K., and Auwerx, J. (2010). Histone methyl transferases and demethylases; can they link metabolism and transcription? *Cell Metabolism*, 12(4):321–327. cited By 101.

Thalacker-Mercer, A., Stec, M., Cui, X., Cross, J., Windham, S., and Bamman, M. (2013). Cluster analysis reveals differential transcript profiles associated with resistance training-induced human skeletal muscle hypertrophy. *Physiol. Genomics*, 45(12):499–507.

Thalacker-Mercer, A. E., Petrella, J. K., and Bamman, M. M. (2009). Does habitual dietary intake influence myofiber hypertrophy in response to resistance training? A cluster analysis. *Appl Physiol Nutr Metab*, 34(4):632–639.

Ulanovskaya, O., Zuhl, A., and Cravatt, B. (2013). Nnmt promotes epigenetic remodeling in cancer by creating a metabolic methylation sink. *Nature Chemical Biology*, 9(5):300–306. cited By 46.

Xia, J. and Wishart, D. (2010). Metpa: A web-based metabolomics tool for pathway analysis and visualization. *Bioinformatics*, 26(18):2342–2344. cited By 95.

Xiao, B., Jing, C., Wilson, J., Walker, P., Vasisht, N., Kelly, G., Howell, S., Taylor, I., Blackburn, M., and Gamblin, S. (2003). Structure and catalytic mechanism of the human histone methyltransferase set7/9. *Nature*, 421(6923):652–656. cited By 232.

Yamane, K., Tateishi, K., Klose, R., Fang, J., Fabrizio, L., Erdjument-Bromage, H., Taylor-Papadimitriou, J., Tempst, P., and Zhang, Y. (2007). Plu-1 is an

h3k4 demethylase involved in transcriptional repression and breast cancer cell proliferation. *Molecular Cell*, 25(6):801–812. cited By 262.

Yu, G., Wang, L. G., and He, Q. Y. (2015). ChIPseeker: an R/Bioconductor package for ChIP peak annotation, comparison and visualization. *Bioinformatics*, 31(14):2382–2383.

CHAPTER 4

CONCLUSIONS AND FUTURE DIRECTIONS

4.1 Conclusions

The previous experiments show the link between decreased methionine availability, decreased SAM pools and decreased H3K4me3. Inspection of the loss H3K4me3 and subsequent changes in gene expression suggests some gene networks may be directly affected by methionine deprivation. However, more work needs to be done to explore this relationship.

4.2 Future Directions

4.2.1 Quantitative ChIP-seq and Peak Parameterization

First, standard ChIP-seq experiments are flawed at several levels due to experimental limitations. It would be useful to characterize H3K4me3 peaks in more detail with high confidence. Traditionally, ChIP-seq relies on peaks being present or absent. With increased complexity in experimental set ups like time courses, or conditions where the loss of signal is expected problems can arise during the experiment and analysis. To address these concerns, several methods have been suggested in order to quantitatively assess the differences in ChIP-seq signal. Methods such as those presented in Orlando et al. (2014) should be used for quantitative analysis. These methods employ a spike in strategy that allows for empirical normalization during alignment and can eliminate problems that

arise from differences in sample preparation and sequencing so true differences between the ChIP-seq signal can be determined. Where standard methods have restricted the analysis, using these quantitative methods will allow us to determine the true differences between H3K4me3 distribution in normal methionine and methionine restricted conditions.

It has already been shown the breadth of H3K4me3 peaks is an important factor in tissue specific gene expression (Benayoun et al., 2014; Chen et al., 2015). This could be expanded upon, and ChIP-seq peak signals could be parameterized (Figure 4.1).

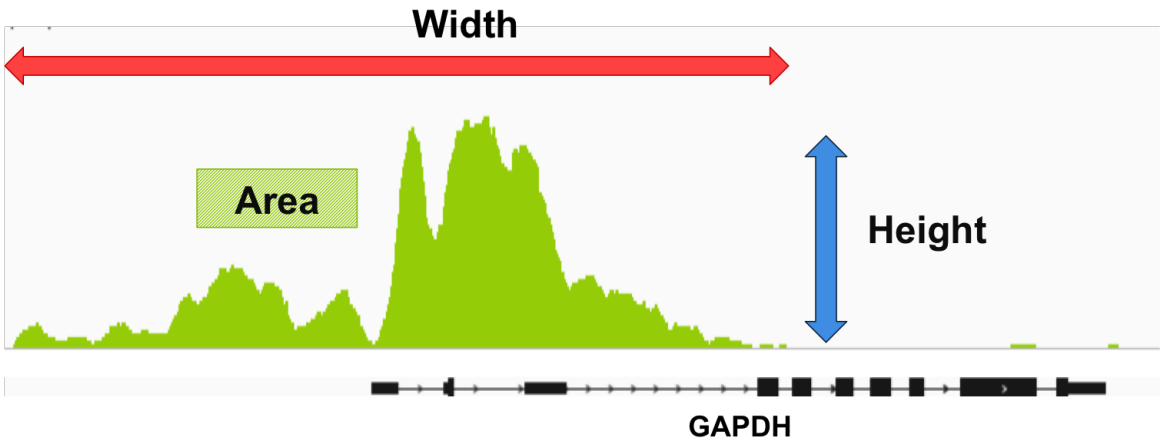

Figure 4.1: Quantitative Peak Parameters

Using quantitative ChIP-seq methodologies, peak parameters such as width, height, and area could be used to determine the absolute differences after methionine restriction.

Not only could breadth (or width) be investigated, but the impact on changes in peak height, area, and others could be investigated. This would be especially interesting in the case of methionine restriction since we observe an overall decrease in H3K4me3 peak signal across the genome. If we could further quantitatively analyze the changes in peak height and area, we may gain

a better insight into how these changes affect gene transcription and cellular identity.

4.2.2 Chromatin Dynamics in Response to Methionine Restriction

So far I have investigated the dynamics of H3K4me3 in response to methionine restriction at the global level. However, it would be interesting to observe the changes of H3K4me3 at each genomic region and determine how this correlates with gene expression. It is possible the genomic context and location of H3K4me3 will play a significant role in how fast a reduction is observed.

To characterize the dynamic response to methionine restriction on histone methylation and the effects on gene transcription at high resolution, ChIP-seq and RNA-seq will need to be performed during a methionine restriction time course. Since decreases in H3K4me3 are observed after only 4 hours, it would be informative to include 0, 2, 4 hour time points in addition to later–6, 8, 12, 24 hour–time points. To analyze the data, quantitative ChIP-seq should be performed using a spike-in strategy to determine the absolute differences in H3K4me3 peaks after methionine restriction.

In addition to this experiment, a parallel rescue experiment could be performed to assess how specifically H3K4me3 is recovered after methionine rescue for 24 hours. At least one additional time point at 48 hours (24 hours after methionine is added back to cells that were methionine restricted for 24 hours) would be necessary to understand what regions of the genome, or which spe-

cific gene sets are recovered. Additional time points after the addition of methionine could also reveal at what rate the recovery takes place.

To analyze the data, the rate of H3K4me3 loss at each gene could be calculated and each gene categorized by how fast it is affected by methionine restriction. This information could give rise to a network of early and late genes that are methionine restriction sensitive.

4.2.3 Changes in H3K4me3 in Response to Methionine Restriction and Effects on Splicing

Alternative splicing is a mechanism that allows cells to expand the diversity of the proteome. Affecting nearly 95% of genes (Pan et al., 2008), alternative splicing is important in cellular identity and differentiation (Barash et al., 2010). Previous studies have identified H3K4me3 as an important player in recruiting splicing machinery and directing alternative splicing in normal and cancer cells (Sims et al., 2007; Podlaha et al., 2014; Curado et al., 2015). With this in mind, it will be important to determine if decreases observed in H3K4me3 after methionine restriction alter the distribution of alternatively spliced transcripts.

To perform these experiments, additional ChIP-seq and deep RNA-seq must be performed to identify alternatively spliced transcripts upon methionine restriction. Alternatively spliced transcripts identified can then be cross referenced to changes observed in H3K4me3 at these genes. If a relationship exists, we hypothesize changes in H3K4me3 at these genes will occur. These changes in H3K4me3 peaks should be further characterized to determine if decreases

or complete loss of H3K4me3 signal are potentially responsible for alternative splicing. Other experiments would need to be performed to confirm any decreases in H3K4me3 peaks at alternatively spliced genes reduce binding of the splicing machinery. For these experiments, ChIP-seq utilizing antibodies for subunits of the splicing machinery will be necessary.

4.2.4 Impact on Other Methylation Events

This thesis only investigates a few histone methylation events and focuses on H3K4me3 since it had the most dramatic decrease in methylation after methionine restriction. However, with the array of histone methylation sites and possibility of mono-, di-, and tri-methylation there is still much to investigate. In addition to histone methylation, DNA methylation also plays a role in regulating gene expression (Bird, 2002). With recent work highlighting the dynamic characteristic of DNA methylation (Smith and Meissner, 2013), it should be investigated further. In addition, decreased folate, the other half of the one carbon metabolic cycle, has been linked to decreased DNA methylation (Crider et al., 2012). Therefore, it is not far reaching to suspect DNA methylation might be altered as well.

LITERATURE CITED

Barash, Y., Calarco, J. A., Gao, W., Pan, Q., Wang, X., Shai, O., Blencowe, B. J., and Frey, B. J. (2010). Deciphering the splicing code. *Nature*, 465(7294):53–59.

Benayoun, B., Pollina, E., Ucar, D., Mahmoudi, S., Karra, K., Wong, E., Devarajan, K., Daugherty, A., Kundaje, A., Mancini, E., Hitz, B., Gupta, R., Rando, T., Baker, J., Snyder, M., Cherry, J., and Brunet, A. (2014). H3k4me3 breadth is linked to cell identity and transcriptional consistency. *Cell*, 158(3):673–688. cited By 52.

Bird, A. (2002). DNA methylation patterns and epigenetic memory. *Genes Dev.*, 16(1):6–21.

Chen, K., Chen, Z., Wu, D., Zhang, L., Lin, X., Su, J., Rodriguez, B., Xi, Y., Xia, Z., Chen, X., Shi, X., Wang, Q., and Li, W. (2015). Broad H3K4me3 is associated with increased transcription elongation and enhancer activity at tumor-suppressor genes. *Nat. Genet.*, 47(10):1149–1157.

Crider, K. S., Yang, T. P., Berry, R. J., and Bailey, L. B. (2012). Folate and DNA methylation: a review of molecular mechanisms and the evidence for folate's role. *Adv Nutr*, 3(1):21–38.

Curado, J., Iannone, C., Tilgner, H., Valcarcel, J., and Guigo, R. (2015). Promoter-like epigenetic signatures in exons displaying cell type-specific splicing. *Genome Biol.*, 16:236.

Orlando, D. A., Chen, M. W., Brown, V. E., Solanki, S., Choi, Y. J., Olson, E. R., Fritz, C. C., Bradner, J. E., and Guenther, M. G. (2014). Quantitative ChIP-Seq normalization reveals global modulation of the epigenome. *Cell Rep*, 9(3):1163–1170.

Pan, Q., Shai, O., Lee, L. J., Frey, B. J., and Blencowe, B. J. (2008). Deep surveying of alternative splicing complexity in the human transcriptome by high-throughput sequencing. *Nat. Genet.*, 40(12):1413–1415.

Podlaha, O., De, S., Gonen, M., and Michor, F. (2014). Histone modifications are associated with transcript isoform diversity in normal and cancer cells. *PLoS Comput. Biol.*, 10(6):e1003611.

Sims, R. J., Millhouse, S., Chen, C. F., Lewis, B. A., Erdjument-Bromage, H., Tempst, P., Manley, J. L., and Reinberg, D. (2007). Recognition of trimethylated histone H3 lysine 4 facilitates the recruitment of transcription postinitiation factors and pre-mRNA splicing. *Mol. Cell*, 28(4):665–676.

Smith, Z. D. and Meissner, A. (2013). DNA methylation: roles in mammalian development. *Nat. Rev. Genet.*, 14(3):204–220.

Appendices

APPENDIX A

CODE FOR RNA-SEQ ANALYSIS

A.1 Generating Counts Table Using HTSeq

Counts tables were generated using HTSeq-0.6.1 for each sample 3/20/2016. The gene annotation gtf file (hg19_genes.gtf) was downloaded from Galaxy on 10/4/2015. It was originally uploaded to the server from Genomes 10/1/2012.

```
htseq-count -f bam
        TopHat/0hr1\RNA\TopHat\Accepted\Hits.bam
        ~/hg19_genes.gtf > Counts/0hr1.htseqcounts.csv

htseq-count -f bam
        TopHat/0hr2\RNA\TopHat\Accepted\Hits.bam
        ~/hg19_genes.gtf > Counts/0hr2.htseqcounts.csv

htseq-count -f bam
        TopHat/24hr1\RNA\TopHat\Accepted\Hits.bam
        ~/hg19_genes.gtf > Counts/24hr1.htseqcounts.csv

htseq-count -f bam
        TopHat/24hr2\RNA\TopHat\Accepted\Hits.bam
        ~/hg19_genes.gtf > Counts/24hr2.htseqcounts.csv
```

A.2 RNA Differential Expression Analysis Using DESeq

```
#install and load DESeq
biocLite("DESeq")
library(DESeq)

countTable<- read.table("CountsfromHTseq.txt",
        header=TRUE,
        row.names=1,
        sep=",")

#remove rows that are where sum is <5 for all genes
x<-rowSums(countTable)>5
countTable<-countTable[x,]
data<-countTable

#create a new DESeq object
cds=newCountDataSet(data,
        c("pMET", "pMET", "mMET", "mMET"))

#New DESeq Pipeline (similar to EdgeR)
#estimate effective library size
cds=estimateSizeFactors(cds)
sizeFactors(cds)

#visualized normalized counts
```

```
head(counts(cds, normalized=TRUE))

#Estimate dispersion (variance between samples)
cds=estimateDispersions(cds)

#Descriptors of dispersion function
str(fitInfo(cds))

#plot dispersion
plotDispEsts(cds)

#Calling differential expression
res=nbinomTest(cds, "pMET", "mMET")
head(res)

#plot log2FC vs mean normalized counts highlighting
   ↪ significant <10$\%$ FDR
plotMA(res, col=ifelse(res$padj>0.05,
         "black",
         "firebrick1"),
         cex.axis=2)

#histogram of pValues
hist(res$pval, breaks=100,
         col="skyblue",
         border="slateblue",
```

```
        main="")

#filter significantly expressed genes
resSig=res[res$padj<0.1,]
head(resSig)

#view most strongly down regulated genes
head(resSig[order(resSig$foldChange), -resSig$baseMean])

#view most strongly up regulated genes
head(resSig[order(-resSig$foldChange, -resSig$baseMean),])

#write results table with differential expression
   ↪ calculations
write.table(res, file="DESeqDiffExpChIP-seqResultsCutoff<5
   ↪ fromHTseqCounts.txt")



#heatmap
cdsBlind = estimateDispersions( cds, method = "blind" )
vsdFull = varianceStabilizingTransformation(cds)
library("RColorBrewer")
library("ggplot2")
select = order(rowMeans(counts(cds)),
        decreasing=TRUE)[1:25]
hmcol = colorRampPalette(brewer.pal(9, "GnBu"))(25)
```

```
heatmap(exprs(vsdFull)[select,],
          col = hmcol, trace="none",
          margin=c(10, 6))



#########################
#Gene Annotations
#########################

#Load the human database
biocLite("org.Hs.eg.db")
library(org.Hs.eg.db)

#Returns what IDs can be converted
keytypes(org.Hs.eg.db)

#make variable for current IDs (fbids) and what to return
   ↪ (cols)
fbids<-rownames(data)
cols<-"SYMBOL"

#search Hs database for keys(current IDs), return SYMBOLS,
   ↪  keys I have are ENSEMBL genes
annots<-select(org.Hs.eg.db, keys=fbids,
          columns=c("SYMBOL"),
          keytype="ENSEMBL")
```

```
write.table(annots,
          file="FromENSEMBLtoSYMBOL.txt",
          sep=",")

#Include Gene Symbols in data table
annotsTable<- cbind(ENSEMBL=rownames(as.data.frame(data)),
          as.data.frame(data)))
newTable = merge(data,
          annots,
          by.x="ENSEMBL")

write.table(newTable,
          file="annotatedOutputFilter<5Reads.txt",sep="\t")
```

APPENDIX B

CODE FOR CHIP-SEQ ANALYSIS

B.1 MACS2 - Calling H3K4me3 Peaks

MACS2 was used to call H3K4me3 peaks using bam files aligned to hg19. Input controls for each sample were used to determine background.

```
MACS2 callpeak
        -t ~/Galaxy176-\[0-3K_Sorted_BAM\].bam
         -c ~/Galaxy169-[0-3I_Sorted_BAM].bam
         -n pMET2
         -f BAM
         -g hs
         -q 0.05
         -B



MACS2 callpeak
        -t ~/Galaxy177-\[24-3K_Sorted_BAM\].bam
        -c ~/Galaxy178-[24-3I_Sorted_BAM\].bam
        -n mMET2
        -f BAM
        -g hs
```

```
        -q 0.05
        -B



MACS2 callpeak
        -t /~/Galaxy175-\[24-2K_Sorted_BAM\].bam
        -c ~/Galaxy168-\[24-2I_Sorted_BAM\].bam
        -n mMET1
        -f BAM
        -g hs
        -q 0.05
        -B

MACS2 callpeak
        -t ~/0-2K_Filtered_SAM.bam
        -c ~/Galaxy129-\[0-2I_Sorted_BAM\].bam
        -n pMET1
        -f BAM
        -g hs
        -q 0.05
        -B
```

B.2 Consensus Peak Set for Downstream Analysis

Using R, replicate peaks called by MACS2 are combined by keeping peaks in replicate 1 and replicate 2 for each condition. Then a consensus peak set is generated by combining peaks found in +MET or peaks found in -MET. A sample input file is generated that includes the paths to MACS2 peak files, MACS2 summit files, and bam files for each sample. This file is used to produce the final results.

```
library(GenomicRanges)
library(ShortRead)
library(rtracklayer)


#Load info file for samples

setwd("~/working_directory")
samples<-read.csv("samples.csv")

#####################################################
# FUNCTION mankeconsensus
# make consensus peak set
# append height, width, area metadata columns
#####################################################
```

```
makeconsensus <- function(PeakFileList){
  for(i in 1:length(PeakFileList)){
    mcols(PeakFileList[[i]]) <- NULL
    if(i == 1){
      ToMerge <- PeakFileList[[i]]
    }else{
      ToMerge <- c(ToMerge,PeakFileList[[i]])

    }
  }
  NonOverlappingSet <- reduce(ToMerge) #removes
    ↪ overlapping peaks
  #counts overlaps between NonOverlappingSet and Peakfile
    ↪ using lapply
  Temp <- do.call(cbind,lapply(PeakFileList,function(x)
    ↪ countOverlaps(NonOverlappingSet,x)))
  Temp[Temp > 1] <- 1 #peaks with more than 1 overlap set
    ↪ to 1
  #add temp to NonOverlappingSet as metadata (1=present in
    ↪  data set, 0=not present)
  elementMetadata(NonOverlappingSet) <- Temp

  return(NonOverlappingSet)
}
```

```
################################
# FUNCTION countarea
# Read in bam files and use bed
# regions to count the # of tags in each
# peak.  Output peak 'area'
################################

countarea<-function(bamfile, bedfile) {
  reads<-readGAlignments(bamfile)
  regions<-bedfile
  reads<-as(reads, "GRanges")
  regions<-as(regions, "GRanges")
  area<-countOverlaps(regions, reads, ignore.strand=TRUE)
  area<-as.data.frame(area)
  return(area)
}



################################
# COMPARE 0-24HR
################################
library(GenomicRanges)

#Load macs2 output files
```

```
myFiles<-as.vector(samples$peak.file)
myData <- lapply(myFiles, read.delim, skip=26)

#Create names for each dataset in myData
n<-samples$name
names(myData)<-n



############################
# MERGE replicate peaks files
############################
myData<-lapply(myData, GRanges)

merge<-mergeByOverlaps(myData[[1]], myData[[2]])

#have to do this funky thing in order to make DataFrame (
    ↪ from GenomicRanges) to actual dataframe
x1<-as.data.frame(GRanges(merge$myData..1..), row.names =
    ↪ NULL, optional=FALSE)
x2<-as.data.frame(GRanges(merge$myData..2..), row.names=
    ↪ NULL, optional=FALSE)

myData[[(length(myData)+1)]]<-cbind(x1, x2)

# name new column in data.frame for merge
```

```
names(myData)[length(myData)]<-"merge0hr"



merge<-mergeByOverlaps(myData[[3]], myData[[4]])

#have to do this funky thing in order to make DataFrame (
    ↪ from GenomicRanges) to actual dataframe
x1<-as.data.frame(GRanges(merge$myData..3..), row.names =
    ↪ NULL, optional=FALSE)
x2<-as.data.frame(GRanges(merge$myData..4..), row.names=
    ↪ NULL, optional=FALSE)

myData[[(length(myData)+1)]]<-cbind(x1, x2)

# name new column in data.frame for merge
names(myData)[length(myData)]<-"merge24hr"



myData<-myData[c(-1,-2,-3,-4)]

names(myData[[1]])<-c("chr", "start", "end", "width.0hr1",
    ↪  "strand.0hr1", "length.0hr1", "summit.0hr1", "
    ↪ pileup.0hr1", "pval.0hr1", "fc.0hr1", "qval.0hr1", "
    ↪ name.0hr1", "chr2", "start2", "end2", "width.0hr2",
    ↪ "strand.0hr2", "length.0hr2", "summit.0hr2", "pileup
    ↪ .0hr2", "pval.0hr2", "fc.0hr2", "qval.0hr2", "name.0
```

```
    ↪ hr2")



names(myData[[2]])<-c("chr", "start", "end", "width.24hr1"
    ↪ , "strand.24hr1", "length.24hr1", "summit.24hr1", "
    ↪ pileup.24hr1", "pval.24hr1", "fc.24hr1", "qval.24hr1
    ↪ ", "name.24hr1", "chr2", "start2", "end2", "width.24
    ↪ hr2", "strand.24hr2", "length.24hr2", "summit.24hr2"
    ↪ , "pileup.24hr2", "pval.24hr2", "fc.24hr2", "qval.24
    ↪ hr2", "name.24hr2")

myData<-lapply(myData, GRanges)

consensus<-makeconsensus(myData)



##################################
# Count number of tags in each peak
##################################
consensus<-as.data.frame(consensus)

# get genomic ranges for each sample and store in variable
area_bed<-subset(consensus, select=seqnames:end)
area_bed<-GRanges(area_bed)
```

```
# set working directory where bam files are
setwd("/Location/BamFiles/")

# get bam files
myFiles<-as.vector(samples$bam.file)

for (i in 1:length(myFiles)){
  count<-countarea(myFiles[[i]], area_bed)
  consensus<-append(consensus, count)
  names(consensus)

}

consensus<-as.data.frame(consensus)
consensus<-GRanges(consensus)



rm(count, area_bed)



###################################
# Export as csv
###################################

setwd("~/working_directory")
```

```
consensus<-as.data.frame(consensus)
names(consensus)<-c("chr", "start", "end", "width", "
    ↪ strand", "merge0hr", "merge24hr", "area.0hr1", "area
    ↪ .0hr2", "area.24hr1", "area.24hr2")


write.csv(consensus, file="024hr-consensusPeak-area.csv")
```

B.3 Annotate Peaks Using Homer Software

Homer Software Suite was used to annotate peaks. From the consensus peak set, the unique peak name, chromosome, start, and end data was subsetted into a new .txt file. This was then used as input for Homer annotatePeaks.pl. After running, the annotation (HomerAnno_024hr.txt) and peak data (024hr-consensusPeakarea.csv) are manually combined by sorting on peak name. This will be the final dataset for analysis.

```
annotatePeaks.pl
        all -for -HomerAnno.txt  hg19 > HomerAnno_024hr.txt
        -annStats  HommerAnnoStats_024hr.txt
```